NNWSI

K. Stablein
extra copy

SANDIA REPORT

SAND85—2701 • Unlimited Release • UC—70
Printed August 1986

Nevada Nuclear Waste Storage Investigations Project

Preliminary Estimates of Groundwater Travel Time and Radionuclide Transport at the Yucca Mountain Repository Site

Y. T. Lin, M. S. Tierney
Scott Sinnock, Editor

Prepared by
Sandia National Laboratories
Albuquerque, New Mexico 87185 and Livermore, California 94550
for the United States Department of Energy
under Contract DE-AC04-76DP00789

"Prepared by Nevada Nuclear Waste Storage Investigations (NNWSI) Project participants as part of the Civilian Radioactive Waste Management Program (CRWM). The NNWSI Project is managed by the Waste Management Project Office (WMPO) of the U. S. Department of Energy, Nevada Operations Office (DOE/NV). NNWSI Project work is sponsored by the Office of Geologic Repositories (OGR) of the DOE Office of Civilian Radioactive Waste Management (OCRWM)."

Issued by Sandia National Laboratories, operated for the United States Department of Energy by Sandia Corporation.

Printed in the United States of America
Available from
National Technical Information Service
U.S. Department of Commerce
5285 Port Royal Road
Springfield, VA 22161

NTIS price codes
Printed copy: A08
Microfiche copy: A01

SAND85-2701

Preliminary Estimates of Groundwater Travel Time and Radionuclide Transport At the Yucca Mountain Repository Site

By

Scott Sinnock (Editor)
Y. T. Lin
M. S. Tierney
and others

ABSTRACT

This report presents the assumptions, methods, and data used in a probabilistic approach to the calculation of groundwater travel times and total radionuclide releases to the water table below Yucca Mountain, Nevada. Assumptions and mathematical principles that serve as the basis for the formulation of the calculational model are described. Data to support the analyses are abstracted from formal and informal reports generated by the staff of such participating organizations as the United States Geological Survey, Los Alamos National Laboratory, Lawrence Livermore National Laboratories, and Sandia National Laboratories, for the Nevada Nuclear Waste Storage Investigations (NNWSI) Project activities. Results from the analyses consist of distributions of groundwater travel time from the disturbed zone to the water table and the cumulative curie releases to the water table. The studies provide some of the information needed in support of requirements for the NNWSI statutory Environmental Assessment and indicate that

- for the upper limit of percolation flux below the repository level at Yucca Mountain, groundwater travel time has a mean of about 43,000 years and a standard deviation of about 12,000 years; less than 1 percent of the calculated groundwater travel times are less than 10,000 years.

- values for cumulative releases of radionuclides, for a 70,000-MTHM inventory of spent fuel, subject to a percolation flux of 0.5 mm/yr, have been estimated at about 6.0×10^{-4} curies of C-14, 2.0×10^{-2} curies of Tc-99, and 5.0×10^{-5} curies of I-129, which would be released to the water table within 10,000 years following repository closure.

Therefore, based on the present model, this evidence indicates that the Yucca Mountain repository site would be in compliance with regulatory requirements.

Contributing Authors

M. J. Eatough	SNL, 6315
J. Foster	Technedyne
M. W. Sharp	SNL, 5164
D. L. Szklarz	Applied Research Inc.
D. L. South	SNL, 6315
B. C. Whittet	SNL, 6315
R. W. Williams	SNL, 6315
D. H. Zeuch	SNL, 6315

CONTENTS

CONTENTS
(continued)

LIST OF FIGURES

LIST OF FIGURES
(continued)

LIST OF TABLES

ACKNOWLEDGMENTS

The authors express their thanks to the following persons who contributed substantial time and effort to the improving the quality of this report. They include F. W. Spencer, Divison 7223, P. G. Kaplan, Division 6315, and G. E. Barr, Division 6312, for the thoughtful critiques of draft versions of the report. Special thanks are extended to R. J. Dreicer, LATA, for technical editing throughout the revision cycles.

1.0 INTRODUCTION

This report was prepared to document analyses of groundwater travel time and radionuclide transport in support of the statutory Environmental Assessment (EA) document of the Nevada Nuclear Storage Investigations (NNWSI) Project (DOE, 1986). The NNWSI Project, administered by the Nevada Operations Office of the Department of Energy (NV-DOE), is responsible for assessing the feasibility of developing a repository for commercial high-level radioactive waste at Yucca Mountain, Nevada (see Figure 1). Sandia National Laboratories (SNL) provides support for the NNWSI Project in the areas of repository design, performance assessment, data base development, and experimental programs for the investigation of thermal and mechanical rock properties at Yucca Mountain. This report was prepared as a part of the performance assessment activities at SNL. The data used in our analyses were provided by various investigators from U.S. Geologic Survey, Los Alamos National Laboratory, Lawrence Livermore National Laboratory, and other principal participants in the activities of the NNWSI Project.

The draft statutory EA (DOE, 1984a) included preliminary performance assessments requiring the calculation and estimates of potential groundwater travel time and cumulative radiological releases to the accessible environment. These performance assessments were used to evaluate certain qualifying and disqualifying conditions required by the DOE with regard to the hydrogeology of the site and total system performance. The calculations of groundwater travel time and cumulative releases of radionuclides presented in the draft EA (DOE, 1984a) were

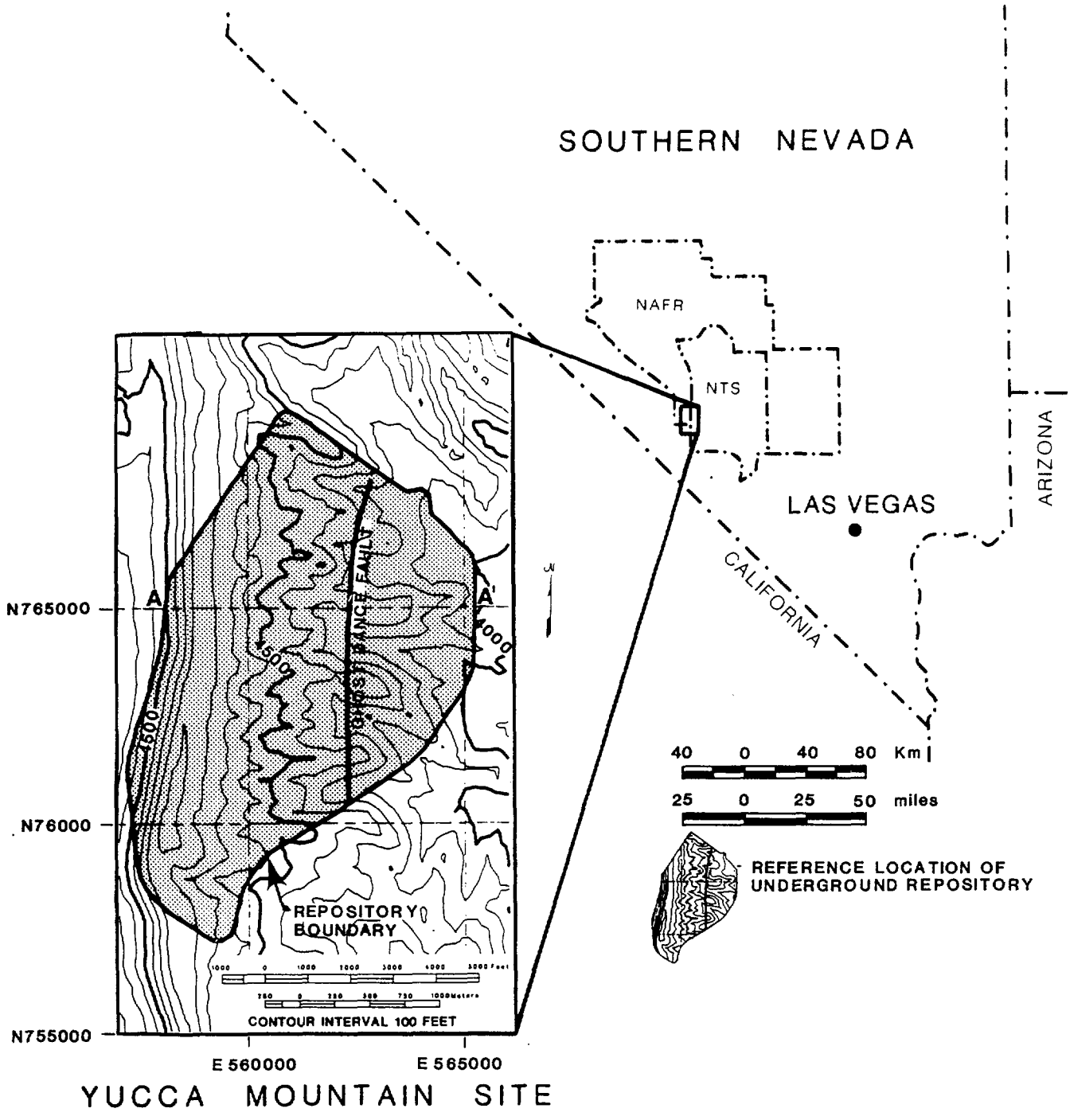

SOURCE: GE/CALMA PRODUCT NO.0119

Figure 1. Location Map of the Yucca Mountain Site, Nevada.

The map shows the reference location of the perimeter drift of the repository (PBQ and D, 1985; GE/CALMA, 1986, Product No. 0119) and the location of the hydrogeologic cross section A-A' shown in Figure 2.

made by means of simulation models available at that time. The model used for predicting cumulative releases, SPARTAN* (Lin, 1985; Sinnock et al., 1984), was based on single, deterministic values of groundwater velocities and dispersionless radionuclide transport through a representative section of hydrogeological units in the unsaturated zone at Yucca Mountain. During the public review and commentary periods for the draft EAs, requests were received from several sources to provide additional support for the conclusions in Sections 6.3.1.1 and 6.4.2 of the final NNWSI EA report (DOE, 1986). The techniques presented here were developed in response to those requests, to account for variabilities in the key parameters used for calculating groundwater travel time and radionuclide transport.

To address the concerns about groundwater travel time, this report presents a probabilistic method for estimating the distribution of groundwater travel times. To address the question of radionuclide transport, the report also presents a probabilistic method consistent with the groundwater travel-time calculations. The report describes the physical and the mathematical bases of the methods, and presents the results of analyses using these methods.

Section 2, following this introduction, describes assumptions, methods, and data used for estimating groundwater travel times. Results of the simulations used for calculating groundwater travel time are also discussed in Section 2. These simulations rely on a wider range of

---

*Simple Performance Assessment of Radionuclide Transport at Nevada.

defining parameters than those used in the draft EA (DOE, 1984a), and provide additional insight and support for judging the reliability of the results presented in Section 6.3.1.1 of the final version of the EA (DOE, 1986).

Section 3 presents the basic assumptions and the methods used for estimating cumulative releases of radionuclides to the water table, and provides background material for assessing the limitations of the conclusions drawn in Section 6.4.2 of the final version of the EA (DOE, 1986).

Section 4 presents the conclusions.

Three appendices are provided as follows:

Appendix A contains estimates of the distribution, mean, and standard deviation of travel time derived by analytical methods.

Appendix B contains the source data for effective porosity, saturated matrix hydraulic conductivity, and relative hydraulic conductivity.

Appendix C contains lists of computer programs for calculating the groundwater travel times and the expected cumulative discharge of the radionuclides.

2.0 GROUNDWATER TRAVEL TIMES

Calculations of groundwater travel times provide useful information for assessing the postclosure performance of a potential high-level nuclear waste repository at Yucca Mountain. In particular, the regulations of both the DOE (1984b) and the Nuclear Regulatory Commission (NRC, 1983) require that pre-waste-emplacement groundwater travel time along the fastest path of likely radionuclide travel from the disturbed zone to the accessible environment shall be at least 1,000 years. Groundwater flow is the most likely means for the movement of substantial amounts of radioactive contaminants from the waste-emplacement area to the accessible environment. Radioactive releases into the accessible environment must remain within limits prescribed by the Environmental Protection Agency (EPA) for the first 10,000 years after permanent closure of the repository (EPA, 1985). Because, in general, contaminants can travel no faster than the groundwater, the groundwater travel time between the subsurface facilities and the accessible environment sets a minimum time before releases of radionuclides can occur and provides a basis for estimating the quantity of such releases thereafter.

Groundwater travel times depend upon the hydraulic properties of geologic units through which water flows, hydrologic conditions at the site, and the length of flow paths. At Yucca Mountain, the flow paths pass through both the unsaturated and saturated zones. This study focuses only on the downward percolation of water through the unsaturated zone. A conceptual hydrogeologic cross section of Yucca Mountain (Figure 2)

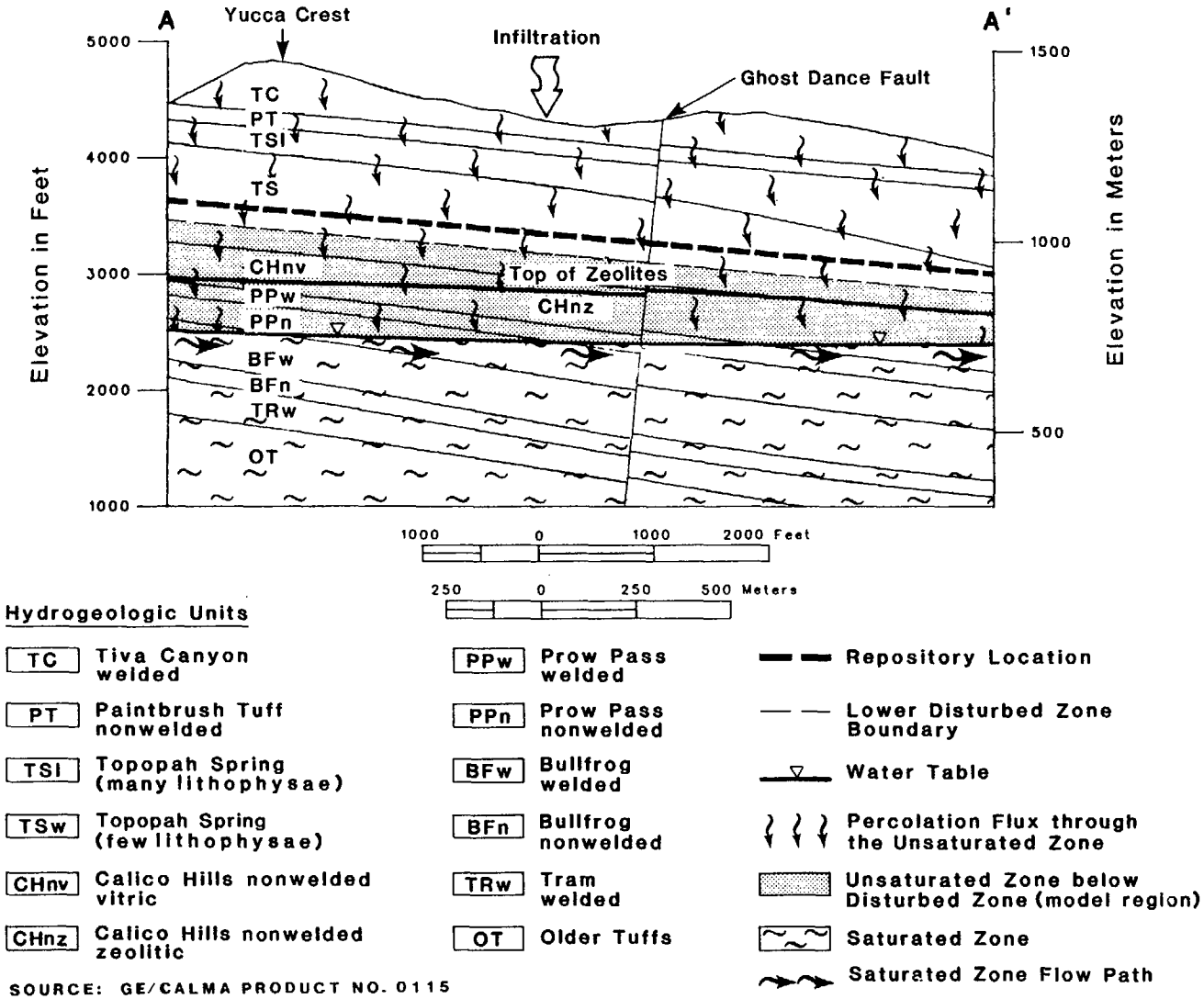

Figure 2. General hydrogeologic cross section at Yucca Mounain.

The wavy arrows show the flow paths, as assumed in this report, from a potential repository through the unsaturated zone to the water table and along the upper portion of the saturated zone toward the accessible environment (5 km away).

illustrates the general flow paths from the waste-emplacement area considered in this report. Montazer and Wilson (1984) present a conceptual model that includes possible lateral flow both above and below the repository level. However, for reasons described in Section 2.1, our approach, hence our conceptual diagram of the likely flow path shown in Figure 2, assumes only vertical flow through the unsaturated zone beneath the repository. The flow passes through the unsaturated zone to the water table, and along a 5-km distance in a downgradient direction along the top portion of the saturated zone leading to the accessible environment.

This chapter is divided into the following sections.

Section 2.1 establishes the conceptual and theoretical bases for calculating groundwater travel times.

Section 2.2 presents a discussion of the data required in the analyses of groundwater travel time.

Section 2.3 details the computational model for calculating groundwater travel time.

Section 2.4 presents selected results of the calculations, including variations based on differing sets of model parameters to indicate the relative sensitivity of simulated travel times to some of the key parameters.

Section 2.5 presents a summary of the groundwater travel time solutions and general conclusions about the probable behavior of the flow system at Yucca Mountain in terms of the regulatory requirements.

2.1 Theoretical Basis for the Calculation of Groundwater Travel Times

The calculation of groundwater travel times depends upon the basic equations selected for analyzing flow behavior. In steady-state flow through a porous rock, the specific discharge (flux) of a fluid is commonly taken as described by the Darcy flow equation (Bear, 1972; Freeze and Cherry, 1979); this is usually expressed in one-dimensional form as

$$q = - K \frac{dh}{d\ell} \qquad (m/yr) \quad , \tag{1}$$

where q is the specific discharge or flux in $m^3/m^2/yr$, K is hydraulic conductivity in m/yr, and $dh/d\ell$ is the hydraulic gradient. The distance along the flow direction is measured by ℓ. The hydraulic head, h, is the sum of the two components, pressure head, Ψ, and elevation head, z. The average linear pore velocity of water particles, V, may, for saturated conditions, be obtained from the equation

$$V = \frac{q}{n_e} \qquad (m/yr) \quad , \tag{2}$$

where n_e is the effective porosity or volume of interconnected pore space available for fluid transmission. Given the velocity for a particle of water, the travel time, t, along a given path may be calculated by using

$$T = \frac{d}{\bar{V}} \qquad \text{(yr)} \quad , \tag{3}$$

where d is the linear distance of the flow path between two points.

Transient infiltration pulses may be transmitted through fractures in the Tiva Canyon welded unit, the uppermost tuff unit of Yucca Mountain (Figure 2), according to several conceptual models for water flow in the unsaturated zone at Yucca Mountain (Montazer and Wilson, 1984; Montazer et al., 1985; Sinnock et al., 1984; Weeks and Wilson, 1984) and simulations of flow (Wang and Narasimhan, 1985 and 1986; Peters et al., 1986). However, the infiltration pulses probably are damped by the matrix pores of the underlying Paintbrush nonwelded unit. The underlying Topopah Spring welded unit responds to the pulses by exhibiting only small changes in saturation, pressure, and potential relative to the steady-state values. The flow field of infiltrating water percolating through deeper units, including the lower part of the Topopah Spring welded unit, which is the target zone for waste emplacement, and the underlying units, probably exhibits a near steady-state behavior representing a long-term average flux.

Because the steady-state flow in the lower portion of the unsaturated zone at Yucca Mountain is probably vertical, the term $dh/d\ell$ is assumed to equal minus one (-1) in our model, which is restricted to the region 50 meters below the repository (from the lower boundary of the disturbed zone to the water table). This means that the flow is driven solely by the elevation head and is along a gradient of unity in the direction of

gravity. Based on this assumption, a reasonable approximation of the velocity of water through the lower portion of the unsaturated zone can be obtained from Equation 2. The flux, q, may be determined independently, or may be determined by theoretical relation to the conductivity, K. The effective porosity, n_e, may be derived from experimental measurements. Therefore, calculations of groundwater travel time can be expressed as a function of only three parameters--namely, the flux, the effective porosity, and the distance of vertical flow. This last parameter is conveniently expressed by the combined thicknesses of the hydrogeologic units, which make up the total thickness between the disturbed zone and the water table for the area beneath the potential repository facilities at Yucca Mountain.

Hydraulic conductivity and pressure head in unsaturated tuff depend on capillary forces in the porous rock. These forces, in turn, are a function of the saturation and the pore size distribution of the rockmass through which flow occurs. At lower saturations, smaller pores with larger capillary forces exert a dominant suction that draws water into the smallest pores with sufficient volume for containing the available water. A decrease in hydraulic conductivity, an increase in suction pressure, and a decrease in effective porosity accompany a decrease in saturation. Given a steady flux of water through the porous rock, it is reasonable to assume (Weeks and Wilson, 1984; p. 2) that an approximate steady-state condition exists whereby (1) hydraulic conductivity adjusts to a value equal to the flux, (2) pressure head is relatively constant in space, and (3) effective pore volume (the pore space available for the free movement of water) becomes a function of the flux.

For steady-state flow through the matrix of porous unsaturated rock, the average linear velocity of a fluid is expressed as

$$V_m = \frac{q}{\theta(q)} \qquad (m/yr) \quad , \tag{4}$$

where θ is the effective moisture content (volume of mobile water per unit volume of porous rock) of the matrix. Equation 4 is the extension of Equation 2 for partially saturated flows. For saturated rock, θ is identical to the effective porosity, but for partially saturated rock, θ is a function of q.

A simple approximation of the dependence of θ on q can be obtained from a power-law expression (Brooks and Corey, 1966) for the wetting-phase relative hydraulic conductivity, as follows:

$$\frac{K}{K_s} = \left(\frac{S - S_r}{1 - S_r}\right)^{\varepsilon} \quad , \tag{5}$$

where

K = effective hydraulic conductivity (m/yr)

K_s = saturated hydraulic conductivity (m/yr)

S = saturation (volume of fluid/void-space volume)

S_r = residual saturation, and

ε = an empirical constant > 0.

Rearranging Equation 5 gives

$$(S - S_r) = (1 - S_r) \left(\frac{K}{K_s} \right)^{1/\varepsilon} \quad . \tag{6}$$

Because

$$\theta = n_b(S - S_r) \quad , \tag{7}$$

where n_b is the bulk porosity of the matrix (void-space volume per unit volume of rock), then

$$\theta = n_b \ (1 - S_r) \left(\frac{K}{K_s} \right)^{1/\varepsilon} \quad . \tag{8}$$

For steady flows and regions of rock removed from infiltration boundaries or capillary fringes, Weeks and Wilson (1984, p. 2) have indicated that under a unity gradient, on the average, the effective hydraulic conductivity, K, will adjust so that

$$K = q \qquad \text{(m/yr)}, \qquad \text{for } q < K_s \ . \tag{9}$$

Therefore, substituting q for K in Equation (8) gives

$$\theta(q) = n_b(1 - S_r) \left(\frac{q}{K_s} \right)^{1/\varepsilon} \qquad \text{for} \quad q < K_s \quad . \tag{10}$$

The term $n_b(1 - S_r)$ is equal to the effective porosity, n_e, if all the pore space in the matrix is interconnected. Thus,

$$\theta(q) = n_e \left(\frac{q}{K_s} \right)^{1/\varepsilon} \qquad \text{for } q < K_s \tag{11}$$

By incorporating Equation 11 into Equation 4, one finds that

$$V_m = \frac{q}{n_e} \left(\frac{K_s}{q} \right)^{1/\varepsilon} \qquad \text{(m/yr)}, \qquad \text{for } q < K_s. \tag{12}$$

If the flux exceeds the largest possible value of hydraulic conductivity of the matrix (i.e., saturated conductivity), then that portion of the flux in excess of saturated hydraulic conductivity will have to move either laterally along the bottom of, or within the low-conductivity region, or vertically downward through fractures. On the assumption that all flow is vertical, the excess flux, q_f, is expected to flow vertically through fractures that dip at angles close to 90° (Scott and Bonk, 1984). If $q \geq K_s$, it is assumed that the water will flow in fractures with a linear velocity, locally, of

$$V_f = \frac{q_f}{n_f} \qquad \text{(m/yr)}, \qquad \text{for } q \geq K_s, \tag{13}$$

where n_f is the effective fracture porosity. Therefore, linear velocity of a water particle moving along a vertical path through the rock matrix or fractures is determined, for our calculations only, by the percolation flux, q, and local values of saturated matrix hydraulic conductivity, K_s, matrix

effective porosity, n_e, fracture effective porosity, n_f, and an empirical constant, ϵ, representing the effects of saturation levels on matrix pore space available for flow.

In the present model, K_s and n_e are treated as random variables because of their spatial variation within each hydrogeologic unit. As described in Section 2.2, their unit-specific statistical parameters are assumed to represent spatial variations of K_s and n_e based on samples collected from the available data. In effect, K_s and n_e are treated as spatially random fields within hydrogeologic units. The effective moisture content, θ (Equation 4), is derived as a function of q, K_s, and n_e (Equation 11), allowing a computation of the local water-particle velocities as follows:

$$V = \begin{cases} \dfrac{q}{n_e}\left(\dfrac{K_s}{q}\right)^{1/\epsilon} & \text{(m/yr)}, \quad \text{if } q < K_s \\ \dfrac{q_f}{n_f} & \text{(m/yr)}, \quad \text{if } q \geq K_s \end{cases} \qquad (14)$$

The fracture porosity, n_f, the residual saturation, S_r, and the Brooks-Corey exponent, ϵ, could also be regarded as spatially random variables. However, because of a lack of sufficient data, S_r and ϵ are assumed to be constant values within each hydrogeologic unit in the present model, and n_f is assumed to be a constant throughout the entire unsaturated portion of the underground site.

The variability of hydraulic parameters may be different in the vertical and horizontal directions. This variability depends on a concept referred to as the correlation length. The correlation length is the minimum distance between two points at which the covariance, C, of a spatially-dependent random variable vanishes (see p. 17 of Feller, 1966). In simpler terms, two values of a random variable are statistically independent if the spatial distance between them exceeds the correlation length. In the vertical direction, the velocity field described by Equation 14 is assumed to be correlated over a distance less than some length ρ_v. Similarly, the values representative of the velocity field at the same depth, but in different horizontal locations of the rock, are assumed to be correlated if the locations are separated by distances of less than ρ_h. Neither ρ_v nor ρ_h has been determined for the hydrogeologic units at Yucca Mountain; therefore, they were defined as free parameters in the calculations. The correlation length in the vertical direction is probably smaller than that in the horizontal direction for vertically stratified tuff at Yucca Mountain.

2.2 Data Required for the Calculation of Groundwater Travel Times

As established in Section 2.1, the data needed for calculating groundwater travel times by our approach include values for the

(1) thickness of each hydrogeologic unit along the assumed vertical flow paths between the disturbed zone and the water table,

(2) effective matrix porosity and effective fracture porosity,

(3) saturated matrix hydraulic conductivity,

(4) the Brooks-Corey Exponent (see Equation 8) for relative conductivity, and

(5) percolation flux between the disturbed zone and the water table.

For each of the parameters, the empirical basis for defining the ranges and distributions used in our calculations, is addressed in the following subsections.

2.2.1 Thickness of the Hydrogeologic Units and the Geometry of the Calculational Grid

A horizontal grid of the repository study area, constructed as a digitized gridded terrain model (GTM) on the Calma Graphics system at SNL (GE/CALMA, 1985), is shown in Figure 3. GTM is defined by a set of elevations and a set of GTM parameters. The parameters include the x-y origin of the orthogonal grid in a three-dimensional spatial model, the grid spacing, and the number of grid points in the x and y directions. The origin of the GTM is located at Nevada state grid (central) coordinates, East 557,000 feet and North 750,000 feet. The distance between grid points along the x and y coordinates is 250 feet (76.2 m). There are 37 grid points in the x direction and 89 in the y direction with 0° orientation. The GTM is three-dimensional. Data defining the elevations (z direction) of stratigraphic contacts, and the water table at each grid point, are from a three-dimensional model of reference

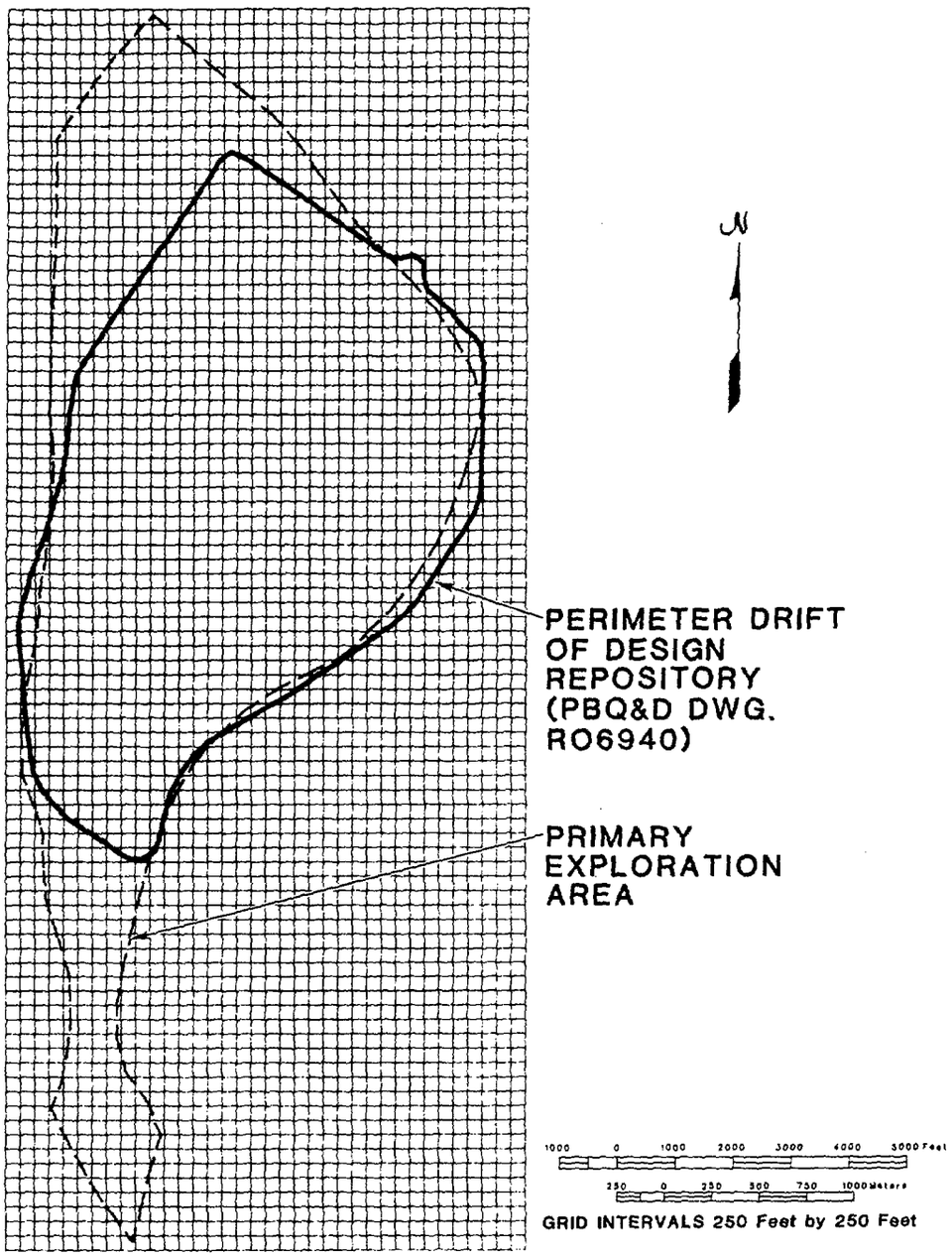

SOURCE: GE/CALMA PRODUCT NO. 0114

Figure 3. Grid map of the calculational elements for the repository study area.

The area enclosed by the perimeter drift is composed of 963 square vertical columns defined by the grid.

thermal/mechanical and hydrological stratigraphy at Yucca Mountain (Ortiz et al., 1985), slightly modified to account for a different interpretation of offsets along Ghost Dance Fault. The depth and elevation level at each point of contact between hydrogeological units, for drill holes, are presented in Appendix B. Elevations of the repository facilities, disturbed zone boundary, and the water table were defined for this study. The volume beneath the repository is represented by 963 square vertical columns of the grid. Digitized data, which define the gridded geometry of the hydrogeological units, repository facilities, disturbed zone boundary, and water table are available from SNL.

The values for the thickness of each unsaturated hydrogeologic unit beneath the disturbed zone were obtained from the three-dimensional graphics model* of the Yucca Mountain Site (Ortiz, et al., 1985). The disturbed zone is assumed to be 50 meters below the midplane of a 45-m-thick envelope containing the underground facilities. Projections of the perimeter drift of the design repository (GE/CALMA, 1986, No. 0119) to the lower boundary of the disturbed zone delineate the area of vertical unsaturated flow used in the calculations. Contours of the thickness of the total unsaturated zone and of each of the seven hydrogeologic units between the disturbed zone and the water table are shown in Figure 4. The range of unit thicknesses and the percentage of total repository area underlain by each unit are listed in Table 1.

---

*The model is maintained on the IGIS computer graphics system of Sandia National Laboratories (GE/CALMA, 1985).

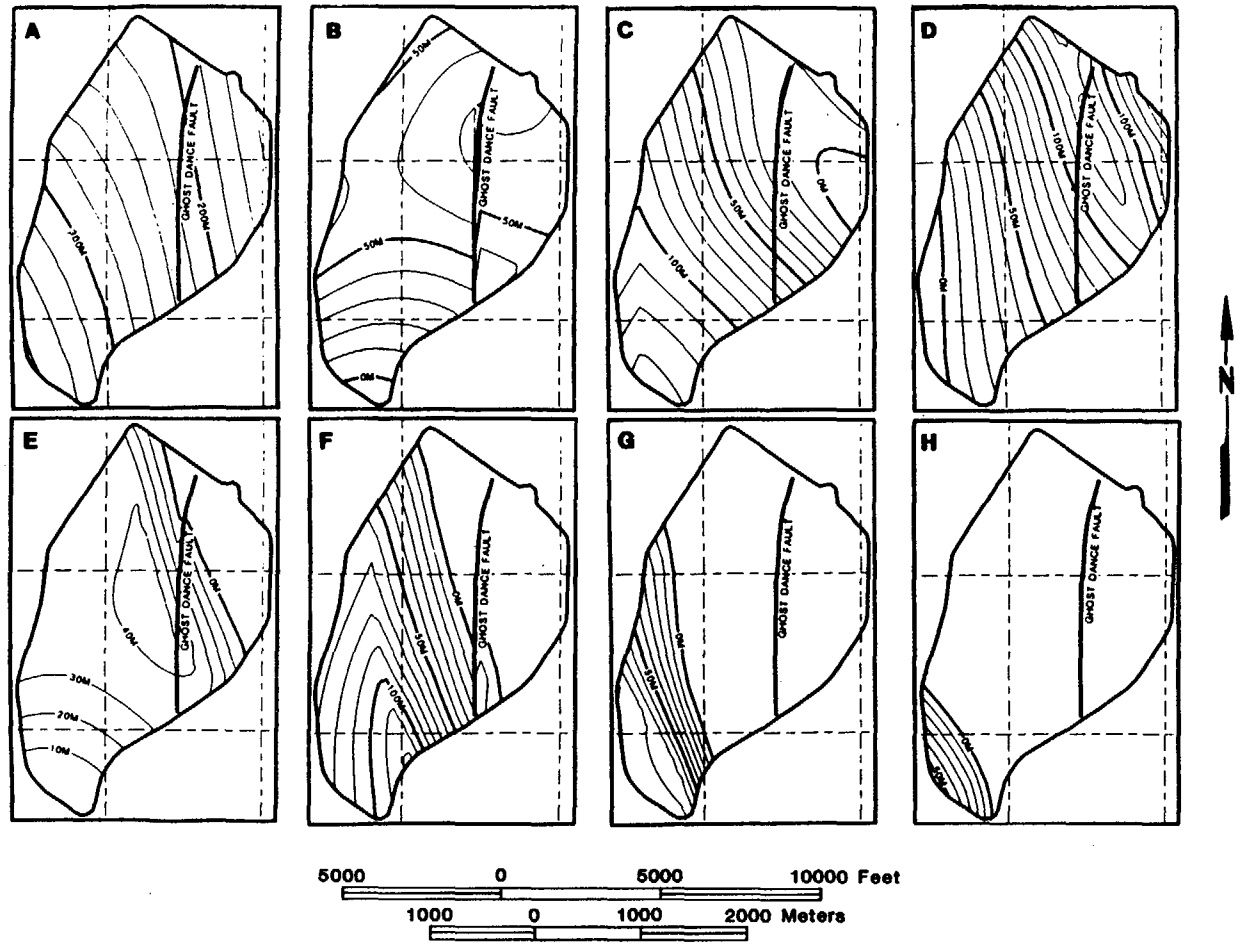

Figure 4. Isopach Contour Maps: (A) Total thickness from disturbed zone to the water table; (B) Thickness of undisturbed Topopah Spring welded unit, TSw; (C) Thickness of the Calico Hills vitric unit, CHnv; (D) Thickness of the Calico Hills zeolitic unit, CHnz; (E) Thickness of the Prow Pass welded unit, PPw; (F) Thickness of the Prow Pass nonwelded unit, PPn, (G) Thickness of the Bullfrog welded unit, BFw; and (H) Thickness of the Bullfrog nonwelded unit, BFn.

TABLE 1

Parameters Used in Groundwater Travel-Time Calculations for the Unsaturated Zone

Parameter \ Hydrogeologic Unit[a]	TSw	CHnv	CHnz	PPw	PPn	BFw	BFn[b]	Remarks
Hydraulic Gradient, (i)	1.0	1.0	1.0	1.0	1.0	1.0	1.0	$i = \partial h/\partial l = \partial \Psi/\partial l + \partial z/\partial l$ where $\partial \Psi/\partial l << 1.0$ and $\partial z/\partial l = \partial z/\partial z = 1.0$, i.e. vertical gravity flow is assumed
Mean Saturated[c] Hydraulic Conductivity K_s (mm/yr)	0.722 (31)	107.168 (8)	0.535 (31)	87.742 (10)	21.637 (7)	118.439 (2)	21.637 (NA)	$\bar{K}_s = \ln^{-1}(\text{mean}[\ln(K_s)])$ Values in parentheses are the number of measurements
$\bar{K}_s - 1\sigma$ (mm/yr)	0.128	1.886	0.0374	29.500	3.302	58.405	3.302	$\ln^{-1}\left(\text{mean}\,[\ln K_s] - \alpha\,[\ln K_s]\right)$
$\bar{K}_s + 1\sigma$ (mm/yr)	4.073	6089.953	7.648	260.967	141.797	240.182	141.797	$\ln^{-1}\left(\text{mean}\,[\ln K_s] + \alpha\,[\ln K_s]\right)$
Mean Effective Porosity $n_e \pm 1\sigma$	0.1062 ±0.0458 (138,12)	0.3239 ±0.0880 (23,6)	0.2693 ±0.0468 (65,10)	0.2382 ±(0.0650) (27,4)	0.2500 ±0.0622 (75,2)	0.2251 ±0.0884 (120,2)	0.2500 ±0.0622 (NA)	$n_e = n_b(1-S_r)$, where n_b is the mean bulk, dry porosity[d] and S_r is residual saturation (S). Ordered pairs in parentheses are number of measurements of n_b and S_r, respectively
Range[e] of Thicknesses (m)	0-72 (98.5)	0-135 (95.3)	0-133 (94.5)	0-44 (83.2)	0-122 (63.1)	0-91 (25.6)	0-55 (7.5)	Thicknesses between disturbed zone and water table for area within the design repository boundaries. Values in parentheses are percents of total repository area underlain by the units.
ϵ[f]	5.9	4.2	7.0	4.0	5.2	4.6	5.2	Empirical constant that represents the effects of the relationship between pore-size distribution and saturation on the amount of the effective porosity, n_e, available for flow; the effect of ϵ is to reduce flow area and thus increase particle velocity relative to values calculated using q/n_e

[a] See Figure 2 for legend.

[b] Assumed to be hydrologically identical to PPn.

[c] Saturated conductivity data is from the Tuff Data Base (TUFFDB) Product No. 2, 1985.

[d] Bulk porosity data is from the Tuff Data Base (TUFFDB) Product No. 1, 1985.

[e] Range of thickness, Interactive Graphics Information System (IGIS), SNL 1985.

[f] ϵ derived in Appendix B by the method of Brooks and Corey (1966).

2.2.2 Effective Porosity

Effective porosity, n_e, was defined in Equation 10 as

$$n_e = n_b(1 - S_r), \tag{15}$$

where n_b is the bulk matrix porosity and S_r is the residual saturation (Peters et al., 1984). To determine an effective porosity for each hydrogeologic unit, information about the bulk matrix porosity and residual saturation for each unit was required.

Given the depth ranges in each drillhole corresponding to each hydrogeologic unit, bulk matrix porosity data were retrieved from the NNWSI Tuff Data Base (TUFFDB, 1985). Bulk porosity data exist for samples collected from only four drillholes--identified as UE-25a#1 (Spengler et al., 1979), USW G1 (Spengler et al., 1981), USW G-4 (Spengler and Chornack, 1984), and USW GU-3 (Scott and Castellanos, 1984). The listing of all bulk porosity data obtained from the Tuff Data Base (TUFFDB, 1985) is presented in Appendix B-1. All porosity measurements are traceable to published NNWSI documents through version 11002 of the TUFFDB. Means and standard deviations of the available porosity values were then calculated for each hydrogeologic unit. A histogram of available porosity measurements for each unit is shown in Figure 5, with a superimposed theoretical curve derived from the calculated mean and standard deviation for a normal distribution.

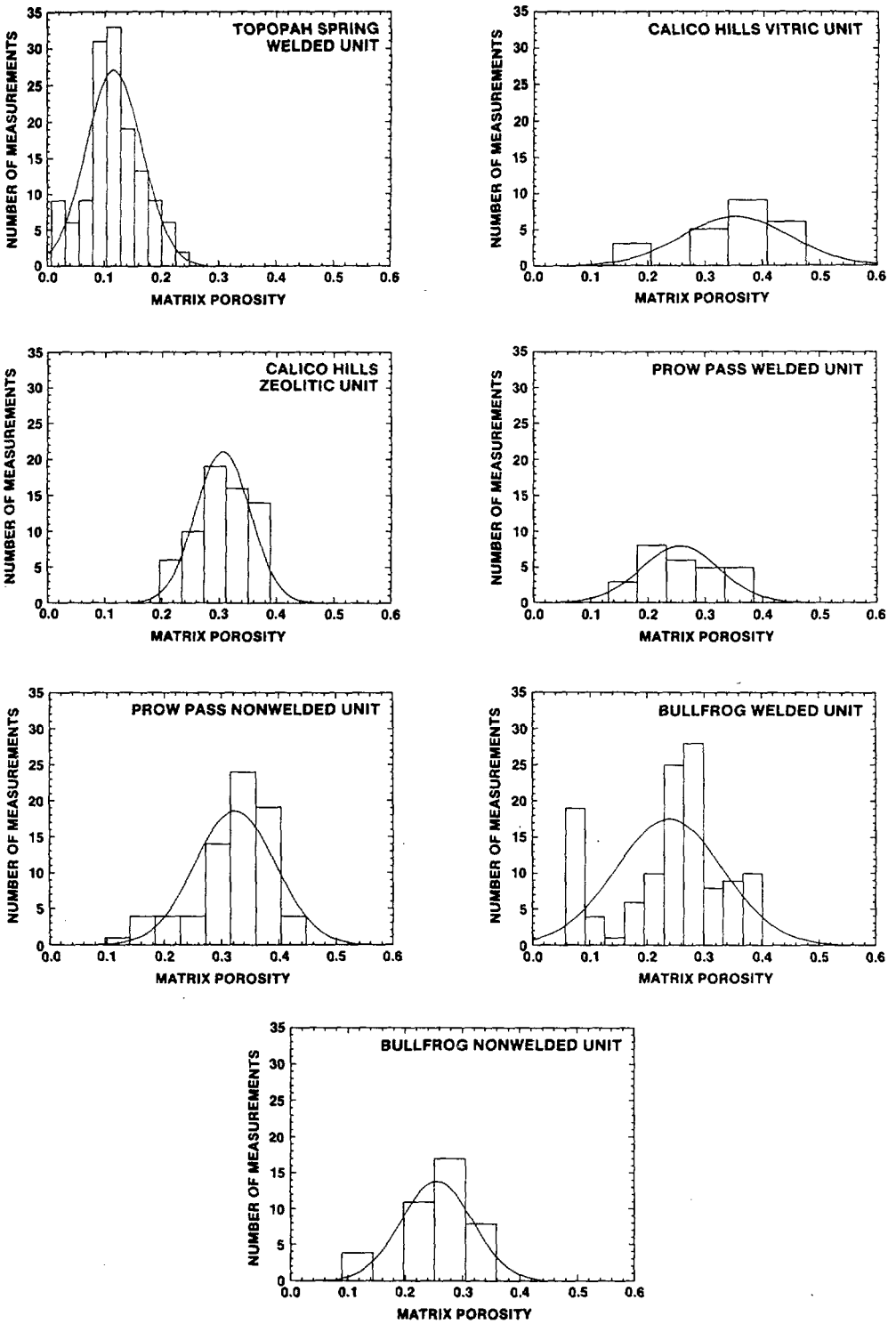

Figure 5. Histograms of bulk matrix porosity for each hydrogeologic unit and their normal distribution curves. These were derived from the calculated means and standard deviations of the sample population represented by the histograms.

Residual saturation values were obtained by Peters et al. (1984) for samples collected from drillholes USW G-4 (Spengler et al., 1984) and USW GU-3 (Scott and Castellanos, 1984). These data were designated for the hydrogeological units based on the depth from which the samples were taken. Given the means of the residual saturation, $\bar{S}_r$, the effective porosity, n_e, were calculated for each sample in each unit by

$$n_e = (1 - \bar{S}_r)\, n_b \quad . \tag{16}$$

The means and standard deviations of effective porosity were then estimated by using the population of samples in each hydrogeologic unit. The data for n_b and S_r, which were used for performing the calculations, are given in Appendix B. The results of these calculations are presented in Table 1.

Few estimated values for effective fracture porosity are available; however, a constant value of 0.0001 was chosen for use in our calculations based on the discussions in Sinnock et al. (1984).

2.2.3 Saturated Matrix Hydraulic Conductivity

Saturated matrix hydraulic conductivity (K_s) data were obtained from Tuff Data Base (TUFFDB, 1985), and Peters et al. (1984). The

drillholes for which data exist are UE-25a#1, USW G-4, and USW GU-3. The available conductivity measurements were grouped by hydrogeologic units (see Appendix B-2). Assuming that a log-normal distribution characterizes the variability of hydraulic conductivity, for the means and standard deviations of the logarithms, conductivity values were calculated for each hydrogeologic unit. Histograms of the logarithms of the available measured values and superimposed theoretically normal distribution curves derived from the calculated means and standard deviations are shown in Figure 6. Table 1 lists the antilog of the mean of the logarithms and the antilog of one standard deviation added to or subtracted from the mean of the logarithms. Conductivity values were calculated in units of m/s for travel-time calculations, but were subsequently converted to mm/yr for presentation in Table 1 and Figure 6.

2.2.4 Brooks-Corey Exponent

For unsaturated materials, the effective porosity must be modified to account for the effects of saturation on the volume of pore space contributing to flow under partially saturated conditions (see Equation 8). One way to estimate the relative conductivity is to apply the power law expression for effective saturation, stated in Equation 5. Brooks and Corey (1966) show that the slope of the relative hydraulic conductivity curve, ε, is related to the slope, $-\lambda$, of the effective saturation curve as a function of pressure head, by the relationship $\varepsilon=3+(2/\lambda)$. The dependence of ε on the water-retention characteristics can be determined by fitting data as closely as possible to a straight line (with a slope of $-\lambda$) when the retention curve is plotted on a log-log

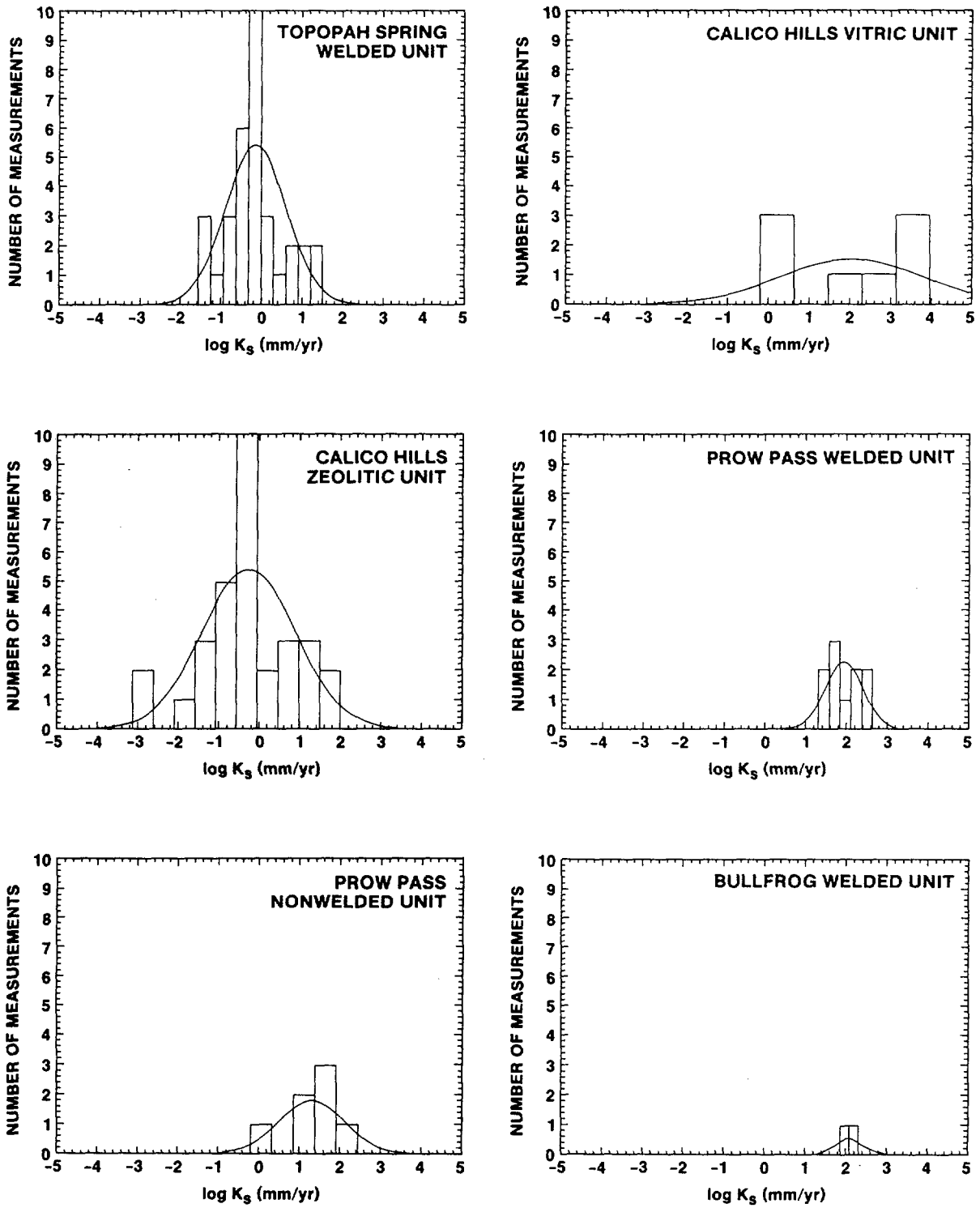

Figure 6. Histograms of the logarithm of saturated matrix hydraulic conductivity and the normal distribution curves. These were derived from the calculated mean and standard deviation of the log[K_S] of the sample population represented by the histograms.

scale. The Brooks-Corey exponent, ϵ, is treated here as a constant, and estimates of it are presented in Appendix B-3. The value, ϵ, for each hydrogeologic unit (see Table 1) was obtained by averaging the estimated ϵ values from the available water-retention curves within each unit.

2.2.5 Percolation Flux

As discussed in Section 2.1, episodic infiltration of surface-water is probably damped by the subsurface rock, and deep percolation is assumed to be in a steady-state condition through and below the waste-emplacement level. According to available information, a steady vertical flux of less than 0.5 mm/yr probably occurs beneath the underground facilities in the matrix of the Topopah Spring welded unit (Montazar et al., 1985; Wilson, 1985; Sinnock et al., 1985). Although no definite value of moisture flux in the Topopah Spring unit and below it has been established, several lines of evidence support an upper bound of 0.5 mm/yr (Wilson, 1985). For this report and for calculations summarized in the NNWSI Project EA, a constant value of 0.5 mm/yr is used as a baseline value for calculations of groundwater travel time. Values of 1.0 mm/yr and 0.1 mm/yr are also used in this report, thus providing a basis for performing a comparative analysis of the effects of flux.

2.3 Calculational Model of the Groundwater Travel-Time Distribution

As described in Section 2.1, unsaturated flow from the boundary of the disturbed zone to the water table may occur in any of the seven hydrologic units. Figure 7 illustrates the three-dimensional geometry of

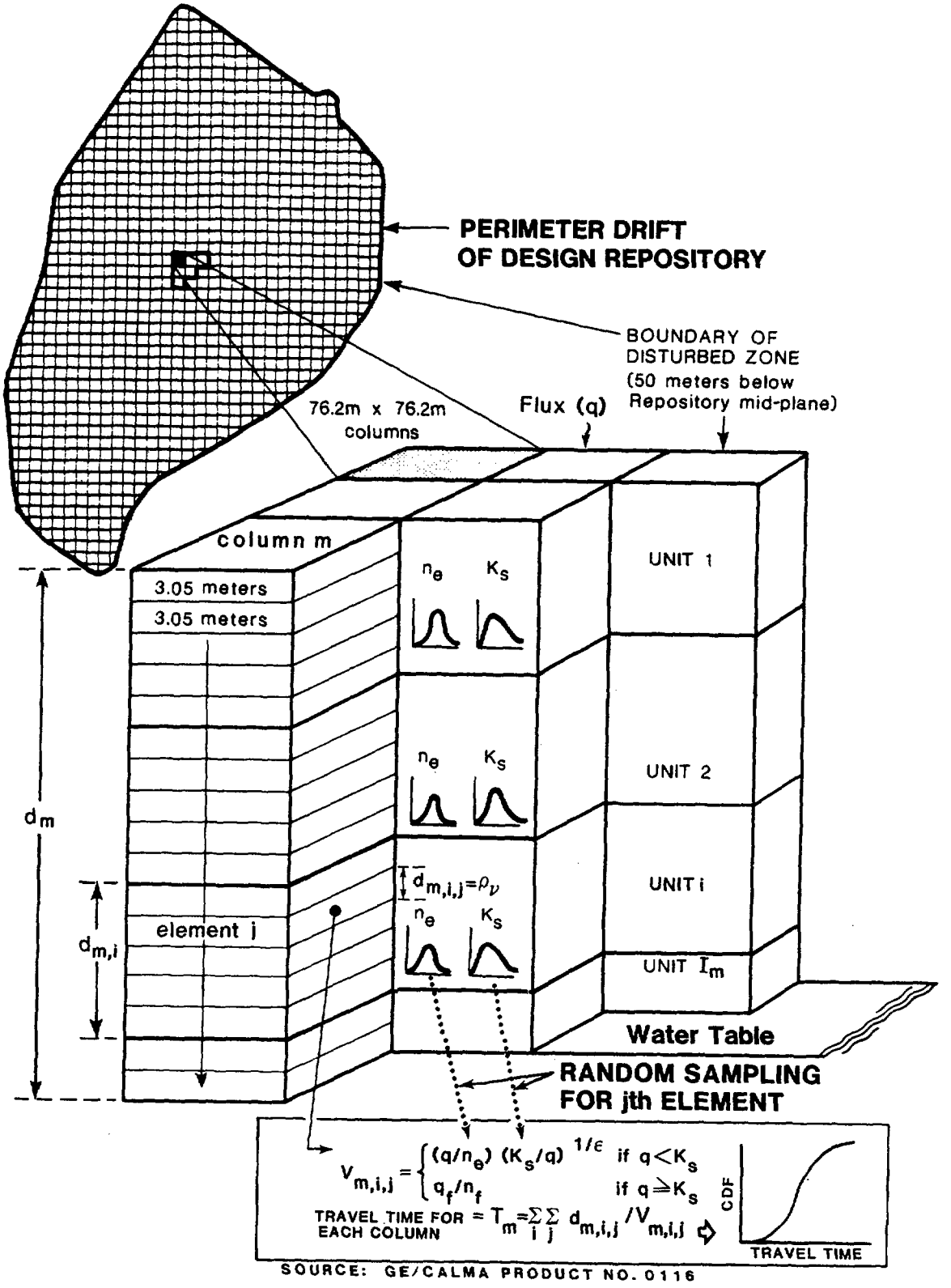

Figure 7. Schematic diagram showing the three-dimensional geometry for modeling groundwater travel time.

the unsaturated zone used in the Monte Carlo simulations of groundwater travel time. In the calculational model, ρ_h is assumed to be 250 ft, the horizontal dimension of the calculational grid shown in Figure 3. The unsaturated zone beneath the disturbed zone was divided into M (963 in the present model) columns of area, $(\rho_h)^2$, each with a vertical length, d_m, equal to the sum of the thickness of the hydrogeologic units that compose column m. The length, d_m, of column m is expressed as

$$d_m = \sum_{i=1}^{I_m} d_{m,i} \qquad (m) \ , \tag{17}$$

where I_m is the number of distinct hydrogeologic units in the column m, and $d_{m,i}$ is the thickness of each unit, i.

Assuming that the thickness of unit i in column m comprises $J_{m,i}$ elements (or slabs) of thickness ρ_v, where ρ_v is the vertical correlation length in unit i, then,

$$J_{m,i} \simeq \frac{d_{m,i}}{\rho_v} \ . \tag{18}$$

We ignore the fact that $d_{m,i}$ may not be an exact multiple of ρ_v. This approximation has little effect on results.

The spatial correlation length for the velocity variable (Equation 14) is related to hydrogeologic parameters such as flux, saturated

hydraulic conductivity, effective matrix porosity, and fracture properties; however, the correlation length for these properties are largely unknown for the tuff units at Yucca Mountain. Different values for the vertical correlation length, ρ_v, were assumed for calculating groundwater travel times in this report. The baseline case uses a vertical correlation length (the thickness of calculational elements) of 10 feet; each column for each hydrologic unit of thickness, $d_{m,i}$ (see Figure 7) was divided into many 10-foot-thick calculational elements (or slabs) for carrying out the calculations of the model. Other cases used different thicknesses for the calculational elements to simulate the vertical correlation length (1-, 50-, and 150-foot-thick slabs and, as a bounding case, the entire unit thickness). The last case (one calculational element per column per unit) is very conservative, because it is unlikely that many water-bearing fractures penetrate the entire thickness of any of the rock units. Longer correlation lengths tend to increase the variance of groundwater travel time and, therefore, tend to be more conservative. A value of 10 feet is assumed to be a baseline representation of the vertical correlation length. The time required for a water particle to travel through element j in unit i of column m is expressed by

$$T_{m,i,j} = \frac{\rho_v}{V_{m,i,j}} = \begin{cases} \dfrac{\rho_v n_e}{q}\left(\dfrac{q}{K_s}\right)^{1/\varepsilon} & \text{(yr)} \quad \text{if } q < K_s \\ \dfrac{\rho_v n_f}{q_f} & \text{(yr)} \quad \text{if } q \geq K_s \end{cases} \tag{19}$$

where the $V_{m,i,j}$ are the velocities of groundwater as computed according to Equation 14; these velocities are treated as independent, identically distributed random variables for each element j, unit i, and column m. $T_{m,i,j}$ are independent random variables with an identical probability density function for each parameter K_s and n_e, sampled within each unit.

The travel time through a unit of thickness $d_{m,i}$ is the sum of the travel times through each of the $J_{m,i}$ elements or slabs in column m; that is,

$$T_{m,i} = \sum_{j=1}^{J_{m,i}} T_{m,i,j} \quad \text{(yr)} . \tag{20}$$

The total travel time, T_m, through I_m units in column m, is the sum of the travel times through each of the I_m units, where

$$T_m = \sum_{i=1}^{I_m} \sum_{j=1}^{J_{m,i}} T_{m,i,j} \quad \text{(yr)} . \tag{21}$$

There are many ways of defining travel time, T, for the entire set of M columns. Because percolation flux is assumed to be uniformly distributed within the boundaries of the disturbed zone, every part of this cross-sectional area of M columns has an equal probability of experiencing the same water flux. Using a uniform weighting implies that each column is chosen at random with equal probability for our derivation

of the distribution of travel time. In this derivation a "realization" of total travel time consists of one set of sampling from K_s and n_e distributions for all of the m, i, and j variables. The distribution of total travel time, T, can be constructed from an ensemble of realizations of the travel time for all M columns, extending from the disturbed zone to the water table.

The mean value of T can be estimated as follows:

$$\bar{T} = \frac{1}{M \cdot R} \sum_{m=1}^{M} \sum_{r=1}^{R} T_m(r) \qquad (yr) \ , \tag{22}$$

where $T_m(r)$ is the r^{th} realization of T_m and R is the number of realizations. The population of $T_m(r)$ is obtained by direct simulation, using the Monte Carlo method.

For the case in which the vertical correlation length is equal to the thickness of the unit, $J_{m,i}$ is equal to 1, and Equation 21 reduces to

$$T_m = \sum_{i=1}^{I_m} T_{m,i} \qquad (yr) \ . \tag{23}$$

An estimate of the mean and variance of the travel-time distribution for the m^{th} column also may be derived analytically by assuming a very small vertical correlation length (i.e., $\rho_v << d_{m,i}$, so that $J_{m,i}$ is very large). Using this assumption and the central limit theorem, the

travel-time distribution through column m of the unsaturated zone can be shown to be approximately normal. The derivation of this analytical solution to travel-time parameters through column m is presented in Appendix A. In this report, however, we have exclusively used direct numerical simulation for calculating the total travel-time distribution and the mean and variance of T. Comparisons of the analytical solution with simulation results will be made in the future.

The algorithm for generating realizations of the travel time is now described for each calculational element. A value for saturated hydraulic conductivity, randomly selected from the appropriate unit-specified distribution in Table 1, is compared with the given value of flux. If the flux value is less than 95 percent of the saturated matrix conductivity, it is assumed that the flow within that element is entirely within the porous rock matrix. The ratio of 0.95 is used for comparing flux with saturated conductivity to account for potential initiation of fracture flow at saturations less than 100 percent. Next, a value of matrix effective porosity is randomly sampled from the appropriate distribution for the unit given in Table 1. The travel time of groundwater flow for each element is then calculated according to Equation 19.

If the ratio of flux to the randomly sampled value of saturated matrix hydraulic conductivity is equal to or greater than 95 percent of the flux, it is assumed that fracture flow occurs for that quantity of flux in excess of the value of saturated matrix conductivity. The travel

time of flow in fractures for that element is then calculated according to the second entry in Equation 19, whereupon a constant value for effective fracture porosity (0.0001) is used in our calculations. The portion of flux remaining in the matrix is used for obtaining a matrix-flow time for each element characterized by groundwater flow through fractures. However, in our model, only the faster one, either fracture-flow time or matrix-flow time, contributes to the travel time used for the element. This procedure is repeated for each vertical element within each hydrogeologic unit (in each of the 963 vertical columns) located between the disturbed zone and the water table. The sum of travel times for all vertical elements within a single column represents the total travel time along that column. As stated earlier, one may repeat this process R number of times, to accumulate R realizations of columnar travel time. Performing the calculations for each of the 963 columns, shown in Figure 7, accounts for the spatial variability of the thickness of the individual hydrogeologic units. A version of the computer code used to perform the calculations is listed in Appendix C.

2.4 Results

This section discusses results of selected groundwater travel-time calculations based on data provided in Section 2.2 and calculational methods described in Section 2.3. Results are presented in several formats including

- isochron contour maps that show the spatial distribution of travel times below the area occupied by underground facilities of the repository;
- histograms that show the number of flow paths (vertical columns in the calculational model, each 5806 m^2 in cross-section) characterized by travel times within certain ranges;
- curves of the cumulative distribution functions (CDF), or cumulative frequency distributions normalized to a total frequency of one, that show the fraction of flow paths with values less than a given value; and
- tables of means and standard deviations of sets of travel-time values for each of the units and the total of the units.

Results of a baseline case are described first, followed by a comparison of these results with travel-time distributions based on variations of selected model parameters. The baseline case is characterized by a set of model parameters that are considered to reflect the current hydrological conditions in the unsaturated zone at Yucca Mountain. Model parameters that are varied, which represent alternative cases, include values for the vertical correlation length, standard deviations of the logarithms of saturated matrix hydraulic conductivity, standard deviations of effective porosity, and the assumed flux through the unsaturated zone. Table 2 presents a summary of the model parameters used in this analysis. The purpose of these variations is to provide insight into the sensitivity of travel-time distributions to some of the assumptions upon which the modeling approach is based.

TABLE 2

Summary of Modeling Parameters

Model Parameters	Vertical Correlation Length ρ_v (ft)	Scaling Factor for $\sigma[\ln K_s]$	Scaling Factor for $\sigma[n_e]$	Flux q (mm/yr)
Case 1 (Baseline)	10	1	1	0.5
Case 2 (Variation on ρ_v)	1, 10, 50, 150, $d_{m,i}$*,+	1	1	0.5
Case 3 (Variation on flux)	10	1	1	0.1, 0.5, 1.0+
Case 4 (Variation on $\sigma[\ln K_s]$)	10	0.2, 1, 2+	1	0.5
Case 5 (Variation on $\sigma[n_e]$)	10	1	0.2, 1, 2+	0.5

* d_i represents the thickness of each hydrogeologic unit.
+ These represent the values that were used for the parametric analysis.

2.4.1 Case 1: The Baseline Case

The model parameters used for the baseline case are defined in the first row of Table 2. The results of groundwater travel-time distributions for the baseline case are shown in Figures 8 through 12, and Table 3. Figure 8 presents maps of travel-time contours for the region composed of 963 columns between the disturbed zone and the water table. Illustrations 8A through 8D present the average travel-time contours obtained for 1, 10, 50, and 100 realizations*, in which all other modeling parameters, as listed in Table 2, remain the same. Figure 8E shows the average travel-time contours calculated by using only mean values for hydraulic conductivity and effective porosity for each hydrogeologic unit. Figures 9A and 9B show contours representing the standard deviations of travel time and the percentage of each column characterized by fracture flow. Figure 10 shows the cumulative distribution curves of travel time based on 1, 10, 50, and 100 realizations. Also shown is a curve derived by using mean values of affective porosity and hydraulic conductivity. Figure 11A provides a histogram of total travel times based on 10 realizations. Figure 11B presents the corresponding cumulative distribution curves for the total travel times and for each of the seven hydrogeologic units. Table 3 shows the means and standard deviations of the travel-time distributions for each of the units and for the total unsaturated area below the

*For more than one realization, the travel-time contours are based on the arithmetic means of the multiple travel-times calculated for each column.

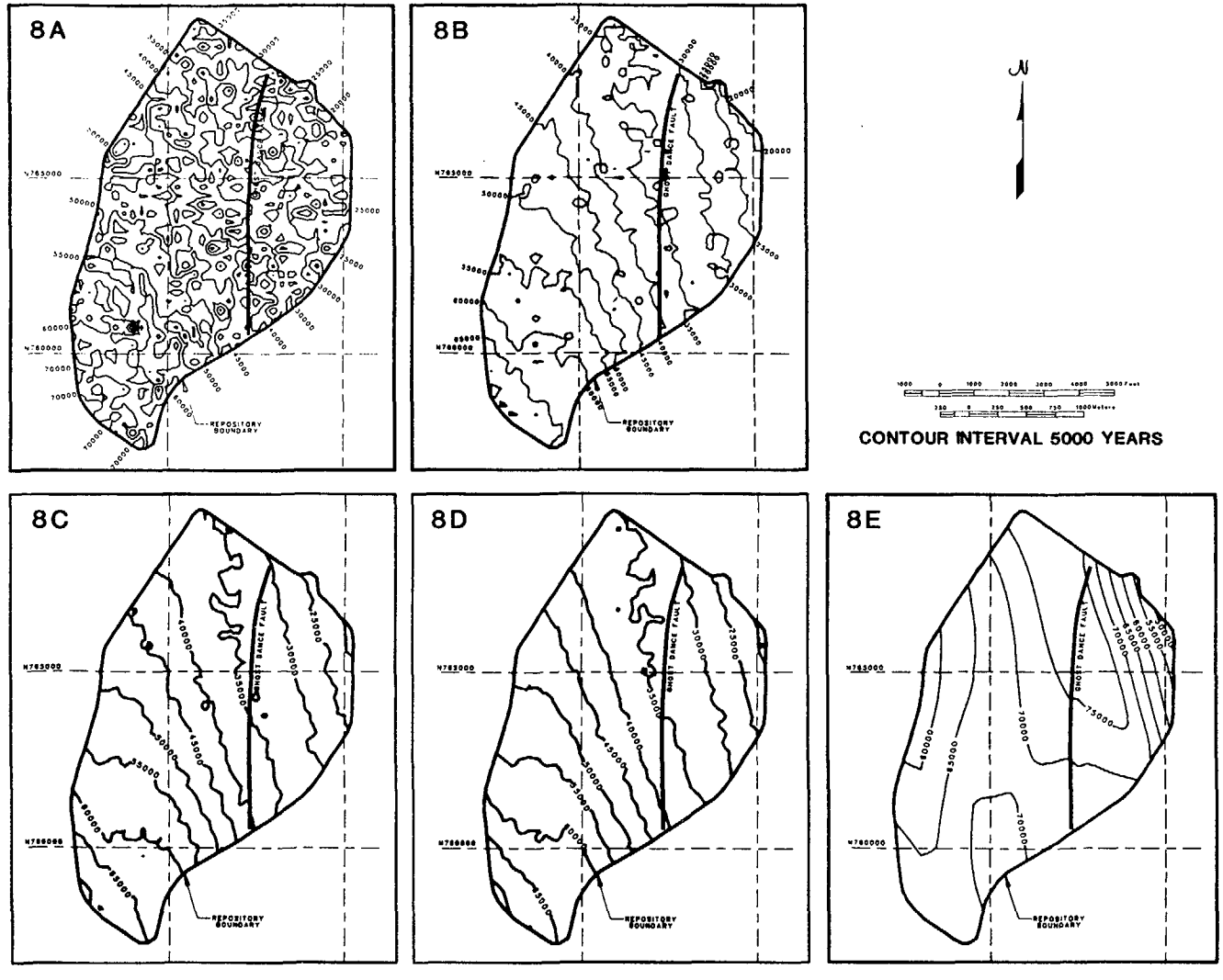

SOURCE: GE/CALMA PRODUCT NOS. 0042, 0082, 0107, 0108, 0109

Figures 8A to 8E. Contour maps of average travel times from the disturbed zone to water table based on (A) 1 realization, (B) 10 realizations, (C) 50 realizations, (D) 100 realizations, and (E) using mean values of effective porosity and hydraulic conductivity for each unit.

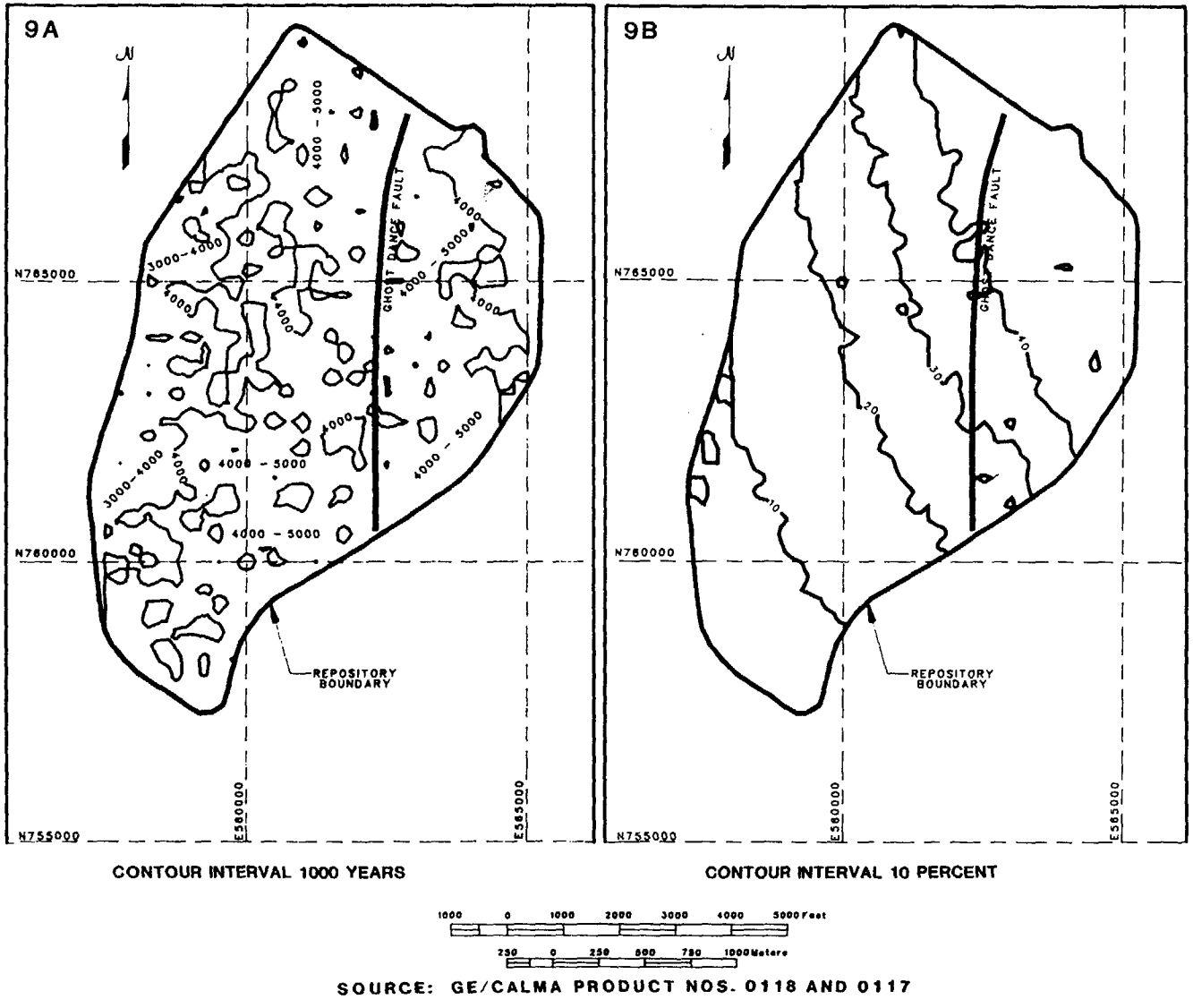

Figures 9A and B. Contour maps of (A) the standard deviation of the travel-times, and (B) percentages of vertical distance characterized by fracture flow, for flux of 0.5 mm/yr using 10-foot-thick calculational elements.

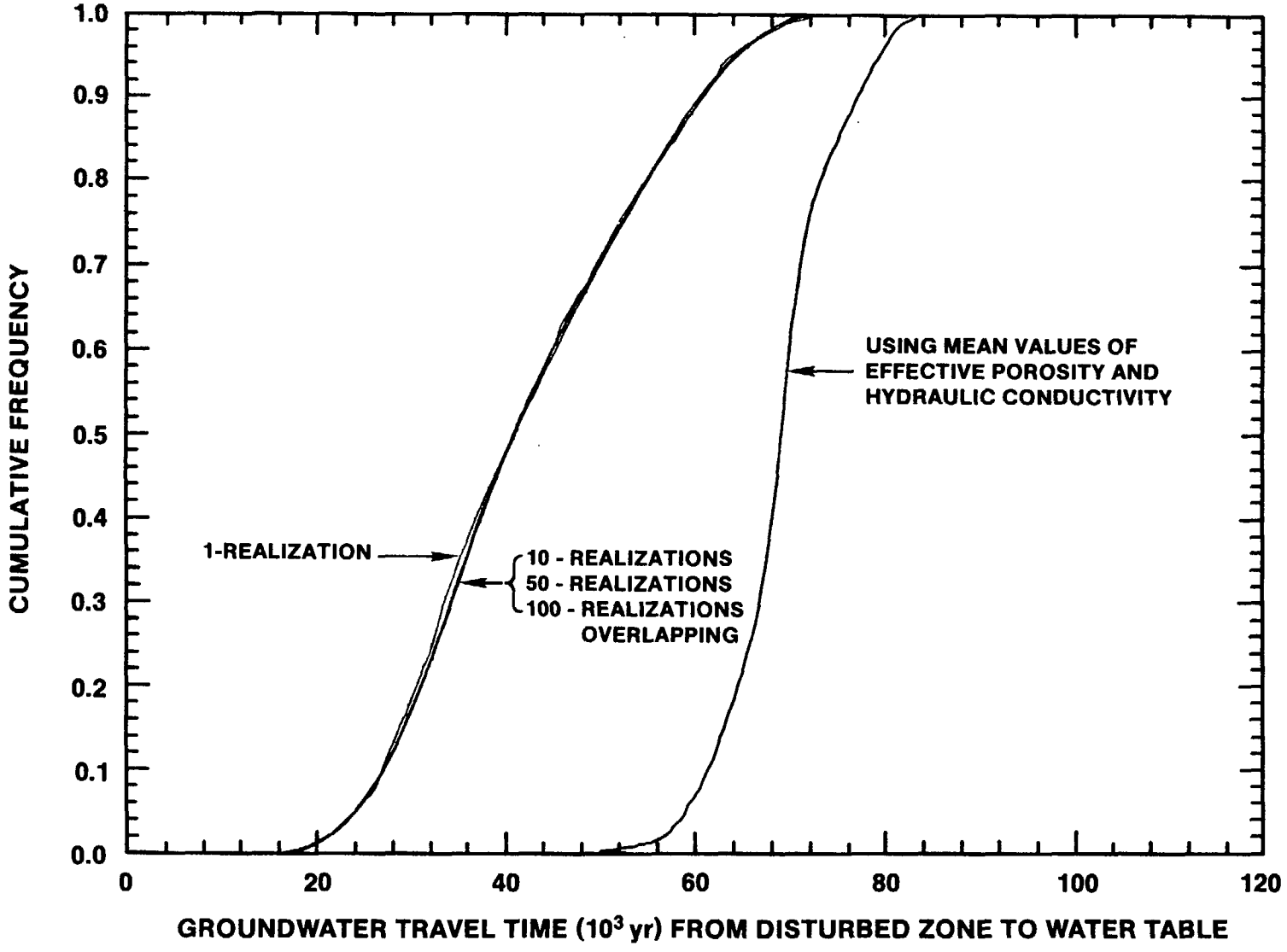

Figure 10. Cummulative distribution curves for 1, 10, 50, and 100 realizations based on randomly selected values Ks and ne and a deterministic curve based on mean values of affective porosity and hydraulic conductivity, for a flux of 0.5 mm/yr using 10-foot-thick calculational elements.

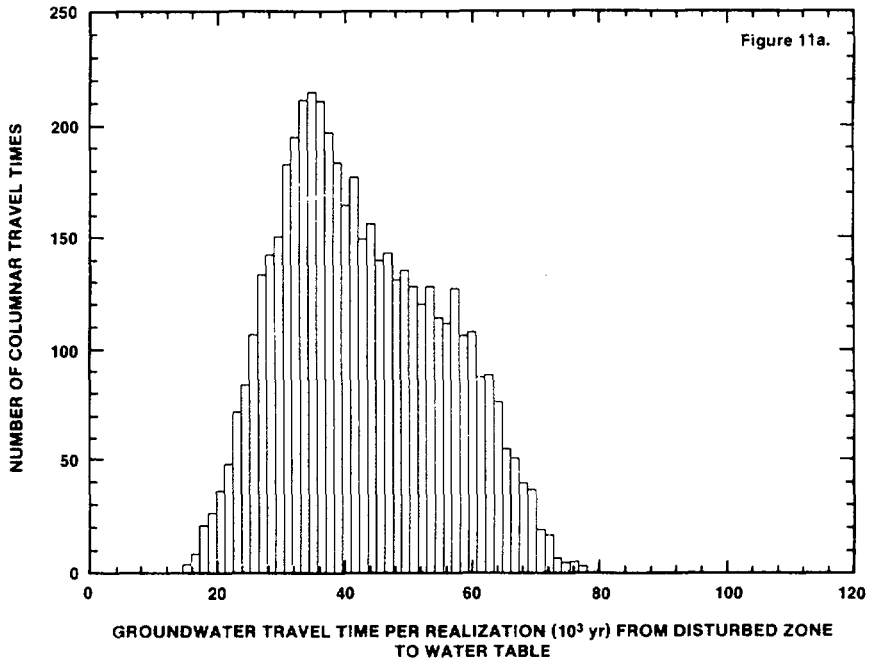

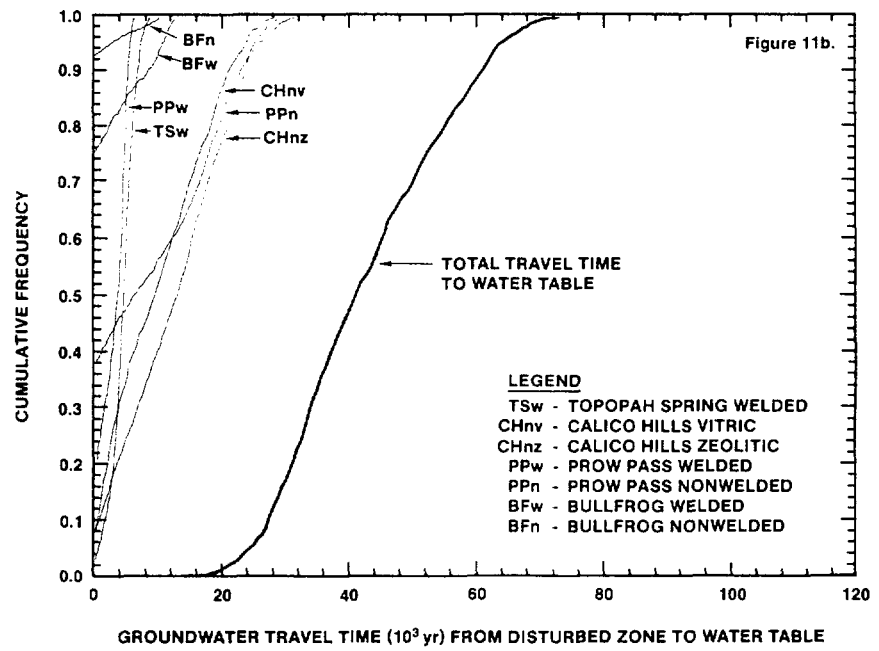

Figures 11A and B. Plots of travel-time distributions based on a flux of 0.5 mm/yr based on 10 realizations using 10-foot-thick calculational elements. (A) Histogram of total travel-time distributions. (B) Cumulative distribution curves for each of the units and the total unsaturated zone. The zero travel-time intercepts for individual hydrogeologic units correspond to the percentage of the repository area not underlain by the unsaturated portions of the units.

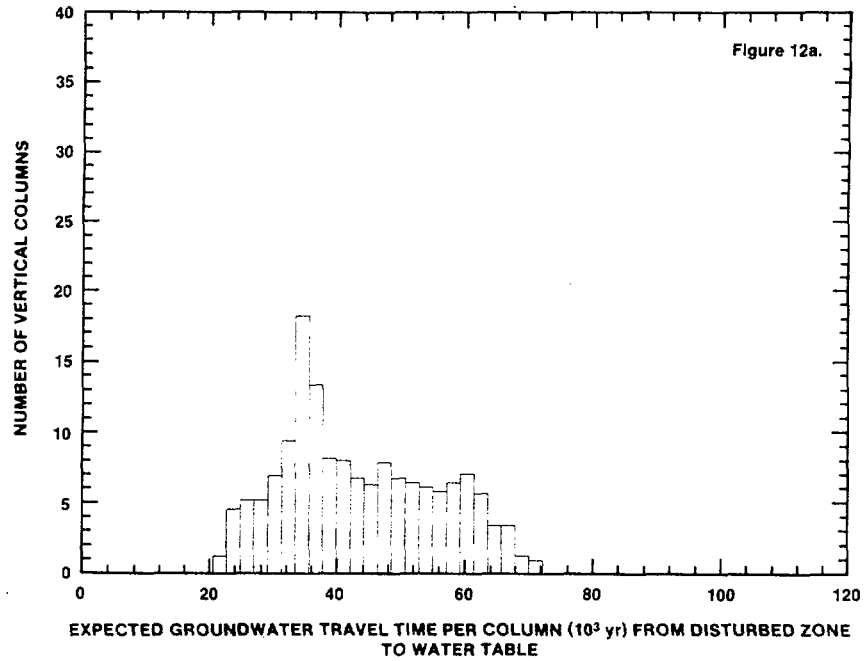

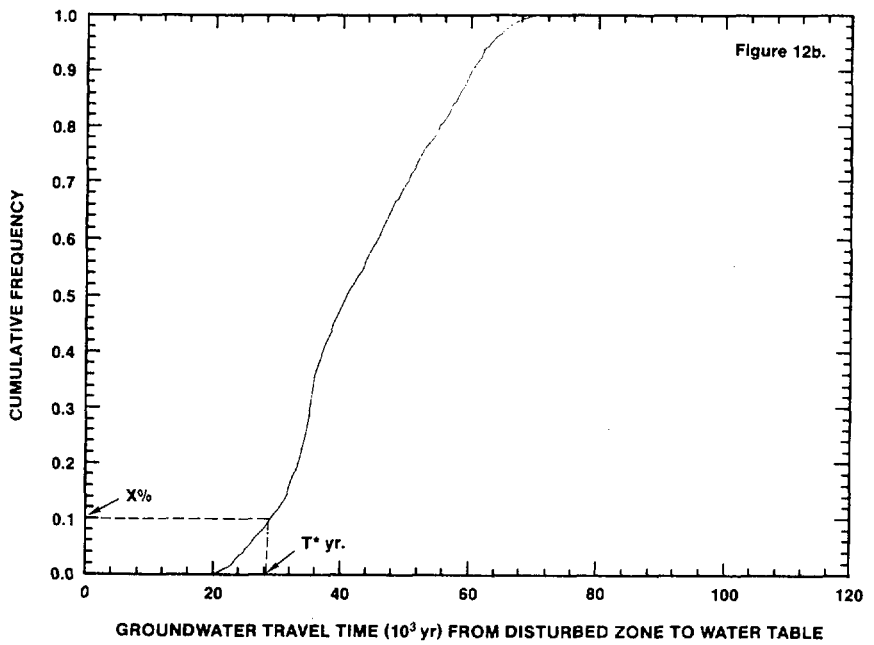

Figures 12A and B. Plots of expected travel-time distributions for a flux of 0.5 mm/yr based on 100 realizations using 10-foot-thick calculational elements. (A) Histogram of the 963 expected values of travel time through each column. (B) Empirical cumulative distribution curve showing x percentiles of flow paths having an average travel time less than some specified value, T*.

TABLE 3

Summary of Travel-Time Values for a Flux of 0.5 mm/yr Based on 10 Realizations and Using 10-Foot-Thick Calculational Elements

Unit	Percentage of Total Repository Area Underlain by the Unit	Mean (yrs)	Standard Deviation (yrs)
Topopah Spring Welded Unit	98.5	4,765	1,920
Calico Hills Vitric Unit	95.3	11,000	7,760
Calico Hills Zeolitized Unit	94.5	13,695	8,145
Prow Pass Welded Unit	83.2	3,915	1,710
Prow Pass Nonwelded Unit	63.1	15,020	8,025
Bullfrog Welded Unit	25.6	6,800	4,085
Bullfrog Nonwelded Unit	7.5	5,445	3,525
Total*		43,265	12,765

*Estimates are for the entire unsaturated zone underlying the disturbed zone.

disturbed zone. Figure 12 shows a histogram of the 963 expected values of travel time corresponding to each of the 963 columns and their cumulative distribution curve based on 100 realizations. Each of the figures will be discussed in the following paragraphs.

The boundaries of the plotted contours on Figures 8A to 8E correspond to the location of the outer perimeter drift of the repository.* The contour maps were generated on the Interactive Graphics and Information Systems (GE/CALMA, Product Nos. CAL0044 (1985) and, CAL0082, CAL0107, CAL0108, and

*The perimeter drift of the repository has been defined as shown in a design drawing by Parsons, Brinkerhoff, Quade, and Douglas, (PBQ&D, 1985; GE/CALMA, 1986, Product No. 0119) an architectural-engineering firm on contract to Sandia to provide a conceptual design of underground facilities for use in the forthcoming NNWSI project Site Characterization Plan.

CAL0109, 1986), which plotted travel times as z values on the GTM of the site (Figure 3). The travel-time values were obtained from the output files of a version of the computer code listed in Appendix C.

Based on the patterns of the contours on Figures 8A to 8E, two overriding conclusions are apparent, as follows: (1) that average travel times increase in a southwesterly direction, from a minimum of about 20,000 years, along the eastern edge of the emplacement area, to a maximum of about 70,000 years in its southwest corner because of the increase in the thickness of the unsaturated rockmass (compare Figures 8A to 8E and 4A to 4H); and (2) that multiple realizations are required for good estimates of the expected values of the columnar travel-time distributions, as evidenced by the smoothing of the contour lines as the number of realizations increase. The irregularity of travel-time contours is most pronounced for a small number of realizations. This can be interpreted as an approximation to the general spatial patterns of actual travel-times caused by the distribution of the hydrogeological properties. However, averaging the values of multiple realizations, for each column, yields a better statistical approximation of the expected values for groundwater travel-time. A comparison of the total travel-time contours obtained for 1, 10, 50, and 100 realizations indicates that increasing the number of realizations reduces the irregularities of average travel-time contours. With a sufficient number of realizations (Figure 8D) the contour lines become fairly smooth, resulting in a close approximation to the expected values. Ten realizations, shown in Figure 8B, were used to illustrate this method for calculating groundwater travel time in the NNWSI EA (DOE, 1986).

time of flow in fractures for that element is then calculated according to the second entry in Equation 19, whereupon a constant value for effective fracture porosity (0.0001) is used in our calculations. The portion of flux remaining in the matrix is used for obtaining a matrix-flow time for each element characterized by groundwater flow through fractures. However, in our model, only the faster one, either fracture-flow time or matrix-flow time, contributes to the travel time used for the element. This procedure is repeated for each vertical element within each hydrogeologic unit (in each of the 963 vertical columns) located between the disturbed zone and the water table. The sum of travel times for all vertical elements within a single column represents the total travel time along that column. As stated earlier, one may repeat this process R number of times, to accumulate R realizations of columnar travel time. Performing the calculations for each of the 963 columns, shown in Figure 7, accounts for the spatial variability of the thickness of the individual hydrogeologic units. A version of the computer code used to perform the calculations is listed in Appendix C.

2.4 Results

This section discusses results of selected groundwater travel-time calculations based on data provided in Section 2.2 and calculational methods described in Section 2.3. Results are presented in several formats including

Please replace page 44 in SAND85-2701, "Preliminary Estimates of Groundwater Travel Time and Radionuclide Transport at the Yucca Mountain Repository Site," by Y.T. Lin et al. with attached new page 44. Thank you.

It is interesting to note that the expected values for travel-time, based on many realizations using random sampling of hydrogeologic parameters, are not the same as those derived by using mean properties in a single deterministic calculation. Figure 8E shows a plot of travel-time contours based solely on mean values for the saturated matrix conductivity and effective porosity as listed in Table 1; other parameters defined in Table 1 remain the same. The difference in patterns is, in part, caused by the effects of using a 10-foot vertical correlation length, which provides a large sampling set of hydraulic conductivity values for the elements in each column. Thus, the sampled properties (K_s, when compared to the assumed constant flux) will result in fracture flow through only some calculational elements for a given column, and there is a limited probability for simulated fracture flow to propagate through many elements (slabs) in the column (Figure 9B). Using only mean hydraulic properties in the calculations ensures that no fracture flow is simulated in any unit, because mean values of hydraulic conductivity (see Table 1) are greater than the assumed constant value of flux of 0.5 mm/yr.

The random sampling of hydraulic properties also produces a variance of the travel-time distribution that includes the effects of the variability of the thickness of the units, as related to the properties of fracture flow in different units, as well as the variability of the hydraulic parameters of the units. Figure 9A shows a contour plot of standard deviations of the columnar travel times. The standard deviations are fairly constant and are generally less than 5,000 years. Figure 9B shows the contours for the percentage fracture flow occurring in the elements through each column. A comparison of Figures 8D and 8E

with Figures 9B and 4A indicates that the changes in travel time from column to column are largely due to the changes in the percentage of fracture flow and to the total thickness of the unsaturated material below the disturbed zone.

Figure 10 shows the cumulative distribution curves based on 1, 10, 50, and 100 realizations using randomly selected values of K_s and n_e. Also shown is a curve derived by using mean values of effective porosity and hydraulic conductivity. These figures were generated from the same data files of travel-time values used to produce the contour maps in Figures 8A to 8E. The empirical cumulative distribution curves show little variation after 10 or more realizations because each realization consists of 963 columnar travel times. This suggests that only a few realizations are sufficient for obtaining a reasonable approximation of the cumulative distribution curve for expected travel times.

Figures 11A and 11B show travel-time distributions in other formats. The histogram (Figure 11A) approximates a probability density function (PDF) of the total travel time, and the cumulative frequency distributions (Figure 11B) illustrate the fraction of travel-time values contributed by individual hydrogeologic units. The minimum and maximum values of such a histogram (i.e., plotting columnar travel time values from all realizations) would extend to zero and infinity, respectively, as the number of realizations approaches infinity. Therefore, the minimum and maximum values from this type of histogram do not represent the range of expected groundwater travel times. Rather, the mean values and multiples of the standard deviations are a better indication of the

range of expected travel times and the reliability of these estimates. Table 3 lists estimates of the means and standard deviations of travel time for each hydrogeologic unit, as well as for the total travel-time. The relatively small values for standard deviations indicate the level of precision possible for estimates of the expected values for groundwater travel times, given the assumption of our model.

Figure 12A provides a histogram of the expected values for travel time through each of 963 columns based on 100 realizations. In this case, it is correct to state that the expected travel times for flow through the unsaturated zone are bounded by a minimum of about 20,000 years and a maximum of about 70,000 years. Note the different shapes and ranges of the histograms and the cumulative distribution curves on Figures 11 and 12. Given a decision-basis value, T*, for the groundwater travel time objective (NRC, 1983) as illustrated in Figure 12B, the fraction of paths having an average travel time less than T* can be identified. Granting the limitations of the modeling assumptions, the groundwater travel-time values represented by Figure 12 indicate a very high likelihood that groundwater travel time from the disturbed zone to the water table at Yucca Mountain will exceed 10,000 years. These results may also provide a rationale based solely on groundwater travel time for an assessment and demonstration of compliance with the EPA requirements for the control of radioactive releases entering the accessible environment. The results shown in Figure 12 can be interpreted as being representative of the fastest paths of likely radionuclide travel from the disturbed zone to the water table on the basis of the present conceptual model. Thus, groundwater travel time

through the unsaturated zone at Yucca Mountain may be adequate to show, with reasonable confidence, that no radionuclides will reach the accessible environment prior to 10,000 years, the time period stipulated for controlled releases by EPA Standards.

Figures 8 to 12 and Table 3 strongly suggest that the requirements for 1,000 years of groundwater travel time from the disturbed zone to the accessible environment can be met solely by flow time within several of the individual hydrogeologic units of the unsaturated zone beneath the disturbed zone at Yucca Mountain. In addition, the total travel times through the unsaturated zone may be sufficient to demonstrate compliance with EPA requirements with regard to the control of radionuclide releases for 10,000 years [(Figure 11B)]. Therefore, such demonstrations may also be based reliably, in a large part, on the estimates of groundwater travel time through the unsaturated zone. The assumptions used in our current analysis are subject to refinement as more data become available and as conceptual understanding of unsaturated flow behavior is improved. Future refinements will occur, particularly in the understanding of the relationships between matrix flow and fracture flow, and the related potential for concentrations of flow by lateral diversion and infiltration pulses.

2.4.2 Case 2: Variations on the Vertical Correlation Length

The implicit vertical correlation length (10 feet) of the baseline case is much less than the thickness of any of the hydrogeologic units (see Figure 4). This results in a large number of independent random

variables (travel times through each of the calculational elements), which are added together to obtain a travel time through a column. Consequently, there is low probability that fracture flow ($q \geq K_s$) will occur through a large number of elements in any single column from the disturbed zone to water table.

To investigate the effects of correlation length on the travel-time distribution, various vertical thicknesses of calculation elements (implicit vertical correlation lengths of 1-, 10-, 50-, 150-ft elements, and for one element equal to the thickness of each unit) were assumed. The model parameters used for this case are defined in Table 2. The calculations of travel time were done in exactly the same way as those for the baseline case, except for the use of different thicknesses for each calculational element.

The resulting cumulative distribution curves for total travel times are plotted in Figure 13. Figure 13 indicates that the variance in the total travel time increases with increases in the correlation length (this observation is analytically derived for a single column in Appendix A). Longer correlation lengths affect the travel-time distribution, especially at the tail ends of the distribution, because of the increasing probability of fracture flow through a significant number of elements that make up each of the columns. Even if the vertical correlation length is assumed to be at least as great as the thickness of each unit (the upper-bound case, $\rho_v = d_{m,i}$), the cumulative distribution is less than 2 percent for a travel time of less than 1,000 years (Figure 13). These results indicate high sensitivity of the travel-

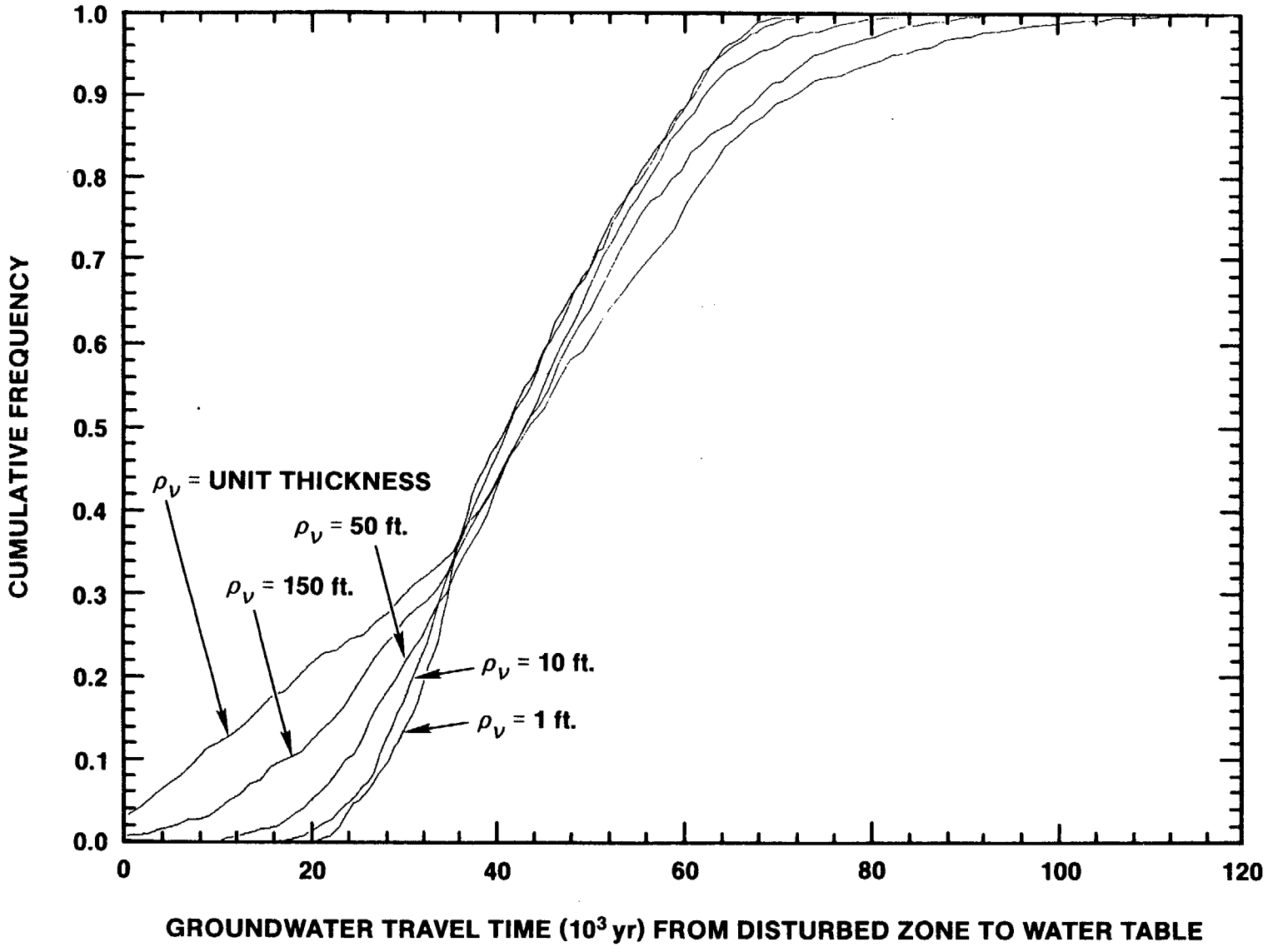

Figure 13. Effects of the thickness of calculated elements (or vertical correlation length) on travel-time distributions based on 1 realization for a flux of 0.5 mm/yr.

time distribution to the, as yet, undetermined correlation length for velocity in each hydrogeologic unit. The bounding case of $\rho_v = d_{m,i}$ may be used with no knowledge of the correlation length, and it is physically improbable. Nevertheless, it may be used for estimating travel times that could occur along structural features where fracture flow might be sustained throughout the entire thickness of a given hydrogeologic unit. Generally, the sensitivity of the travel times to the correlation lengths suggests how prudent it is to perform a carefully designed testing program for determining the correlation length of all key parameters influencing flow velocities.

Because of the uncertainty about the data used in calculations of pre-waste-emplacement groundwater travel time, the effects of variability in flux, saturated matrix hydraulic conductivity, and effective porosity were investigated to gain some insight into the sensitivity of the travel time to these parameters. The following three subsections treat variations based on each of the hydrogeologic parameters.

2.4.3 Case 3: Variations on the Flux

A reasonable and conservative estimate of the upper-bound on flux of 0.5 mm/yr (Wilson, 1985) was used for the baseline-case travel-time calculations. A value twice that of this upper bound is probably an unrealistically high estimate of flux. Nevertheless, a histogram of associated travel times (Figure 14) suggests that the 1,000-year requirement would be satisfied even under a flux value of 1 mm/yr. The

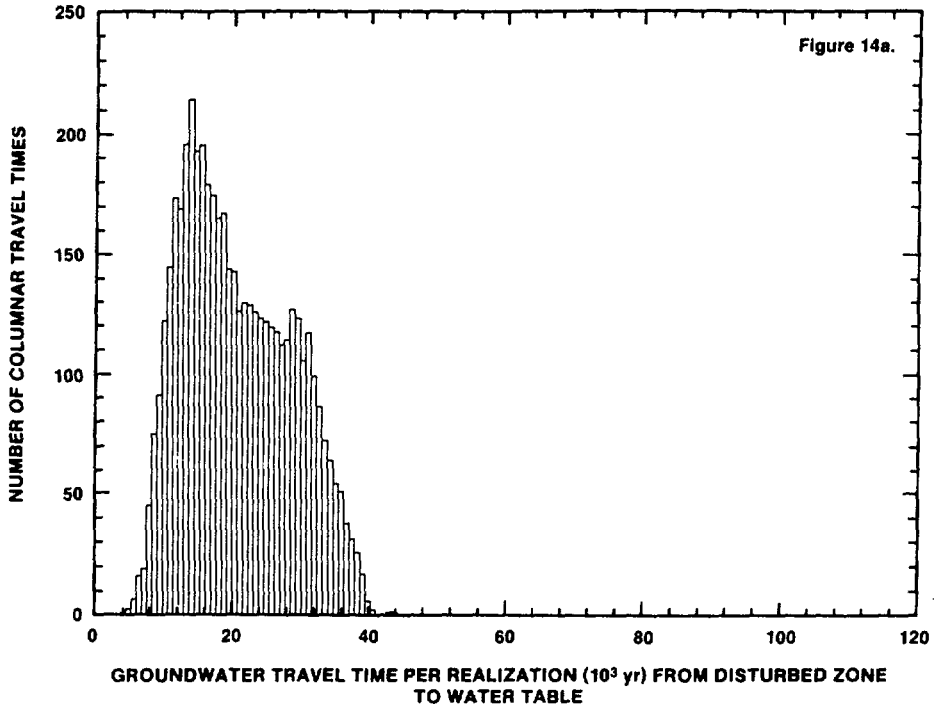

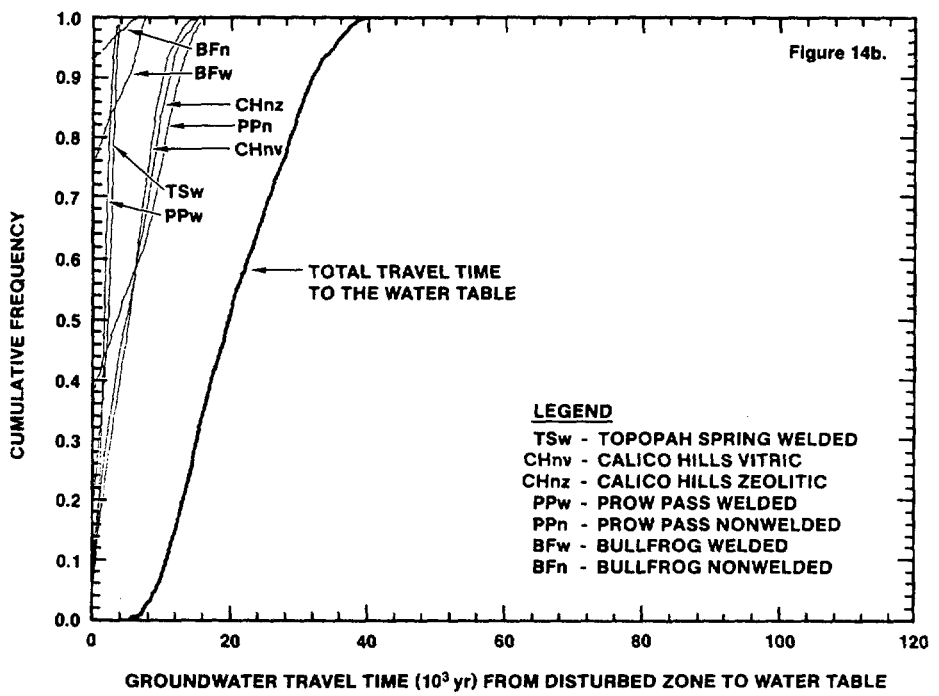

Figures 14A and B. Plots of travel-time distributions for a flux of 1.0 mm/yr based on 10 realizations using 10-foot- thick calculational elements. (A) Histogram of total travel times. (B) Cumulative distribution curves for each of the units and the total unsaturated zone. The zero travel-time intercepts for individual hydrogeologic units correspond to the percent of the repository area not underlain by the unsaturated portions of the units.

histogram in Figure 14 is the conservative (see discussion in Section 2.4.1) frequency plot of all 9630 travel times from 10 realizations (i.e., 10 realizations of 963 columns).

Figure 15 shows the travel-time distributions obtained for flux values of 0.1, 0.5, and 1.0 mm/yr where all other modeling parameters listed in Table 1 are retained. A value of flux of 0.1 mm/yr or less is consistent with available data on hydraulic properties of the rock matrix and observed field conditions of moisture tension and saturation (Peters et al., 1985; Sinnock et al., 1984; Montazer and Wilson, 1985; and Weeks and Wilson, 1984). The cumulative distribution functions provide a means of interpreting, probabilistically, whether the 1,000-year travel-time requirement would be satisfied. Figure 15 indicates that a very small proportion of flow paths have a travel time of less than 10,000 years for a flux value of 0.1 mm/yr. On the other hand, a substantial proportion of flow paths have a travel time of less than 10,000 years for a flux value of 1 mm/yr. This indicates that according to the present model, the travel-time distribution is very sensitive to the percolation flux, and that site characterization activities that reduce the uncertainty about the flux from the repository level downward would be very useful.

2.4.4 Case 4: Variations on the Saturated Hydraulic Conductivity

The effects of the range of variability of saturated matrix hydraulic conductivity within each hydrogeologic unit was examined by varying the standard deviations of the natural logarithm of the baseline conductivity values given in Table 1. Results, based on scaling factors of 0.2

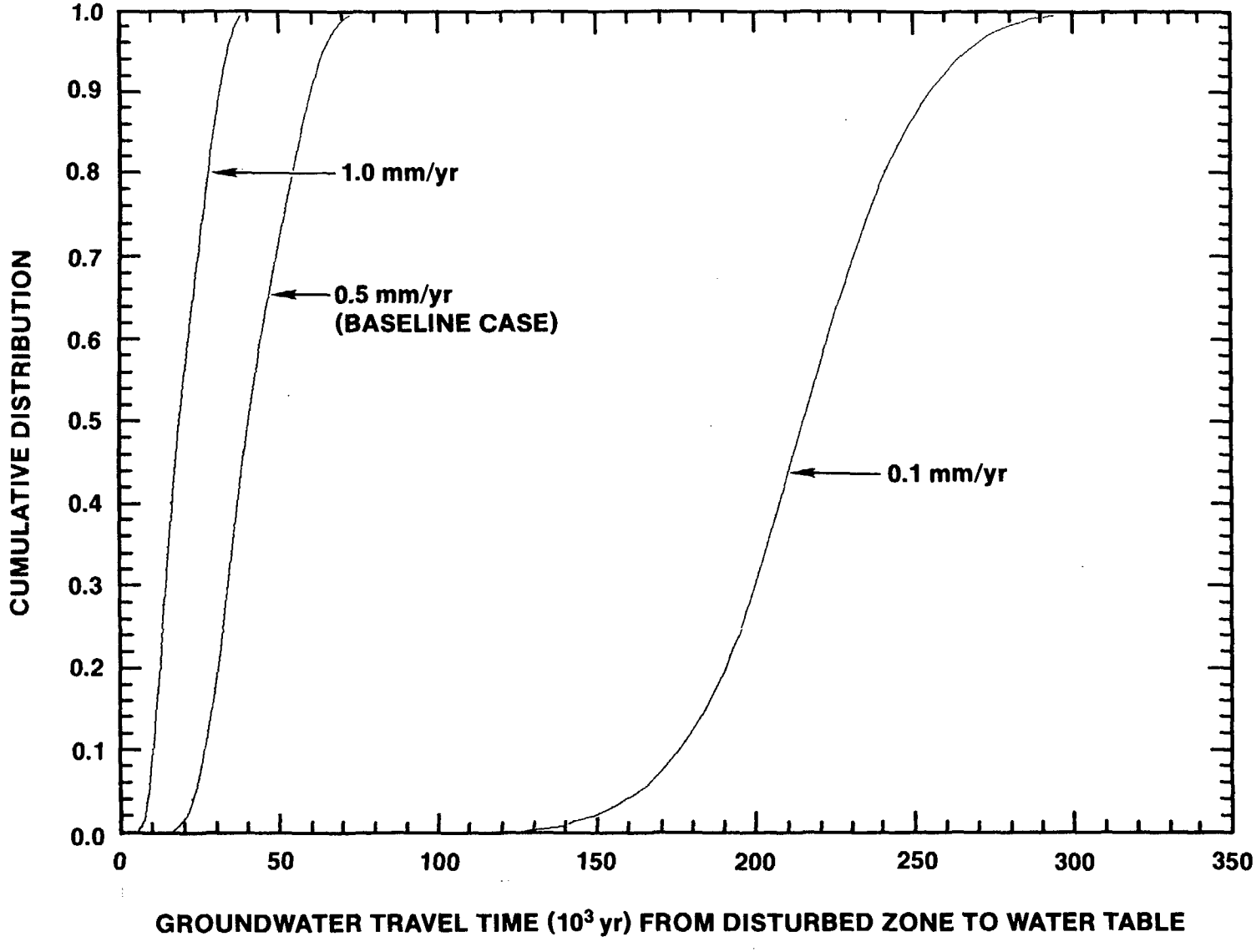

Figure 15. Effects of various flux values on travel time. Cumulative probability density curves for a flux of 0.1, 0.5, and 1.0 mm/yr based on 10 realizations using 10-foot-thick calculational elements.

and 2.0 for the standard deviation are illustrated in Figure 16. This figure shows that the travel times are quite sensitive to variations of standard deviations of saturated matrix hydraulic conductivity, though not as sensitive as the range of travel-time values are to variations in mean value of flux (Figure 15) or correlation lengths (Figure 13). Uncertainty about the standard deviations of $\ln(K_s)$ affects the mean and variance of the travel-time distribution. Therefore, it is important to obtain a good estimate of saturated matrix hydraulic conductivity for each hydrogeologic unit because the lower end of the CDF is sensitive to the uncertainty in K_s, which governs the assumptions about fracture flow ($q \geq K_s$).

2.4.5 Case 5: Variations on the Effective Porosity

The variation of effective matrix porosity within each hydrogeologic unit apparently has less effect on travel time than do the variations of other parameters (Figure 17). This is because the matrix porosities for individual hydrogeologic units have relatively small standard deviations, and because the matrix porosities are so much larger than fracture porosities. Figure 17 shows that the effect of changing the standard deviations of the matrix porosity is the least sensitive of the effects presented in these variations in hydrogeologic parameters. Varying the effective matrix porosity affects only the matrix flow, though such flow contributes to the bulk of travel time in any given column. Uncertainties about the effective fracture porosity values may affect the estimates at the low end of the travel-time distribution. The apparent lack of sensitivity to matrix porosity values should not act as a

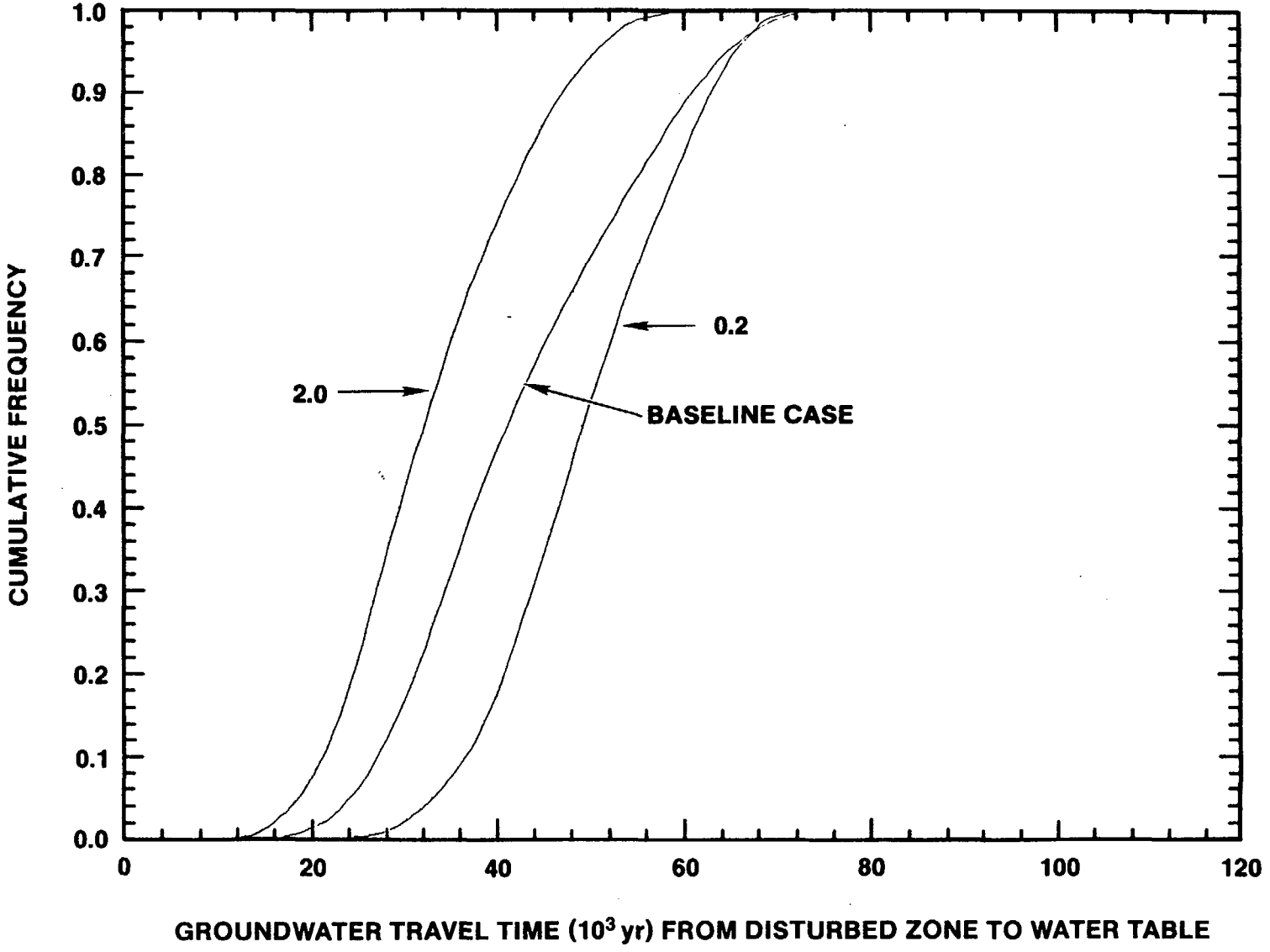

Figure 16. Effects of variations of the standard deviation of saturated hydraulic conductivity. Travel-time cumulative probability density curves are shown for values of the standard deviations of ln K_S scaled at 0.2, 1.0, and 2.0 times that of the baseline case.

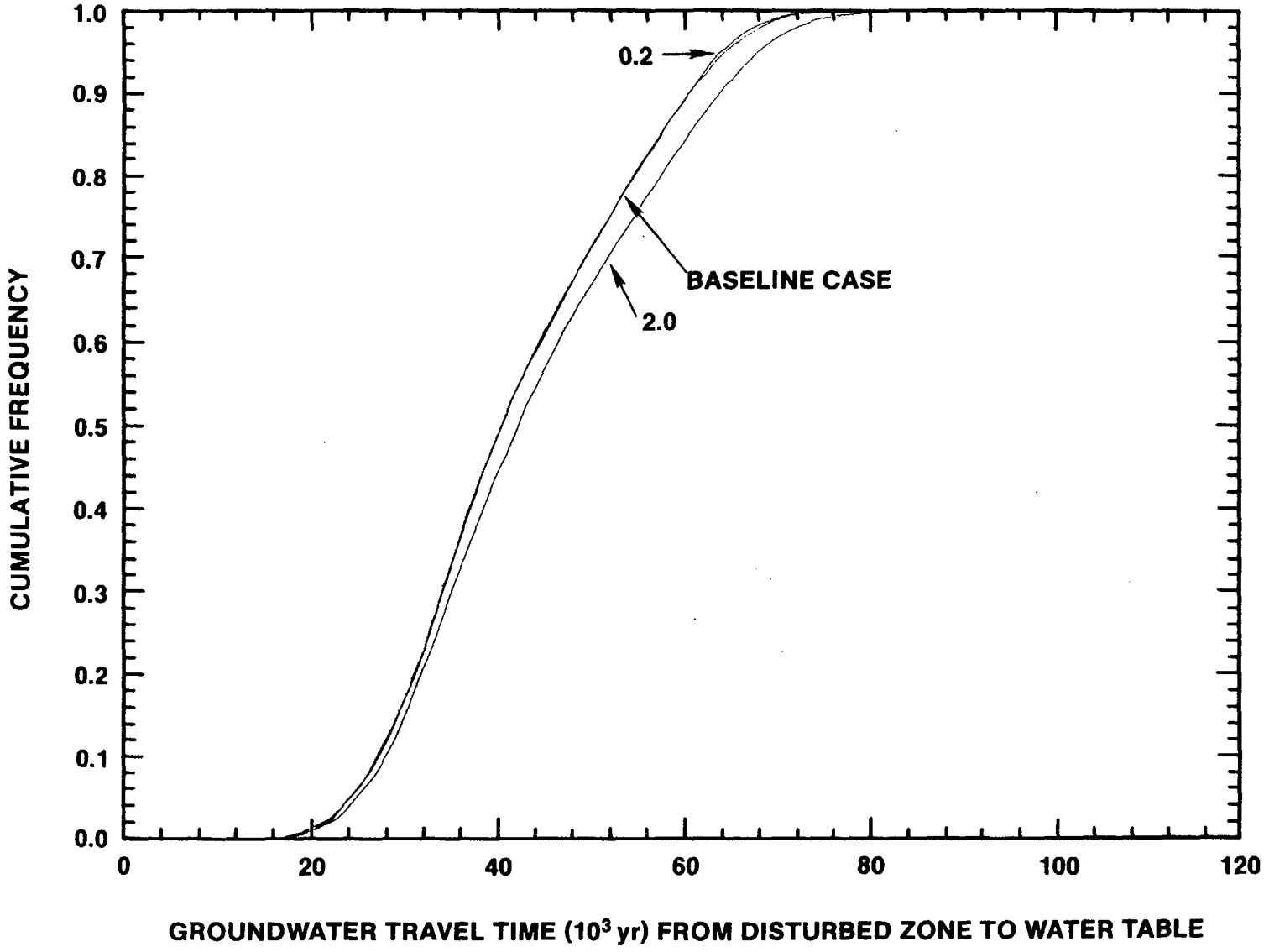

Figure 17. Effects of variations of the standard deviation on effective porosity. Travel time cumulative probability density curves are shown for values of the standard deviation of n_e scaled at 0.2, 1.0, and 2.0 times that of the baseline case.

deterrent against the performance of a carefully designed experimental program to ensure a high degree of reliability in the porosity data. In general, porosity measurements are relatively inexpensive to obtain. Furthermore, porosity is likely to be closely correlated with parameters that are more difficult to measure, such as hydraulic conductivity. From this perspective, the spatial distribution of porosity values should be included in the site characterization activities.

2.5 Summary of Groundwater Travel Times

As presented in this chapter, the following conclusions are drawn from this study for estimating groundwater travel times in the unsaturated zone at Yucca Mountain.

1) If the percolating flux, q, is less the than average saturated matrix hydraulic conductivity, K_s, and if matrix suction can draw water from fractures at the same rate as it moves within matrix blocks, then the groundwater travel times from the disturbed zone to the water table will exceed 1,000 years with a very high level of probability and are likely to exceed 10,000 years as well, also with a high level of probability.

2) The travel-time distribution is apparently most sensitive to flux, correlation lengths, and spatial variations of saturated matrix hydraulic conductivity. Less sensitivity is attributed to effective porosity. A good estimate of means, standard deviations, and spatial and cross correlations of all hydrogeologic parameters, is strongly recommended.

3) Potential lateral flow and the concentration of flux down fault zones need to be investigated before the cumulative distribution function can be interpreted as representative of the fastest paths of likely radionuclide travel. Further refinement of the present model will be necessary, as conceptual understanding of flow in unsaturated fractured porous tuff and additional data are acquired for Yucca Mountain site.

4) In most cases, hydraulic data are insufficient for performing geostatistical analyses. Site-characterization studies should provide the hydrogeologic data needed for modeling the ground-water travel time based on site statistics.

3.0 RADIONUCLIDE TRANSPORT FROM THE WASTE-EMPLACEMENT AREA TO THE WATER TABLE

This section describes the mathematical models and calculational techniques used for predicting releases of radionuclides from the waste-emplacement area to the water table. A theoretical basis for predicting system behavior is derived in Section 3.1, which contains the three following subsections: 3.1.1 describes the formula for the mass release rate from the waste canister; 3.1.2 establishes the necessary connections between these mass-release rates and the simulation model for predicting radionuclide transport to the water table; and 3.1.3 develops the transport model, consistent with the model for predicting groundwater travel time distributions described in Chapter 2. Section 3.2 explains how the transport model was used for calculating the cumulative release of radionuclides to the water table which is included in Subsection 6.4.2 of the NNWSI EA (DOE, 1986).

3.1 Theoretical Basis for Calculating Radionuclide Release

3.1.1 Mass Release From the Waste Canister

For the basis of this analysis, a single canister is taken as the unit of waste inventory. The reference canister is assumed to contain 3.33 metric tons of heavy metal (MTHM) in the form of spent-fuel rods or pellets. It is estimated that about 21,000 canisters (or 70,000 MTHM) can be emplaced in the underground facilities of the candidate site at Yucca Mountain. The disposal horizon is assumed to have an effective

area of 510 ha (1260 acres). The composition of spent fuel, in terms of radioactivity present at various times after removal from the reactor, can be found in "Technology for Commercial Radioactive Waste Management" (DOE, 1979). Ten-year-old spent fuel is assumed to be present at the time of closure of the repository.

For the calculations in this section, it is assumed that canister failure to contain and isolate radioactive material may occur at any time following repository closure; $t = 0$ represents the time at closure. During the interval in which canisters remain intact, $0 < t < T_c$, no radioactive waste material will be released from the canisters. At some point in time, at $t = T_c$, a breach in a canister could occur, allowing water to come into contact with the spent-fuel pellets. No matter how canister failure occurs, the time-to-failure of even a single canister may be treated as a random variable with an associated cumulative distribution function defined for the interval $(0,\infty)$. Our current knowledge of the potential for canister failure is insufficient for estimating such a distribution, therefore, we have treated T_c as a fixed parameter.

Water in partially saturated rock will not flow into the space between the borehole and canister unless sufficient suction is exerted in the space or local hydraulic conductivity allows ponding of sufficient water near the space to cause positive pressure at the face of the borehole. The circumstances under which water could reach the waste form in a partially saturated environment are not yet understood. One may, however, estimate a maximum rate at which water could steadily enter and leave a breached canister under any circumstances. This maximum rate is

the product of the percolation flux, q, at the repository level and an effective water-intercept area for the canister, A, which can be taken to be the projected area of the canister in a plane perpendicular to the direction of flow, assuming the absence of mechanisms that concentrate flow at the canisters. If the protective effects of the spent-fuel cladding and canister materials are ignored, it is easily seen that the maximum rate of dissolution of uranium dioxide (the spent-fuel matrix), is $q\ A\ S_m$ (kg/yr), where S_m is the solubility limit for uranium oxide, in units of kg/m^3.

As the spent-fuel matrix is dissolved, radionuclides embedded in the matrix will become available for conversion to a liquid phase at a maximum rate, $q\ A\ S_m\ f_i(t)$, where $f_i(t)$ is the ratio of mass of the i^{th} radionuclide to the mass of the spent-fuel matrix at any time, t. Not all radionuclides released as the matrix dissolves will themselves be converted to a liquid phase; the solubility limits of the radionuclide-bearing compound that can enter the liquid phase are usually different from the solubility limit of the spent-fuel matrix. If the solubility limit of the compound bearing the i^{th} radionuclide, S_i, is greater than or equal to S_m, then all radionuclides that are released through dissolution of the matrix will be converted to the liquid phase at the same maximum rate as the matrix material. If, on the other hand, $S_i < S_m$, the corresponding radionuclides that become exposed to water through dissolution of the matrix will be converted into two forms as follows: (1) a liquid phase at a maximum rate of $q\ A\ S_i\ f_i(t)$ and (2) a solid phase, in the form of a precipitate (or possibly a solid suspension), at a maximum rate of $q\ A\ (S_m - S_i)\ f_i(t)$. It is assumed that radionuclides converted to the second of these forms cannot be

transported by water; the precipitates are assumed to remain within or very near the canisters and--for modeling purposes--are treated as undissolved spent-fuel matrix. Thus, the maximum rate at which the mass of the i^{th} radionuclide enters a liquid phase within the canister is expressed as $q\ A\ \bar{S}_i\ f_i(t)$, where $\bar{S}_i$ is the lesser of the solubility limits S_m and S_i. If steady flow through the canister is maintained, and if water residence time in the canister is small, compared to the half-life of the i^{th} nuclide, $q\ A\ \bar{S}_i\ f\ (t)$ is an upper-bound approximation of the rate of release of the mass of the i^{th} radionuclide from the canister by advection. Mass transfer from the canister by molecular diffusion is probably not significant for canisters emplaced in boreholes in partially saturated rock.

The fraction of mass per canister in the form of the i^{th} radionuclide at any time is, by definition,

$$f_i(t) = \frac{m_i(t)}{M(t)} \quad , \tag{24}$$

where $m_i(t)$ is the mass of the i^{th} radionuclide remaining in a canister, at time t, and M(t) is the mass of the spent-fuel matrix remaining in a canister at time t. For typical dissolution rates of the waste matrix expected at Yucca Mountain, M(t) can be set to its value at closure, for example, M_o, without introducing a significant source of error in the calculations described in Section 3.2. Thus, an upper-bound approximation to the mass release rate from a reference canister is

$$R_i = \frac{q\ A\ \bar{S}_i}{M_o}\ m_i(t), \qquad (kg/yr) \tag{25}$$

and the fractional release rate for the i^{th} nuclide in units of parts per year is

$$R_i = \frac{q\ A\ \bar{S}_i}{M_o} \qquad (yr^{-1}) \ . \tag{26}$$

This fractional release rate is not the one used in making comparisons with the regulatory numerical criteria in 10 CFR 60.113 (the long-term release performance objective for the engineered-barrier system). The maximum rate allowed by the regulatory criteria is based on the mass release rate of Equation 26 divided by the ratio of the mass of the i^{th} nuclide present 1,000 years after closure to the mass, M_o. See Sinnock et al. (1984; page 3 and Table 1) for a discussion of the ratios of allowable releases in the context of the NRC performance objectives.

3.1.2 The Source Term for Radionuclide Transport Calculations

For reasons stated in Section 3.1.3, the radionuclides that would contribute significantly to releases at the water table for the first 100,000 years after closure are the non retarded nuclides C-14, I-129, and TC-99. Because each of these nuclides is characterized as a single-member decay chain, the appropriate equation for describing the mass of the i^{th} one of these remaining in a canister at any time, t, is

$$\frac{dm_i}{dt} = \begin{cases} -\lambda_i m_i & 0 \leq t \leq T_c \\ -(\lambda_i + R_i)m_i & t > T_c \end{cases} , \qquad (27)$$

where all variables were defined in Section 3.1.1, except for λ_i, which represents the decay constant of the i^{th} nuclide. The solution of Equation 27 is therefore,

$$m_i(t) = \begin{cases} m_i(0)\, e^{-\lambda_i t} & 0 \leq t \leq T_c \\ m_i(0)\, e^{-\lambda_i t}\, e^{-R_i(t-T_c)} & t > T_c \end{cases} , \qquad (28)$$

Thus, the total mass-release rate from the waste inventory of the i^{th} nuclide is expressed as

$$N\, R_i\, m_i(t) \cdot u(t - T_c) \qquad (kg/yr) , \qquad (29)$$

where N = the number of waste canisters,

$$u(x) = \begin{cases} 0 \text{ if } x \leq 0 \\ 1 \text{ if } x > 0 \end{cases} \quad \text{(the unit step function)}, \qquad (30)$$

and $m_i(t)$ is given by Equation 28. The concentration of the i^{th} radionuclide in the aqueous phase, at any point $z > 0$ below the repository level ($z = 0$), and any time $t > 0$, is denoted by $C_i(z,t)$ in Section 3.1.3. The concentration at the repository level, $C_i(0,t)$, for conditions of steady, vertically downward flow, is found by dividing Equation 29 by the total discharge of water through the repository, $q\, A_R$

(m^3/yr), where q is the flux in units of $m^3/m^2/yr$, and A_R denotes the projection of the repository area onto the plane of the water table. Thus, the time-dependent concentration of the i^{th} radionuclide at the underground facility is given by

$$C_i(0,t) = \frac{NR_i}{q\ A_R}\ m_i(t)\ u(t-T_c) \qquad (kg/m^3) \quad . \tag{31}$$

Equation 31 is a time-dependent boundary condition on the transport equation, which will be developed below.

3.1.3 Radionuclide Transport Between the Underground Facilities and the Water Table

The equation used for calculating transport of an aqueous-phase radionuclide from the underground facilities to the water table is

$$\frac{\partial C_i}{\partial t} + \frac{q}{\theta r_i}\ \frac{\partial C_i}{\partial z} = -\lambda_i C_i \ , \tag{32}$$

where

$C_i(z,t)$ = concentration of the i^{th} radionuclide (kg/m^3 of water) at distance, z, below the repository (z = 0), at time t;

$\theta(z)$ = volumetric moisture content (m^3 of water/m^3 of rock) at distance, z, below the repository;

$r_i(z)$ = an effective retardation factor for the i^{th} radionuclide;

q = flux ($m^3/m^2/yr$); and

λ = decay constant for the i^{th} radionuclide.

Equation 32 is derived from the general continuity equation for transport of a radioactive contaminant in a porous, fractured medium (Dudley et al., 1986). In going from the general continuity equation to Equation 32, several assumptions are made.

First, it is assumed that the flow is one-dimensional and steady, and that, consequently, the percolation flux, q, is constant along the path from the underground facilities ($z = 0$) to a point $z > 0$. In steady flow, θ and r_i will be functions of position only, as indicated above. These variables will be assigned in a manner consistent with the formulation of water travel time in Section 2 (see Equation 11).

Second, Equation 32 contains no term that accounts for hydrodynamic dispersion. The reason for this will become clear as the solution is developed below, where a new independent variable (travel time) is introduced, to account for hydrodynamic dispersion.

Third, Equation 32 contains no terms that account for molecular diffusion. Molecular diffusion is ignored because its rate is relatively small compared with rates of mass transport by advection under the

expected hydrologic conditions at Yucca Mountain. Based on effective diffusivities given by Daniels et al. (1982), the Peclet number ranges from 14 to 143 for a 0.5-mm/yr flux in the matrix.

Finally, Equation 32 applies only to transport of radionuclides that are single-member decay chains. The reason for this limitation will also become clear as the solution is developed below. However, a brief explanation for this is that only certain nonsorbing radionuclides, all of which are single-member decay chains, can be transported the full distance between the emplacement area and the water table during the time period of 10,000 to 100,000 years after repository closure.

Equation 32 is solved, therefore, subject to the time-dependent boundary condition expressed in Equation 31. However, it is convenient to introduce a new independent variable in place of z, that is,

$$T(z)_i = \int_0^z \frac{\theta r_i}{q}\, dz \quad . \tag{33}$$

For obvious reasons, this new variable can be called transport time. When r_i is set equal to 1 (no retardation), and z is taken as the distance between the repository and the water table, T_i is identical with the groundwater travel time through a column of rock units defined in Section 2, provided, of course, that moisture content, θ, is interpreted as described in Equation 11.

In terms of transport time, Equation 32 becomes

$$\frac{\partial C_i}{\partial t} + \frac{\partial C_i}{\partial T_i} = - \lambda_i C_i \quad . \tag{34}$$

The solution of this equation, subject to the initial condition

$$C_i(T_i,0) = 0, \qquad T_i > 0 \quad , \tag{35}$$

and the boundary condition (from Equations 28 and 31),

$$C_i(0,t) = \frac{NR_i}{q\ A_R}\, m_i(0) e^{-\lambda_i t}\, e^{-R_i(t - T_c)}\, u(t - T_c) \ , \quad t > 0 \ , \tag{36}$$

is easily found. Applying the Laplace transformation in time to Equations 34 and 36, one finds that

$$C_i(T_i,t) = C_i(0,\ t-T_i)\ e^{-\lambda_i T_i}\ u(t - T_i) \qquad (kg/m^3). \tag{37}$$

If T_i is now interpreted as the transport time through a column of rock of total thickness d (i.e., z = d in Equation 37), then the discharge to the water table at some time t > 0, given T_i, is evidently

$$Q_i(t|T_i) = \alpha_i\ q\ C_i(T_i,t) \qquad (Ci/m^2 \cdot yr) \ , \tag{38}$$

where the conversion from mass in kilograms to radioactivity in curies is made, using the specific activity of the i^{th} radionuclide, α_i. It

follows that the cumulative discharge in curies (in the form of the i^{th} radionuclide) up to some time $t > 0$, given T_i, is

$$X_i\ (t|T_i) = \int_0^t Q_i\ (t'|T_i)dt' \qquad (Ci/m^2)\ . \tag{39}$$

Consecutive substitution of Equations 36 to 38 into Equation 39 leads to a simple integral over time that can be evaluated. One finds that

$$X_i\ (t|T_i) = \psi_i\ (t)\ \ e^{-\lambda_i\ \tau}\ [1 - e^{-(\lambda_i + R_i)\tau}]u(\tau)\ \ (Ci/m^2), \tag{40}$$

where the following auxiliary variables have been introduced to keep the formulae conveniently short:

$$\tau = t - (T_c + T_i)\ (yr), \text{ and} \tag{41}$$

$$\psi_i = \frac{\alpha_i N\ m_i(0)}{A_R}\ \frac{R_i e^{-\lambda_i t}}{(\lambda_i + R_i)} \qquad (Ci/m^2)\ .$$

Note that the first factor in the expression for ψ_i can be interpreted as the areal density of the activity of the i^{th} radionuclide in the repository in Ci/m^2, at $t = 0$.

Equation 40 expresses cumulative discharge of the i^{th} radionuclide as a function of time since closure and a transport time, T_i. Because the unit step function, $u(\tau)$, appears as a factor, the cumulative

discharge will be zero for times equal to less than the sum of T_c and T_i. In Section 3.1.2, a value of T_c of about 1,000 years is adopted, and in Section 2 it is shown that expected water travel times through a column of rock units in the unsaturated zone below the emplacement area are of the order of 40,000 years at 0.5-mm/yr percolation flux. At this upper-limit value of flux, the earliest radionuclides released as part of the cumulative discharge would travel at the full linear velocity of the water with no retardation. Radionuclides of this type in the Yucca Mountain repository's potential reference inventory appear to be C-14, I-129, and possibly Tc-99 (DOE, 1984; Table 6-43); all three of them are single-member decay chains and, therefore, fall into the category of radionuclides for which the transport Equation 32 is valid.

The transport of other radioactive elements containing nuclides with single-member decay chains (such as cesium and strontium) could also be correctly treated by Equation 32, but the retardation factors for these elements are enormous; for instance, for cesium $r_i \simeq 40{,}000$, and for strontium, $r_i \simeq 21{,}000$ (DOE, 1984). Such strongly retarded radionuclides are effectively immobile and would not be transported to the water table within any realistic time scale, so long as the very low percolation fluxes prevailed at Yucca Mountain. Obviously, the same is true for strongly retarded compounds containing radionuclides, which are parts of multi-member decay chains, such as americium, neptunium, and uranium. Uranium appears to be the least retarded of these, with r_i of the order of 10 or more (DOE, 1984; Table 6-9). But if the time scales that are of interest are restricted to 100,000 years or less, even uranium will not contribute significantly to cumulative discharges; at

0.5 mm/yr flux, the transport times for uranium would be more than 100,000 years and one would find justification for ignoring this element (and certainly any other element with a higher retardation factor) in a calculation of cumulative releases up to 10,000 years. These observations indicate that we can ignore, with some justification, the complication of including multi-member decay chains in the formulation of the transport Equation 32.

Next, we show how hydrodynamic dispersion can be included in the transport problem. The cumulative discharge expressed by Equation 40 can be regarded as a function of two variables, that is, time, which is a free parameter, and transport time, T_i, which, as seen in Chapter 2, is a random variable whose distribution is determined by flux and the distribution of hydrologic properties throughout the rock column under consideration. In Appendix A it is shown that under certain weak conditions the travel-time distribution for a specific column of rock units is approximately normal with a calculable mean, T, and variance σ_T^2. If we limit considerations to nonretarded elements such as carbon, iodine, and technetium, then the distribution of the variable, τ, defined in Equation 41, will also be normal with the mean expressed as

$$\bar{\tau} = t - (T_c + \bar{T}) \quad , \tag{42}$$

and variance σ_τ^2. In other words, the probability density function (PDF) of τ is

$$p(\tau) = \frac{1}{\sqrt{2\pi}\,\sigma_T} e^{-(\tau-\bar{\tau})^2/2\sigma_T^2} \quad . \tag{43}$$

Using this result and Equation 41 the expected cumulative discharge at any time can be calculated as

$$X_i(t) = \psi_i(t) \int_0^\infty e^{-\lambda_i \tau} \left[1 - e^{-(\lambda_i + R_i)\tau}\right] p(\tau) d\tau \quad . \tag{44}$$

After evaluation of the integral in the last expression, we have

$$X_i(t) = \frac{\psi_i(t)}{2} \left\{ e^{-\lambda_i(\bar{\tau} + \frac{1}{2}\lambda_i\sigma_T^2)} \left[1 + \text{erf}\left(\frac{\bar{\tau} + \lambda_i\sigma_T^2}{\sqrt{2}\,\sigma_T}\right)\right] - e^{-R_i(\bar{\tau} - \frac{1}{2}R_i\sigma_T^2)} \left[1 + \text{erf}\left(\frac{\bar{\tau} - R_i\sigma_T^2}{\sqrt{2}\,\sigma_T}\right)\right] \right\}, \tag{45}$$

where erf(x) is the error function (National Bureau of Standards, 1964; p. 297). The listing of a FORTRAN program for evaluating the expression in Equation 45 is shown in Appendix C. An analytical expression for the variance of the cumulative discharge can also be derived; but for reasons mentioned below, such an expression was not needed for purposes of this report.*

*Note that other variables in Equation 44 could also be considered as random variables--in particular, the waste canister containment time, T_c; such an extension was not considered in the work leading to this report.

Note that the expected cumulative discharge, Equation 45, applies to a single column of rock units, the m^{th} one, and has units of Ci/m^2.* The dependence on the particular rock column has, so far, been suppressed for the sake of a simplified notation. However, one sees that virtually every parameter appearing either explicitly or implicitly in Equation 45 (except time and the radionuclide decay constants) could depend upon the location of the rock column within the repository area (i.e., ψ_i, R_i, T_c, $\bar{T}$, and s_T^2 could all be functions of the coordinates of the m^{th} column--see Appendix A). This dependence is now recognized by simply inserting the label m (for the m^{th} column) in the definition of the cumulative discharge in Equation 40, i.e.,

$$X_i(t|T_i) \text{ is replaced by } X_i(t|T_i, m),$$

and in the definition of the expected cumulative discharge Equation 45,

$$X_i(t) \text{ is replaced by } X_i(t,m).$$

Using this notation and the results of Section 3.1.2, one can express the total cumulative release to the water table in the form of the i^{th} radionuclide up to time t: if the disposal area is divided into m columns of equal area, A_R/M, then the total cumulative release $D_i(t)$ is approximated by

*Note that we have temporarily dropped reference to the column m up to this point to simplify the notation; the subscript m will be added later in the arguments.

$$D_i(t) \doteq \frac{A_R}{M} \sum_{m=1}^{M} X_i(t|T_i, m) \qquad (Ci) \quad . \tag{46}$$

Note that $D_i(t)$ is a function of the M variables $T_i(m)$, m = 1,2,...m. As noted in Section 2.3, the M transport times are approximately, normally distributed random variables; hence $D_i(t)$ is a random variable for any fixed time t. The distribution of $D_i(t)$ will probably have to be constructed by direct simulation with the use of a random number generator. The expected total cumulative release can be expressed directly, however, without the use of random sampling by

$$D_i(t) \doteq \frac{A_R}{M} \sum_{m=1}^{M} X_i(t,m) \qquad (Ci) \quad . \tag{47}$$

The terms in the sum of Equation 47 are calculated for each one of M columns using Equation 45 and values of $T_i(m)$, $\sigma_T^2(m)$ appropriate for the rock-unit column m.

Although an expression for the variance of the cumulative discharges, $X_i(t|T_i,m)$, is not given in this report, it is worth noting that if the transport times, $T_i(m)$, m = 1,2...M are assumed to be independent random variables, then

$$\text{Var}\,[D_i(t)] \doteq \left(\frac{A_R}{M}\right)^2 \sum_{m=1}^{M} \text{Var}\,[X_i(t|T_i,m)] \quad . \tag{48}$$

Finally, note that the assumption of uncorrelated transport times $T_i(m)$ is realistic only if the characteristic size of each of the M columns is no smaller than the spatial correlation length in the horizontal direction, ρ_h, defined in Section 2.1. As mentioned in that section, the distances over which relevant rock hydrologic properties of the Yucca Mountain Site are correlated are unknown.

3.2 Calculations of the Cumulative Releases to the Water Table

The expression for expected total cumulative release, Equation 47, provides a formula for estimating releases of radionuclides into the water table beneath Yucca Mountain, which is entirely consistent with the theoretical and calculational models of groundwater travel time described in Section 2. But, because of the very tight schedule for producing the final version of the EA for Yucca Mountain, it was not possible to estimate releases using Equation 47. What was actually done in the time allowed for estimating releases to the water table is explained below.

It was first assumed that the water travel-time distribution for the entire repository, i.e., as expressed in Equation A-23, could be approximated by a normal distribution with the mean and variance equal to the sample mean and sample variance obtained from the numerical simulations of groundwater travel time (see the baseline case in Section 2.4). Then we multiplied the expression in Equation 40 by the repository area, A_R, and the normal PDF and integrated the product over all values of travel time to obtain an expression that, apart from the constant A_R, is

identical with Equation 45. A short FORTRAN code (Appendix C-2) was written and used for evaluating the expression. Results for a 0.5-mm/yr flux are shown in Table 4.

TABLE 4

Estimates of Cumulative Releases to the Water Table Calculated With the Normal Approximation to the Distribution of Water Travel Times for the Entire Disposal Area[a]

Species	Curies Released by 10,000 Years	Curies Released by 100,000 Years
C-14	6.0×10^{-4}	1.4×10^{-2}
I-129	5.0×10^{-5}	0.3
TC-99	2.0×10^{-2}	97.0

[a] Parameters used in Equation 45 are as follows: $\bar{N} = 21{,}000$, $R_i = 2.5 \times 10^{-9}$/yr, $q = 0.5$ mm/yr, $\bar{T} = 43{,}270$ yr, $\sigma_T = 12{,}800$ yr, $T_c = 3{,}000$ years. For radionuclide parameters, see Table 6-42 of DOE (1986), or Table 1 of Lin (1985)

The error incurred by approximating the groundwater travel-time distribution by a normal distribution has not been carefully estimated. In Appendix A we note that Equation A-23 cannot be normal unless the means and variances of the travel-time distributions associated with the M rock-unit columns are identical. In effect, this approximation distorts the rock-unit thickness distribution in such a way as to make the means and variances indicated for all columns equal to the estimated mean and variance associated with the travel-time distribution for the entire repository. Some insight into the error incurred through use of a normal-distribution approximation may be gained by inspecting

Figure 18, which is adapted from Figure 11B in Section 2.4. The solid-line curve represents the empirical cumulative distribution function of 9630 samples of water-travel times obtained with the numerical simulator described in Section 2.4. The sample mean of this distribution is 43,270 years, and the sample standard deviation is 12,800 years. The dashed-line curve represents a normal CDF with a mean equal to 43,270 years and a standard deviation equal to 12,000 years. A comparison of the two curves shows that the normal approximation gives more weight to the shorter travel times (< 18,000 years) than is given by the empirical cumulative frequency (which should be a close, if not exact, representation of Equation A-23). This fact suggests that our use, as described in the EA, of the normal-distribution approximations for calculations of releases to the water table has led to overestimates of the cumulative release of all nuclides during 10,000 years. In other words, use of the normal approximation was inadvertently conservative for the 10,000-year time scale. It is harder to see effects of the approximation on the calculations of cumulative releases up to 100,000 years. The fact that the normal CDF lies below (or is less steep than) the empirical distribution in the central part of the curves (roughly 20,000 to 50,000 years from closure) may indicate that we have underestimated cumulative releases of all nuclides during 100,000 years, by an amount that is unknown but probably insignificant.

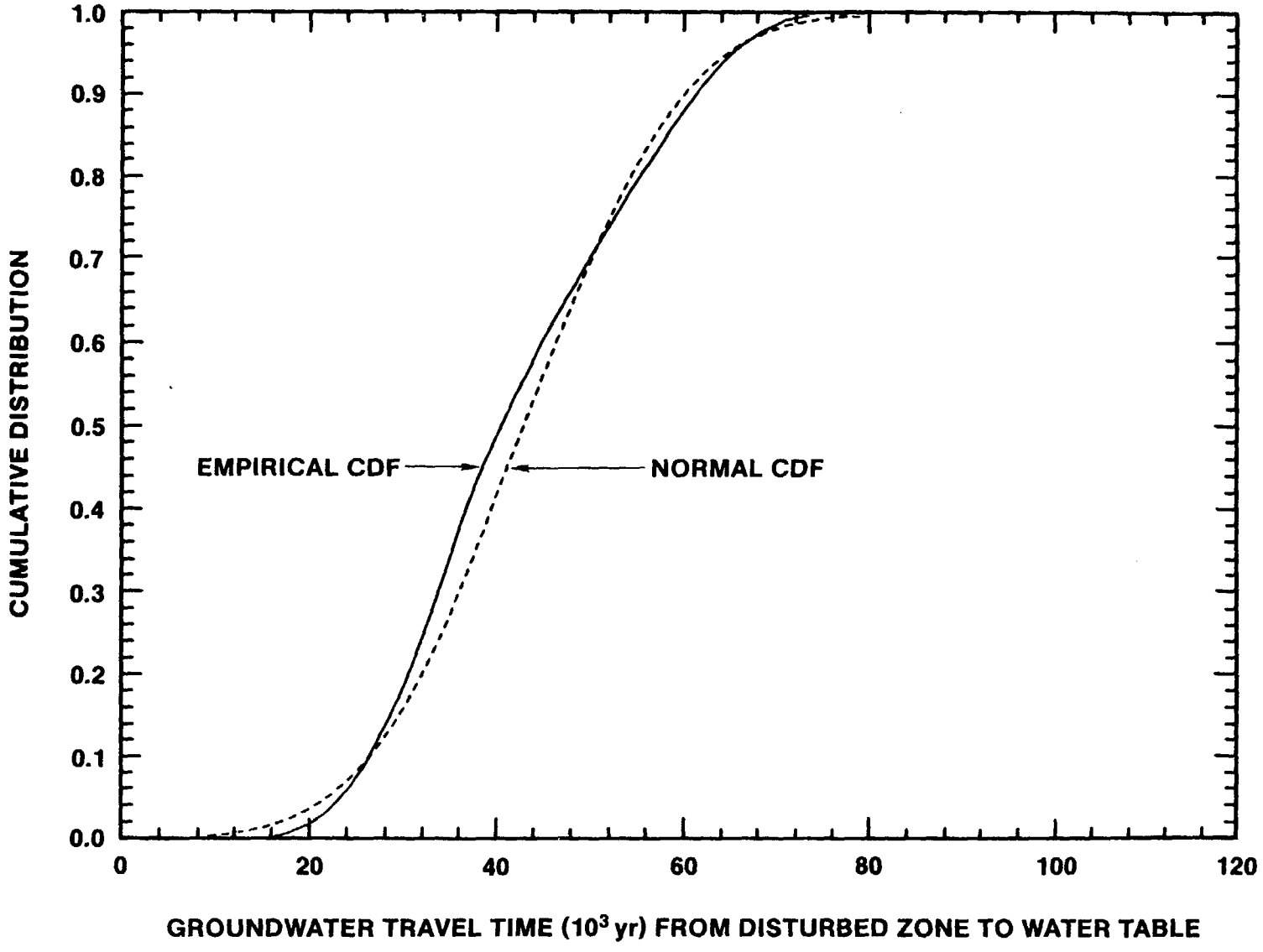

Figure 18. Comparison of cumulative distribution functions between the results from numerical simulation (Figure 11B, Section 2.4) and the mathematical normal distribution.

4.0 CONCLUSIONS

This report is intended to document the physical and mathematical bases of results used to support arguments in Sections 6.3.1.1 and 6.4.2 of the NNWSI Project statutory environmental assessment document (DOE, 1986). The methods described in that report were based on the current understanding of processes operating at Yucca Mountain.

A probabilistic method was devised for calculating the distribution of groundwater travel time from the disturbed zone to the water table and is described in Chapter 2. Major assumptions behind this method are that (1) water travels vertically downward through the unsaturated zone below the disturbed zone, (2) quasi-steady flow conditions prevail between the disturbed zone and the water table, and (3) water flows through the porous matrix unless it is diverted into fractures where percolation flux exceeds the saturated matrix hydraulic conductivity. The water velocity is determined by relationships between percolation flux, saturated matrix hydraulic conductivity, effective matrix porosity, and fracture porosity. All of these parameters are assumed to be statistically independent quantities in the present model, because available hydrogeologic data are insufficient for determining the degree of correlation. The spatial correlation length of the velocity field is treated as a free parameter, although there is reason to believe velocity-field correlations are related to spatial correlations of the primary hydrologic variables.

Application of the probabilistic method of Chapter 2, to a 963-column, rock-unit model of Yucca Mountain gives results that indicate that, for 0.5-mm/yr percolation flux, groundwater travel time has a mean of about 43,000 years and a standard deviation of about 12,000 years. Because 0.5 mm/yr is believed to be an upper limit on the percolation flux below repository level at Yucca Mountain, the results of this application suggest that less than 1 percent of the calculated groundwater travel times are less than 10,000 years.

A method for calculating cumulative releases of radioactivity through the groundwater flow pathway is described in Chapter 3; this method uses the distribution of groundwater travel times derived in Chapter 2 to incorporate the effects of hydrodynamic dispersion in the calculation of the transport of soluble contaminants from the disturbed zone to the water table. However, given the time constraints on the present report, the need for calculational simplicity dictated that actual calculations of cumulative releases of radionuclides to the water table be made with a normal-distribution approximation to the distributions obtained by the Monte Carlo method of Chapter 2. The method for estimating cumulative releases of radionuclides to the water table was applied to a 70,000-MTHM inventory of spent fuel located at the repository level at Yucca Mountain and subject to a percolation flux of 0.5 mm/yr. This calculation shows that the cumulative releases to the water table at 10,000 years following repository closure would be about 6.0×10^{-4} curies of C-14, 2.0×10^{-2} curies of Tc-99, and 5.0×10^{-5} curies of I-129. This small amount of radioactive material is about one ten-millionth of the amount allowed to be released in 10,000 years as stipulated by EPA standards in 40 CFR Part 191 (Appendix A, Table 1 et seq.).

The assumptions and data used in the analyses presented in this report are, of course, subject to change or refinement, if necessary, as new information becomes available through NNWSI Project activities.

REFERENCES

Bear, J., Dynamics of Fluids in Porous Media, Elsevier, New York, 1972.

Brooks, R. H., and Corey, A. T., 1966, "Properties of Porous Media Affecting Fluid Flow," Journal of the Irrigation and Drainage Division, Proceedings of the American Society of Civil Engineers, pp. 61-89, June 1966.

Daniels, W. R., et al., 1982, "Summary Report on the Geochemistry of Yucca Mountain and Environs," LA-9328-MS, Los Alamos National Laboratory, Los Alamos, New Mexico.

DOE (U.S. Department of Energy), 1979, "Technology for Commercial Radioactive Waste Management," DOE/ET-0028, Volume I-V.

DOE (U.S. Department of Energy), 1984a, "Nuclear Waste Policy Act Draft Environmental Assessment Yucca Mountain Site, Nevada Research and Development Area, Nevada," DOE/RW-0012.

DOE (U.S. Department of Energy), 1984b, "10 CFR Part 960 General Guidelines for Recommendation of Sites for Nuclear Waste Repositories: Final Siting Guidelines," Code of Federal Regulations, Federal Register, v. 49, n. 236, pp. 49714-47770, December 6, 1984.

DOE (U.S. Department of Energy), 1986, "Nuclear Waste Policy Act Environmental Assessment of the Nevada Nuclear Waste Storage Investigations (NNWSI) Project."

Dudley, A. L., Peters, R. R., Tierney, M. S., Klavetter, E. A., Gauthier, J. H., and Wilson, M., 1986 (in preparation), "Total Systems Performance Assessment Code (TOSPAC), Volume I: Physical and Mathematical Bases," SAND85-0002, Sandia National Laboratories, Albuquerque, New Mexico.

EPA (U.S. Environmental Protection Agency), 1985, 40 CFR Part 191, "Environmental Standards for Management and Disposal of Spent Fuel, High Level and Transuranic Radioactive Wastes; Final Rule," Code of Federal Regulations, Federal Register, Vol. 50, No. 182, pp. 38066-38089, September 19, 1985.

Feller, W., 1966, An Introduction to Probability Theory and Its Applications, Volume II, 626 pp., John Wiley and Sons, Inc., New York.

Freeze, R. A., and Cherry, J. A., 1979, Groundwater, Prentice-Hall, Inc., New Jersey.

GE/CALMA, 1985, Interactive Graphic and Information Systems, Product Nos. CAL0044, CAL0047 to CAL0053, and CAL0060, Report 0310, Sandia National Laboratories, Albuquerque, New Mexico.

GE/CALMA, 1986, Interactive Graphic and Information Systems, Product Numbers: CAL0114, CAL0118, CAL011, CAL0094, CAL0082, CAL0107 to CAL0109, Department 6310, Sandia National Laboratories, Albuquerque, New Mexico.

Klavetter, E. A., and Peters, R. R., 1985, "Estimation of Hydrologic Properties of an Unsaturated, Fractured Rock Mass," SAND84-2642, Sandia National Laboratories, Albuquerque, New Mexico.

Lin, Y. T., 1985, "SPARTAN--A Simple Performance Assessment Code for the Nevada Nuclear Waste Storage Investigations Project," SAND85-0602, Sandia National Laboratories, Albuquerque, New Mexico.

Montazer, P., and Wilson, E. W., 1984, "Conceptual Hydrologic Model of Flow in the Unsaturated Zone, Yucca Mountain, Nevada," Water-Resource Investigations Report 84-4345, U.S. Geological Survey, Lakewood, Colorado.

Montazer, P., Weeks, E. P., Thamir, F., Yard, S. N., and Hofrichter, P. B., 1985, "Monitoring the Vadose Zone in Fractured Tuff, Yucca Mountain, Nevada, Proceeding of the Characterization and Monitoring of the Vadose (Unsaturated) Zone Conference, National Water Well Association, November 19-21, 1985.

National Bureau of Standards, 1964, Handbook of Mathematical Functions, edited by M. Abramowitz and I. A. Stegun, Applied Mathematics Series 55, U.S. Department of Commerce, Washington, D.C.

NRC (U.S. Regulatory Commission), 1983, 10 CFR Part 60, "Disposal of High-Level Radioactive Waste in Geologic Repositories: Technical Criteria," Code of Federal Regulations, Federal Register, Vol. 48, No. 120, pp. 28194-28220, June 21, 1983.

Ortiz, T. S., Williams, R. L., Nimick, F. B., Whittet, B. C., and South, D. L., 1985, "A Three-Dimensional Model of Reference Thermal/ Mechanical Stratigraphy at Yucca Mountain, Nye County, Nevada," SAND84-1076, Sandia National Laboratories, Albuquerque, New Mexico.

PBQ&D, 1985, Parsons, Brinckerhoff, Quade, and Douglas, Drawing No. R06940, GE/CALMA No. 0119.

Peters, R. R., Klavetter, E. A., Hall, I. J., Blair, S. C., Heller, P. R., and Gee, G. W., 1984, "Fracture and Matrix Hydrologic Characteristics of Tuffaceous Materials from Yucca Mountain, Nye County, Nevada," SAND84-1471, Sandia National Laboratories, Albuquerque, New Mexico.

Peters, R. R., Gauthier, J. H., and Dudley, A. L., 1986, "The Effect of Percolation Rate on Water-Travel Time in Deep, Partially Saturated Zones," SAND85-0854, Sandia National Laboratories, Albuquerque, New Mexico.

Scott, R. B. and Castellanos, M., 1984, "Stratigraphic and Structural Relations of Volcanic Rocks in Drill Holes USW GU-3 and USW G-3, Yucca Mountain, Nye County, Nevada," USGS-OFR-84-491, Open-File Report, U.S. Geological Survey, Denver, Colorado.

Sinnock, S., Lin, Y. T., and Brannen, J. P., 1984, "Preliminary Bounds on the Expected Postclosure Performance of the Yucca Mountain Repository Site, Southern Nevada," SAND84-1492, Sandia National Laboratories, Albuquerque, New Mexico.

Spengler, R. W., and Chornack, M. P., 1984. "Stratigraphic and Structural Characteristics of Volcanic Rocks in Core Hole USW G-4, Yucca Mountain, Nye County, Nevada," with a section of geophysical logs by D. C. Muller and J. E. Kibler, USGS-OFR-84-789, Open-File Report, U.S. Geological Survey, Denver, Colorado.

Spengler, R. W., Muller, D. C., and Livermore, R. B., 1979, "Preliminary Report on the Geology and Geophysics of Drill Hole UE-25a#1, Yucca Mountain, Nevada Test Site," USGS-OFR-79-1244, Open-File Report, U.S. Geological Survey, Denver, Colorado.

Spengler, R. W., Byers, Jr., F. M., and Warner, J. B., 1981, "Stratigraphy and Structure of Volcanic Rocks in Drill Hole USW G-1, Yucca Mountain, Nye County, Nevada," USGS-OFR-81-1349, Open-File Report, U.S. Geological Survey, Denver, Colorado.

TUFFDB, 1985, System-2000 Tuff Data Base, Version 11002, Product Nos. 1 and 2, Sandia National Laboratories, Albuquerque, New Mexico.

Wang, J. S. Y., and Narasimhan, T. N., 1985, "Hydrologic Mechanisms Governing Fluid Flow in Partially Saturated, Fractured, Pourous Tuff at Yucca Mountain," SAND84-7202 (LBL-18473), Sandia National Laboratories, Albuquerque, New Mexico.

Wang, J. S. Y., and Narasimhan, T. N., 1986, "Hydrologic Mechanisms Governing Partially Saturated Fluid Flow in Fractured Welded Units and Porous Nonwelded Units at Yucca Mountain," SAND-7114 (LBL-21022), Sandia National Laboratories, Albuquerque, New Mexico.

Weeks, E. P., and Wilson, E. W., 1984, "Preliminary Evaluation of Hydrologic Properties of Cores of Unsaturated Tuff, Test Well USW H-1, Yucca Mountain, Nevada, Water-Resources Investigations Report 84-4193, U.S. Geological Survey, Denver, Colorado.

Wilson, W. E., 1985, "Unsaturated Zone Flux at Yucca Mountain, Nevada," attached to a letter from W. E. Wilson to D. L. Vieth dated December 24, 1985, U. S. Geoloical Survey, Denver, Colorado.

APPENDIX A

ESTIMATION OF THE DISTRIBUTION, MEAN, AND STANDARD DEVIATION OF TRAVEL TIME BY ANALYTICAL METHODS

The disturbed-zone boundary below the repository area is assumed to be divided into M patches of equal area. Below the m^{th} patch ($1 \leq m \leq M$) there extends a vertical column of rock reaching to the water table; the column includes I_m rock units, each with distinctive hydrologic properties. The key hydrologic properties for the i^{th} unit are as follows:

$K_s(i)$ = the saturated matrix hydraulic conductivity (m/yr)

$n_e(i)$ = the effective matrix porosity

$q(i)$ = the specific discharge in the vertical direction (the percolation flux in m^3/m^2 yr)

$n_f(i)$ = the effective fracture porosity

$\varepsilon(i)$ = an empirical constant in the power-law relation between relative hydraulic conductivity and saturation of the matrix.

Within each unit, K_s, n_e, and n_f are assumed to be stationary spatial series, as is the velocity field to be derived from these parameters. The velocity field is assumed to have a vertical correlation length, ρ_v, and a horizontal correlation length, ρ_h. The statistical properties of K_s and n_e, are assumed to be derivable from tests performed on core samples taken from each defined rock unit.

The percolation flux, q, is assumed to be uniform in all M columns, as is the value of the fracture porosity, n_f; fractures are ubiquitous (i.e., fracture spacing approaches zero), but flow occurs in fractures only if $q > K_s$ locally; otherwise, flow is confined to the rock matrix. Fractures are also assumed to be vertically oriented (dip of fracture plane = 90°), and in this model the choice of a vertical correlation length for the velocity field probably amounts to a choice of the average depth of penetration of a fracture in a rock unit.

As presented in Section 2, the calculation of a groundwater travel time distribution for all paths of likely radionuclide transport from the disturbed zone to the water table begins with the estimation of the travel-time distribution through a single unit.

A-1 Travel-Time Distribution Through a Single Unit

For unit i, the thickness $d_{m,i}$ in column m is divided into N slabs of thickness ρ_v, where

$$N \simeq \frac{d_{m,i}}{\rho_v} \quad , \tag{A-1}$$

and the n^{th} slab is centered at some depth, Z_n, measured from the top of the unit (Figure A-1)

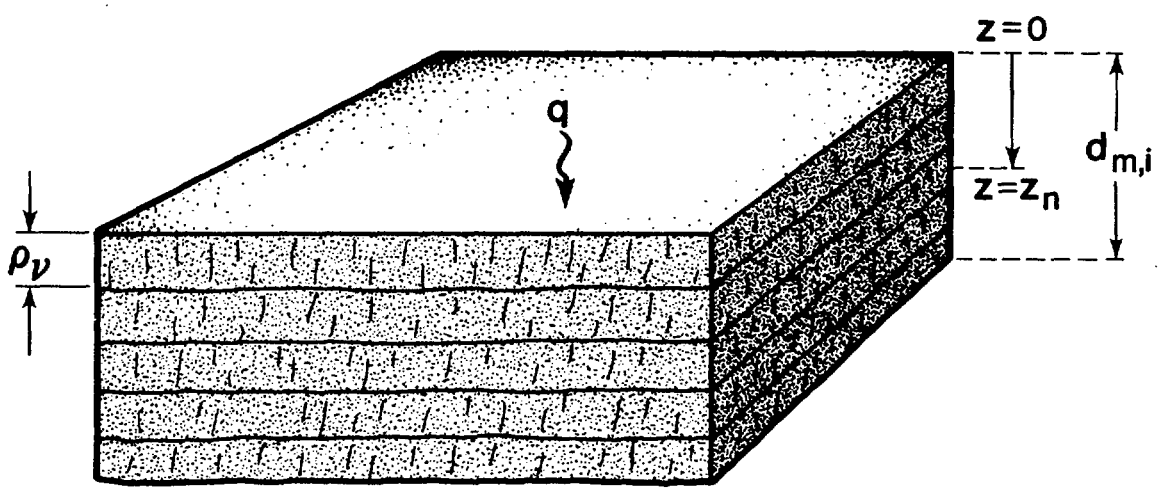

Figure A-1. Schematic diagram illustrating a single unit of thickness, $d_{m,i}$, in column m with a correlation length of ρ_v.

The time required for a water particle to traverse the n^{th} slab is

$$\Delta T_n = \int_{Z_n - \rho_v/2}^{Z_n + \rho_v/2} \frac{dz}{V_n} \quad , \qquad \text{(A-2)}$$

where V_n is an effective linear velocity determined by the percolation flux q and the values of the hydrologic parameters K_s, n_e, n_f, etc., in the n^{th} slab. This effective linear velocity is a function of position within the n^{th} slab through its dependence on the hydrologic parameters which are here assumed to be random functions of position, i.e.,

$$V_n(z) = f[K_s(z),\ n_e(z),\ \ldots].$$

$V_n(z)$ is assumed to be piecewise continuous within each slab; consequently, the mean-value theorem of integral calculus can be used to simplify Equation A-2, i.e.,

$$\Delta T_n = \frac{\rho_v}{V_n(Z_n^*)} \quad , \quad (Z_n - \rho_v/2,\ Z_n + \rho_v/2) \qquad \text{(A-3)}$$

where Z_n^* belongs to $(Z_n - \rho_v/2,\ Z_n + \rho/2)$. The purpose of this simple construction is obviously to ensure that the $V_n(Z_n^*)$, $n = 1, 2, \ldots, N$

and, therefore, the ΔT_n are each independent random variables. Independence can always be guaranteed by choosing ρ_v large enough so that travel times in each of the N slabs are, effectively, uncorrelated. Recall that the vertical correlation length, ρ_v, is a free parameter in the model of groundwater travel time described in Chapter 2.

The total travel time through a unit of thickness $d_{m,i}$ is the sum of the travel times through each of the N slabs so that,

$$T(d_{m,i}) = \sum_{n=1}^{N} \Delta T_n \quad . \tag{A-4}$$

The ΔT_n, n = 1,2, . . .,N, are assumed to be independent random variables taking values for the interval (o,∞). The spatial series from which each ΔT_n is derived is assumed to be stationary; hence, the ΔT_n should be identically distributed with a common probability density function (PDF), g(t), associated with each independent column. In other words, for every n,

$$P_r \{\Delta T_n < t\} = \int_o^t g(\tau)d\tau, \text{ and}$$

$$E(\Delta T_n) = \int_o^\infty \tau g(\tau)\, d\tau, \tag{A-5}$$

[where $E(\cdot)$ is the expectation], and

$$Var(\Delta T_n) = \int_o^\infty [\tau - E(\Delta T_n)]^2 g(\tau)d\tau \quad .$$

It follows that the total travel time through the unit has a PDF that is the N-fold convolution of g with itself (Feller, 1966; pp. 6-7). This fact points to the correct way of calculating the travel-time distribution through a rock unit, although the correct method proves to be impracticable in the present model because the analytic form of g(t) is unknown. Instead, one must resort to direct numerical simulation to construct the PDF, and it becomes most efficient to apply numerical simulation to the entire problem.

Another way of estimating the travel-time distribution for a unit of thickness $d_{m,i}$, uses a central limit theorem (Feller, 1966, p. 253) that states that if $Y_1, Y_2, \ldots Y_n$ are mutually independent random variables with a common PDF, and

$$E(Y_n) = 0, \quad Var(Y_n) = 1,$$

then as $N \rightarrow \infty$ the distribution of the normalized sums,

$$S_N = \frac{Y_1 + \ldots + Y_N}{\sqrt{N}} , \qquad \text{(A-6)}$$

tends toward the standard normal distribution with PDF equal to

$$\frac{1}{\sqrt{2\pi}} e^{-Y^2/2} .$$

In the present case, the central limit theorem can be applied formally by first defining a new random variable

$$Y_n = \frac{\Delta T_n - E(\Delta T_n)}{[Var(\Delta T_n)]^{1/2}}, \qquad \text{(A-7)}$$

and assuming that $\rho_v << d_{m,i}$ (i.e., in Equation A-1, N becomes large). It then follows that $T(d_{m,i})$ is approximately normally distributed. Upon substituting Equation A-3 into Equation A-7 and comparing the normal distribution with mean $\bar{T}$ and variance σ_T^2 we get

$$\bar{T} \equiv E\,[T(d_{m,i})] = d_{m,i}\, E(V_n^{-1}) \quad , \text{ and} \qquad \text{(A-8)}$$

$$\sigma_T^2 \equiv Var\,[T(d_{m,i})] = d_{m,i}\, \rho_v\, Var\,(V_n^{-1}) \quad . \qquad \text{(A-9)}$$

One sees that the expected travel time, $\bar{T}$, is derived by what intuition would suggest--the unit thickness multiplied by the expectation of the reciprocal effective linear velocity. The variance in the travel time, $T(d_{m,i})$, is proportional to the correlation length, ρ_v.

A-2 Estimates of the Mean and Variance of Travel Time Through a Unit

The mean and variance of $T(d_{m,i})$ are, respectively, proportional to the mean and variance of $1/V_n$ by Equations A-8 and A-9. From the discussion involving Equations 4 and 13 of Section 2 we get

$$V_n^{-1} = \begin{cases} \dfrac{\theta}{q} & \text{if } q < K_s \ , \\ \dfrac{n_f}{q} & \text{if } q \geq K_s . \end{cases} \qquad \text{(A-10)}$$

Substituting the dependence of θ into q, K_s and n_e in Equation A-10, one obtains

$$V_n^{-1} = \begin{cases} \left(\dfrac{n_e}{q}\right)\left(\dfrac{q}{K_s}\right)^{1/\varepsilon} & \text{if } q < K_s \ , \\ \dfrac{n_f}{q} & \text{if } q \geq K_s \ . \end{cases} \qquad \text{(A-11)}$$

If the saturated matrix hydraulic conductivity, K_s, is assumed to be log-normally distributed, K_s has a cumulative distribution function (CDF) of the form

$$F(k) = P_r\left\{K_s \leq k\right\} = \frac{1}{\sqrt{2\pi}\ \sigma_\ell} \int_o^k \exp\left[\frac{-(\ell n\ z - \ell n\ z_o)^2}{2\sigma_\ell^{\,2}}\right]\frac{dz}{z} \ , \qquad \text{(A-12)}$$

where $E(K_s) = z_o\ e^{\sigma_\ell^{\,2}/2}$

$$Var(K_s) = z_o^{\,2}\ e^{\sigma_\ell^{\,2}}\ (e^{\sigma_\ell^{\,2}} - 1)$$

This standard, two-parameter distribution was also adopted for K_s in the numerical studies in Section 2.

The expectation of V_n^{-1} can be calculated if we assume that n_e, K_s, ε, and n_f are mutually independent random variables.* The

*This may not be true; n_e, K_s, and ε all depend on pore-size distribution and may be closely correlated.

conditional expectation of V_n^{-1}, given n_e, ε, and n_f, is first calculated using Equations A-11 and A-12

$$E(V_n^{-1} | n_e, \varepsilon, n_f) = \frac{n_f}{q} F(q) + n_e q^{1/\varepsilon - 1} \int_q^\infty k^{-1/\varepsilon} f(k) dk \quad , \text{ and} \qquad \text{(A-13)}$$

where $F(\cdot)$ is the log-normal CDF and $f(\cdot)$ is the associated PDF. The integral in the second term on the right-hand side of Equation A-13 can be evaluated and the result expressed rather concisely if some new notation is introduced. Redefine the CDF in Equation A-12 as

$$F(k | \ell n\ z_o, \sigma_\ell^{\ 2}),$$

making explicit the dependence on the two parameters, $\ell n\ z_o$ and $\sigma_e^{\ 2}$. Then Equation A-13 can be written as

$$E(V_n^{-1} | n_e, \varepsilon, n_f) = \frac{n_f}{q} F(q | \ell n\ z_o, \sigma_\ell^{\ 2})$$

$$+ \frac{n_e}{q} [1 - F(q | \ell n\ z_1, \sigma_\ell^{\ 2})]\ e^{-1/\varepsilon}\ [\ell n\ z_1 - \ell n\ q + \sigma_\ell^{\ 2}/2\varepsilon], \qquad \text{(A-14)}$$

where

$$\ell n\ z_1 \equiv \ell n\ z_o - \frac{\sigma_\ell^{\ 2}}{\varepsilon}.$$

Removing the conditioning on the remaining random variables is easy except for the variable ε, about which little is known; for ε, one must take a typical value for the unit. Thus, if

$\bar{n}_f \equiv E(n_f)$ and

$\bar{n}_e \equiv E(n_e)$ and

ε = a constant,

then the unconditional expectation of the groundwater travel-time is approximately

$$\bar{T} \cong d_{m,i} E(V_n^{-1}) = \frac{d_{m,i}}{q}\left\{ \bar{n}_f F(q|\ell n\, z_o, \sigma_\ell^2) + \bar{n}_e [1 - F(q|\ell n\, z_1, \sigma_\ell^2)]\, e^{1/\varepsilon [\ell n\, z_1 - \ell n\, q + \sigma_\ell^2/2\varepsilon]}\right\} \quad \text{(A-15)}$$

To estimate the variance in groundwater travel time, one first observes that

$$\sigma_T^2 = d_{m,i}\rho_v \mathrm{Var}(V_n^{-1}) = d_{m,i}\,\rho_v E\left\{\left[V_n^{-1} - E(V_n^{-1})\right]^2\right\}$$

$$= d_{m,i}\rho_v\left\{\left[E(V_n^{-1})\right]^2 - \left[E(V_n^{-1})\right]^2\right\} = d_{m,i}\rho_v E\left[(V_n^{-1})\right]^2 - \frac{\rho_v}{d_{m,i}}\bar{T}^2 . \quad \text{(A-16)}$$

Using Equation A-12 and arguments identical to the ones used in developing $E(V_n^{-1})$ through equations A-13 to A-15, one finds first that

$$E[(V_n^{-1})^2 | n_e, \varepsilon, n_f] = \frac{n_f^2}{q^2} F(q|\ell n\, z_o, \sigma_\ell^2) + \frac{n_e^2}{q^2}[1 - F(q|\ell n\, z_2, \sigma_\ell^2)]\, e^{-2/\varepsilon [\ell n\, z_2 - \ell n\, q + \sigma_\ell^2/\varepsilon]}$$

where $\ell n\, z_2 \equiv \ell n\, z_o - \frac{2\sigma_\ell^2}{\varepsilon} = \ell n\, z_1 - \frac{\sigma_\ell^2}{\varepsilon}$ (A-17)

Then, upon observing that

$$E(n_f^2) = Var(n_f) + (\bar{n}_f)^2 \quad , \text{ and}$$

$$E(n_e^2) = Var(n_e) + (\bar{n}_e)^2 \quad ,$$

one can remove the conditioning on n_e, ε, n_f in Equation A-17 to finally obtain

$$E\left[(V_n^{-1})^2\right] = \frac{1}{q^2}\left\{\left[Var(n_f) + (\bar{n}_f)^2\right] \cdot F(q|\ell n\ z_o,\ \sigma_\ell^2)\right. \tag{A-18}$$

$$\left. + \left[Var(n_e) + (\bar{n}_e)^2\right] \cdot \left[1 - F(q|\ell n\ z_2,\ \sigma_\ell^2)\right] \cdot e^{-2/\varepsilon\left[\ell n\ z_2 - \ell n\ q + \sigma_\ell^2/\varepsilon\right]}\right\} \quad .$$

Equations A-15 through A-18 give estimates of the mean and variance of the water travel time through a rock unit of thickness $d_{m,i}$ in terms of percolation flux and simple statistical measures (mean and variance) of the natural variability of key hydrologic parameters.

To summarize, if the vertical correlation length, ρ_v, is small compared to the thickness of a rock unit, $d_{m,i}$, then the water travel times through the unit are approximately normally distributed with mean, $\bar{T}$, and variance, σ_T^2, as described by equations A-15 through A-18 of this appendix.

A-3 Travel-Time Distributions Through a Column of Rock Units

If the travel-time distribution for a single rock unit is taken to be a normal distribution with defined mean, $\bar{T}$, and variance, σ_T^2, then the

travel-time distribution for the m^{th} column of rock units should also be a normal distribution with mean

$$\bar{T}(m) \equiv \sum_{i=1}^{I_m} \bar{T}_i, \qquad \text{(A-19)}$$

where $\bar{T}_i \equiv \bar{T}\,[d_{m,i}]$ is prescribed by Equation A-15, and I_m is the number of rock units in the m^{th} column. The variance is given by

$$\sigma_T^2(m) \equiv \sum_{i=1}^{I_m} \sigma_T^2(i), \qquad \text{(A-20)}$$

where $\sigma_T^2(i) \equiv \sigma_T^2[d_{m,i}]$ is prescribed by Equations A-16 through A-18.

A-4 Travel-Time Distributions for Water Particles Released at Any Point in the Disturbed-Zone Boundary Below the Repository Area

The surface describing the disturbed-zone boundary under the repository area is divided into M patches of equal area; the m^{th} patch will be centered at coordinates (x_m, y_m), which also specify the location of the m^{th} rock column. The probability that a water particle released in the m^{th} patch will reach the water table in a time interval less than t will be taken as the travel-time distribution for the m^{th} column described in Section A-3. Under the assumptions of A-3, these distributions are normal CDFs with different means and variances that differ mainly because of the different unit thicknesses appearing under each of the M patches; these CDFs may also be regarded as conditional probabilities and defined as follows:

$F_c(t|m)$ = probability that a water particle will reach the water table in time $\leq$ t, given that particle is released in the m^{th} patch, or column, $(1 \leq m \leq M)$.

If p(m) is the probability that a water particle is released in the m^{th} patch at t = 0, then the unconditional probability that a particle released at any point on the disturbed-zone boundary at t = 0 will reach the water table in a time less than, or equal to, t > 0 is

$$\sum_{m=1}^{M} F_c(t|m)p(m) \quad . \tag{A-21}$$

This is the desired travel-time distribution. To proceed further, one must have the form of p(m). Here, we will assume that release from each of the M patches is equally probable, i.e.,

$$p(m) = \frac{1}{M} \qquad m = 1,2, \ . \ . \ . \ M \quad . \tag{A-22}$$

Then the desired travel-time distribution (CDF) is

$$\frac{1}{M} \sum_{m=1}^{M} F_c(t|m) \quad . \tag{A-23}$$

Note that this is not a normal distribution (the weighted sum of normal distributions is not normal unless each distribution has the same mean and variance).

The mean and variance of the travel-time distribution, Equation A-23, are easily computed; the mean of Equation A-23 is just the arithmetic average of the column means, i.e.,

$$\frac{1}{M} \sum_{m=1}^{M} \bar{T}(m), \qquad \bar{T}(m) \text{ as given by Equation A-19.} \tag{A-24}$$

The variance of the travel-time distribution, Equation A-23, is

$$\frac{1}{M} \sum_{m=1}^{M} \sigma_T^2(m) + \frac{1}{M} \sum_{m=1}^{M} \bar{T}^2(m) - \frac{1}{M^2} \left[\sum_{m=1}^{M} T(m) \right]^2 , \tag{A-25}$$

with $\sigma_T^2(m)$ as given by Equation A-20. Note that the last two terms in Equation A-25 constitute the variance of the column means, $\bar{T}(m)$.

A-5 Summary

The analytical model developed in earlier sections of this appendix shows that

(1) the travel-time distribution through a rock unit, having thickness $d_{m,i}$, is approximately normal, with mean and variance given by Equations A-15 and A-16, respectively, and the auxiliary equations A-12 and A-17. The approximation to a normal distribution is strongest when ρ_v, the correlation length for the velocity field, is small compared to $d_{m,i}$. The variance in travel time is proportional to $d_{m,i}$ and ρ_v;

(2) the travel-time distribution through the m^{th} column of rock units is also approximately normal with mean and variance as given by Equations A-19 and A-20, respectively;

(3) the travel-time distribution for a water particle released at any point on the disturbed-zone boundary below the repository area is the arithmetic average of the travel-time distributions through the M rock columns described in item (2) above; in general, it is not a normal distribution.

The relationships developed in this appendix provide a means of calculating the distribution of water travel times between the disturbed-zone boundary and the water table, without recourse to Monte Carlo simulations of the type described in Chapter 2, provided, of course, that the assumptions made in developing these relations are valid. The analytical relationships developed in this appendix have not yet been tested for agreement with results of the Monte Carlo simulations.

APPENDIX B

SOURCE DATA FOR ESTIMATING EFFECTIVE POROSITY, SATURATED MATRIX HYDRAULIC CONDUCTIVITY, AND RELATIVE HYDRAULIC CONDUCTIVITY

Statistical distributions were compiled from the hydraulic parameters needed for calculating travel times for each of the seven hydrogeologic units. The means and standard deviations of effective matrix porosity and saturated matrix hydraulic conductivity, and the Brooks-Corey exponent for the relative hydraulic conductivity, are presented in the following subsections.

B-1 Effective Matrix Porosity Data

To estimate the effective porosity, n_e, for each hydrogeologic unit, the matrix porosity, n_b, and residual saturation, S_r, of each unit were compiled. Porosity data and hydrogeologic stratigraphic designators exist for only four drillholes, UE-25a#1, USW G-1, USW G-4, and USW GU-3. Hydrological stratigraphies for these holes, as a function of depth (drilling distance) are presented in Table B-1. Given the depth ranges in each drillhole for each hydrogeologic unit, matrix porosity and depth data on a unit-by-unit basis across all four drillholes were retrieved from NNWSI Tuff Data Base (TUFFDB, 1985). The results in the percentage values are presented in Table B-2. At the end of each hydrogeologic unit, the mean and standard deviation of matrix porosity ($\bar{n}_b$ and $\sigma[n_b]$) are given. Plots of matrix porosity as a function of depth for each drillhole are shown in Figure B-1.

Residual saturation values were obtained from Peters et al. (1984). Using the hydrogeologic stratigraphies for drillholes USW G-4 and USW GU-3 (Table B-3) the data were organized by hydrogeologic units. These data are presented in Table B-3 along with drillhole names and depths of the specimens from which the measurements were taken. The mean values, $\bar{S}_r$, are presented below the tables for each hydrological unit.

Given means and standard deviations for the matrix porosities and residual saturations for each unit, means and standard deviations for the effective porosity, n_e, were calculated by

$$\bar{n}_e = (1 - \bar{S}_r)\bar{n}_b \quad \text{and} \tag{B-1}$$

$$\sigma[n_e] = (1 - \bar{S}_r)\ \sigma[n_b] \quad . \tag{B-2}$$

The results of these calculations are presented in Table B-4.

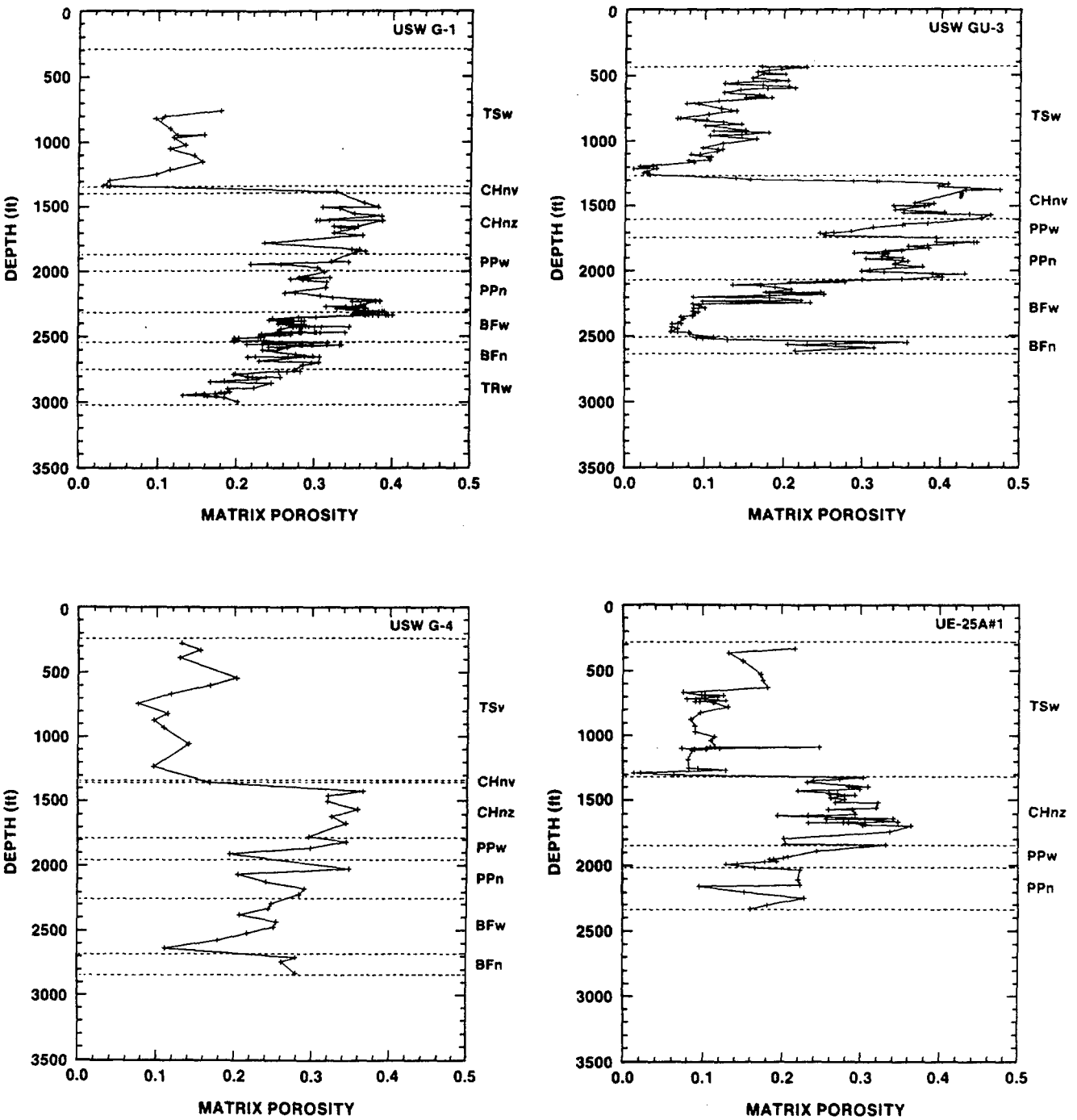

Figure B-1. Plots of porosity data as a function of depth for drillholes UE-25a#1, USW G-1, USW G-4, and USW G-U3.

TABLE B-1

Effective Matrix Porosity and Residual Saturation for Each Hydrogeologic Unit

Hydrological Unit*	Drill Hole: UE-25 a#1 Elev[a] (ft)	UE-25 a#1 Depth[b] (ft)	USW G-1 Elev[a] (ft)	USW G-1 Depth[b] (ft)	USW G-4 Elev[a] (ft)	USW G-4 Depth[b] (ft)	USW G-3 Elev[a] (ft)	USW G-3 Depth[b] (ft)	Matrix Porosity n_b: Number of Samples	Mean	Standard Deviation	Residual Saturations S_r: Number of Samples	Mean	Standard Deviation
TCw	3904	30	4289	60	4137	30	4857	ND	NC	NC	NC	NC	NC	NC
PTn	3739	195	ND	ND	4049	118	4514	343	NC	NC	NC	NC	NC	NC
TS1	3656	277	4069	280	3924	243	4427	430	NC	NC	NC	NC	NC	NC
DZ	2759	1175	3113	1236	3020	1145	3642	1215	NA	NA	NA	NA	NA	NA
TSw	2673	1261	3062	1287	2876	1288	3670	1187	137	0.117	0.049	12	0.091	0.092
CHnv	ND	ND	3007	1342	2824	1343	3299	1560	23	0.354	0.092	6	0.085	0.066
CHnz	2100	1834	2548	1801	2411	1756	ND	ND	65	0.306	0.048	9	0.121	0.267
PPw	2092	1842	2481	1868	2380	1787	3258	1601	27	0.256	0.069	4	0.069	0.038
PPn	1925	2009	2552	1997	2213	1954	3111	1746	74	0.324	0.699	2	0.228	0.094
BFw	ND	ND	2032	2317	1917	2250	2789	2070	120	0.239	0.939	2	0.058	0.003
BFn	ND	ND	1710	2639	1424	2743	ND	ND	40	0.256	0.621	ND	ND	ND

* See Figure 2 for legend.
[a] Corrected elevation to the base of the unit.
[b] Corrected depth as to the base of the unit.
ND No data.
NC Not calculated.
DZ Lower disturbed zone boundary.
NA Not applied.

TABLE B-2

Matrix Porosity Data for Each Hydrogeologic Unit*

Unit	Hole	Depth (ft)	Elevation (ft)	Matrix Porosity (%)
TSw	UE-25a#1	328.00	3606.40	21.79
TSw	UE-25a#1	360.00	3574.40	13.33
TSw	UE-25a#1	421.00	3513.40	15.14
TSw	UE-25a#1	524.00	3410.40	17.41
TSw	UE-25a#1	569.00	3365.40	17.72
TSw	UE-25a#1	623.00	3311.40	18.29
TSw	UE-25a#1	660.00	3274.40	7.57
TSw	UE-25a#1	680.25	3254.15	10.20
TSw	UE-25a#1	680.25	3254.15	9.84
TSw	UE-25a#1	681.35	3253.05	10.32
TSw	UE-25a#1	681.35	3253.05	12.60
TSw	UE-25a#1	696.85	3237.55	11.90
TSw	UE-25a#1	708.55	3225.85	9.13
TSw	UE-25a#1	708.55	3225.85	8.00
TSw	UE-25a#1	723.00	3211.40	12.90
TSw	UE-25a#1	730.60	3203.80	9.06
TSw	UE-25a#1	730.60	3203.80	9.60
TSw	UE-25a#1	733.00	3201.40	11.42
TSw	UE-25a#1	739.00	3195.40	11.30
TSw	UE-25a#1	772.00	3162.40	13.23
TSw	UE-25a#1	816.00	3118.40	9.77
TSw	UE-25a#1	866.00	3068.40	8.56
TSw	UE-25a#1	921.00	3013.40	9.06
TSw	UE-25a#1	969.00	2965.40	9.06
TSw	UE-25a#1	1010.00	2924.40	11.51
TSw	UE-25a#1	1040.00	2894.40	11.07
TSw	UE-25a#1	1090.00	2844.40	11.67
TSw	UE-25a#1	1090.00	2844.40	11.02
TSw	UE-25a#1	1091.40	2843.00	24.90
TSw	UE-25a#1	1101.10	2833.30	12.20
TSw	UE-25a#1	1101.10	2833.30	7.39
TSw	UE-25a#1	1101.85	2832.55	10.55
TSw	UE-25a#1	1106.30	2828.10	8.98
TSw	UE-25a#1	1106.30	2828.10	10.42
TSw	UE-25a#1	1112.00	2822.40	8.70
TSw	UE-25a#1	1183.00	2751.40	8.17
TSw	UE-25a#1	1249.00	2685.40	8.27
TSw	UE-25a#1	1253.00	2681.40	9.41
TSw	UE-25a#1	1266.00	2668.40	12.90
TSw	UE-25a#1	1285.55	2648.85	2.14
TSw	UE-25a#1	1285.80	2648.60	1.28
TSw	UE-25a#1	1304.00	2630.40	6.36
TSw	USW GU-3	435.20	ND	17.19
TSw	USW GU-3	435.80	4420.80	22.87

*From Tuff Data Base System 2000 - Source TUFFBD Product No. 1, 1986.
ND-No data.

Table B-2 (continued)

Unit	Hole	Depth (ft)	Elevation (ft)	Matrix Porosity (%)
TSw	USW GU-3	452.50	4404.10	19.61
TSw	USW GU-3	461.10	ND	18.04
TSw	USW GU-3	475.80	4380.80	16.60
TSw	USW GU-3	490.40	4366.20	20.16
TSw	USW GU-3	492.20	4364.40	17.32
TSw	USW GU-3	519.80	4336.80	16.00
TSw	USW GU-3	542.70	4313.90	20.48
TSw	USW GU-3	543.60	4313.00	18.97
TSw	USW GU-3	552.30	ND	14.06
TSw	USW GU-3	561.00	4295.60	12.45
TSw	USW GU-3	576.00	ND	17.27
TSw	USW GU-3	586.50	4270.10	20.63
TSw	USW GU-3	600.10	4256.50	21.43
TSw	USW GU-3	600.30	4256.30	17.86
TSw	USW GU-3	610.30	ND	14.46
TSw	USW GU-3	631.10	4225.50	12.35
TSw	USW GU-3	652.00	4204.60	16.86
TSw	USW GU-3	660.30	ND	17.44
TSw	USW GU-3	669.40	4187.20	15.14
TSw	USW GU-3	670.40	4186.20	18.43
TSw	USW GU-3	693.70	4162.90	11.65
TSw	USW GU-3	712.40	4144.20	7.57
TSw	USW GU-3	713.18	ND	9.09
TSw	USW GU-3	753.00	4103.60	11.95
TSw	USW GU-3	753.40	4103.20	12.00
TSw	USW GU-3	765.00	ND	13.20
TSw	USW GU-3	770.00	4086.60	13.94
TSw	USW GU-3	795.00	4061.60	10.36
TSw	USW GU-3	825.60	ND	6.75
TSw	USW GU-3	826.30	4030.30	6.43
TSw	USW GU-3	837.30	4019.30	10.16
TSw	USW GU-3	841.00	4015.60	8.70
TSw	USW GU-3	857.10	3999.50	12.26
TSw	USW GU-3	873.60	3983.00	14.62
TSw	USW GU-3	884.10	ND	10.00
TSw	USW GU-3	921.50	3935.10	15.18
TSw	USW GU-3	923.70	3932.90	15.08
TSw	USW GU-3	925.00	ND	11.07
TSw	USW GU-3	938.40	3918.20	18.08
TSw	USW GU-3	953.80	3902.80	14.62
TSw	USW GU-3	957.70	ND	10.59
TSw	USW GU-3	986.60	3870.00	16.54
TSw	USW GU-3	1023.60	3833.00	12.20
TSw	USW GU-3	1055.80	ND	9.65
TSw	USW GU-3	1069.30	3787.30	11.58
TSw	USW GU-3	1069.80	3786.80	12.16
TSw	USW GU-3	1084.80	3771.80	11.49
TSw	USW GU-3	1104.40	3752.20	9.34

Table B-2 (continued)

Unit	Hole	Depth (ft)	Elevation (ft)	Matrix Porosity (%)
TSw	USW GU-3	1108.90	ND	8.20
TSw	USW GU-3	1124.40	3732.20	10.77
TSw	USW GU-3	1131.10	3725.50	10.42
TSw	USW GU-3	1149.20	3707.40	10.59
TSw	USW GU-3	1152.30	3704.30	7.87
TSw	USW GU-3	1165.90	ND	8.56
TSw	USW GU-3	1194.90	3661.70	1.70
TSw	USW GU-3	1196.00	3660.60	3.33
TSw	USW GU-3	1213.20	ND	0.85
TSw	USW GU-3	1214.10	3642.50	3.80
TSw	USW GU-3	1234.40	3622.20	2.53
TSw	USW GU-3	1247.00	3609.60	2.11
TSw	USW GU-3	1247.60	3609.00	2.53
TSw	USW GU-3	1261.80	ND	2.93
TSw	USW G-1	751.80	3596.80	17.93
TSw	USW G-1	795.00	3553.60	10.71
TSw	USW G-1	810.00	3538.60	9.56
TSw	USW G-1	810.00	3538.60	10.36
TSw	USW G-1	890.30	3458.30	11.42
TSw	USW G-1	939.00	3409.60	15.83
TSw	USW G-1	939.00	3409.60	12.35
TSw	USW G-1	959.40	3389.20	11.90
TSw	USW G-1	1017.60	3331.00	13.39
TSw	USW G-1	1047.10	3301.50	11.37
TSw	USW G-1	1100.10	3248.50	14.57
TSw	USW G-1	1151.10	3197.50	15.63
TSw	USW G-1	1210.70	3137.90	11.42
TSw	USW G-1	1245.00	3103.60	9.69
TSw	USW G-1	1288.40	3060.20	3.73
TSw	USW G-1	1330.00	3018.60	2.94
TSw	USW G-1	1330.00	3018.60	3.36
TSw	USW G-1	1330.00	3018.60	3.77
TSw	USW G-1	1332.80	3015.80	3.75
TSw	USW G-4	280.40	ND	13.23
TSw	USW G-4	332.30	ND	15.63
TSw	USW G-4	390.30	ND	12.99
TSw	USW G-4	548.40	ND	20.32
TSw	USW G-4	602.60	ND	16.93
TSw	USW G-4	668.60	ND	11.86
TSw	USW G-4	742.50	ND	7.60
TSw	USW G-4	821.20	ND	11.46
TSw	USW G-4	875.50	ND	9.69
TSw	USW G-4	937.60	ND	10.94
TSw	USW G-4	1064.50	ND	14.12
TSw	USW G-4	1239.20	ND	9.65
			Mean	11.68
			Standard Deviation =	4.87

Table B-2 (continued)

Unit	Hole	Depth (ft)	Elevation (ft)	Matrix Porosity (%)
CHnv	USW GU-3	1287.90	3568.70	13.92
CHnv	USW GU-3	1297.80	3558.80	15.74
CHnv	USW GU-3	1310.90	ND	28.88
CHnv	USW GU-3	1312.10	3544.50	32.19
CHnv	USW GU-3	1312.60	3544.00	31.91
CHnv	USW GU-3	1330.40	3526.20	40.97
CHnv	USW GU-3	1351.30	3505.30	39.83
CHnv	USW GU-3	1377.70	3478.90	47.64
CHnv	USW GU-3	1378.10	3478.50	43.29
CHnv	USW GU-3	1477.20	ND	36.77
CHnv	USW GU-3	1481.90	3374.70	39.21
CHnv	USW GU-3	1497.20	3359.40	38.53
CHnv	USW GU-3	1497.80	3358.80	38.03
CHnv	USW GU-3	1501.80	ND	34.08
CHnv	USW GU-3	1503.00	3353.60	37.99
CHnv	USW GU-3	1533.80	3322.80	34.29
CHnv	USW GU-3	1549.00	3307.60	40.55
CHnv	USW GU-3	1554.90	3301.70	35.34
CHnv	USW GU-3	1566.00	ND	43.72
CHnv	USW GU-3	1571.10	3285.50	46.41
CHnv	USW GU-3	1594.60	3262.00	45.23
CHnv	USW G-1	1385.20	2963.40	32.91
CHnv	USW G-4	1361.50	ND	16.88
CHnv	USW G-1	1667.00	2681.60	35.25
CHnv	USW G-1	1705.50	2643.10	32.62
CHnv	USW G-1	1722.30	2626.30	36.29
CHnv	USW G-1	1784.50	2564.10	23.66
CHnv	USW G-1	1832.00	2516.60	35.86
CHnv	USW G-1	1832.00	2516.60	34.87
CHnv	USW G-1	1847.00	2501.60	36.59
CHnv	USW G-1	1847.00	2501.60	35.54
CHnv	USW G-4	1431.50	ND	36.64
CHnv	USW G-4	1468.20	ND	32.16
CHnv	USW G-4	1511.40	ND	32.05
CHnv	USW G-4	1570.30	ND	35.93
CHnv	USW G-4	1627.20	ND	32.62
CHnv	USW G-4	1678.40	ND	34.45
CHnv	USW G-4	1784.30	ND	29.66
			Mean	35.41
			Standard Deviation =	9.25

Table B-2 (continued)

Unit	Hole	Depth (ft)	Elevation (ft)	Matrix Porosity (%)
CHnz	UE-25a#1	1324.00	2610.40	30.47
CHnz	UE-25a#1	1338.00	2596.40	27.49
CHnz	UE-25a#1	1349.00	2585.40	24.14
CHnz	UE-25a#1	1361.00	2573.40	23.38
CHnz	UE-25a#1	1394.90	2539.50	31.11
CHnz	UE-25a#1	1394.90	2539.50	28.64
CHnz	UE-25a#1	1411.00	2523.40	30.04
CHnz	UE-25a#1	1423.80	2510.60	22.17
CHnz	UE-25a#1	1446.40	2488.00	27.19
CHnz	UE-25a#1	1446.40	2488.00	26.15
CHnz	UE-25a#1	1461.20	2473.20	29.41
CHnz	UE-25a#1	1464.00	2470.40	28.09
CHnz	UE-25a#1	1478.40	2456.00	26.39
CHnz	UE-25a#1	1478.40	2456.00	26.32
CHnz	UE-25a#1	1490.00	2444.40	28.10
CHnz	UE-25a#1	1513.60	2420.80	26.94
CHnz	UE-25a#1	1516.00	2418.40	32.34
CHnz	UE-25a#1	1555.00	2379.40	32.11
CHnz	UE-25a#1	1566.45	2367.95	26.01
CHnz	UE-25a#1	1568.00	2366.40	29.11
CHnz	UE-25a#1	1605.00	2329.40	29.50
CHnz	UE-25a#1	1612.20	2322.20	23.45
CHnz	UE-25a#1	1612.20	2322.20	19.62
CHnz	UE-25a#1	1638.00	2296.40	34.33
CHnz	UE-25a#1	1641.50	2292.90	25.81
CHnz	UE-25a#1	1641.50	2292.90	30.74
CHnz	UE-25a#1	1662.00	2272.40	34.90
CHnz	UE-25a#1	1667.85	2266.55	23.53
CHnz	UE-25a#1	1667.85	2266.55	28.63
CHnz	UE-25a#1	1667.85	2266.55	28.00
CHnz	UE-25a#1	1680.50	2253.90	30.74
CHnz	UE-25a#1	1686.00	2248.40	30.47
CHnz	UE-25a#1	1692.00	2242.40	36.60
CHnz	UE-25a#1	1741.00	2193.40	33.90
CHnz	UE-25a#1	1791.00	2143.40	20.40
CHnz	UE-25a#1	1833.00	2101.40	20.58
CHnz	UE-25a#1	1842.00	2092.40	33.33
CHnz	USW G-1	1469.90	ND	36.51
CHnz	USW G-1	1503.00	2845.60	38.31
CHnz	USW G-1	1505.00	2843.60	31.14
CHnz	USW G-1	1514.80	2833.80	33.33
CHnz	USW G-1	1553.00	2795.60	35.22
CHnz	USW G-1	1571.20	2777.40	38.75
CHnz	USW G-1	1606.00	2742.60	30.80
CHnz	USW G-1	1606.00	2742.60	32.00
CHnz	USW G-1	1606.00	2742.60	30.36
CHnz	USW G-1	1606.00	2742.60	38.87
CHnz	USW G-1	1652.00	2696.60	35.71
CHnz	USW G-1	1652.00	2696.60	32.62
CHnz	USW G-1	1663.50	2685.10	33.47

Table B-2 (continued)

Unit	Hole	Depth (ft)	Elevation (ft)	Matrix Porosity (%)
CHnz	USW G-1	1667.00	2681.60	35.25
CHnz	USW G-1	1705.50	2643.10	32.62
CHnz	USW G-1	1722.30	2626.30	36.29
CHnz	USW G-1	1784.50	2564.10	23.66
CHnz	USW G-1	1832.00	2516.60	35.86
CHnz	USW G-1	1832.00	2516.60	34.87
CHnz	USW G-1	1847.00	2501.60	36.59
CHnz	USW G-1	1846.00	2501.60	35.34
CHnz	USW G-4	1431.50	ND	36.64
CHnz	USW G-4	1468.20	ND	32.16
CHnz	USW G-4	1511.40	ND	32.05
CHnz	USW G-4	1570.30	ND	35.93
CHnz	USW G-4	1627.20	ND	32.62
CHnz	USW G-4	1678.40	ND	34.45
CHnz	USW G-4	1784.30	ND	29.66
			Mean	30.64
			Standard Deviation =	4.76

Table B-2 (continued)

Unit	Hole	Depth (ft)	Elevation (ft)	Matrix Porosity (%)
PPw	UE-25a#1	1888.00	2046.40	24.62
PPw	UE-25a#1	1930.00	2004.40	21.00
PPw	UE-25a#1	1930.00	2004.40	21.00
PPw	UE-25a#1	1942.00	1992.40	20.38
PPw	UE-25a#1	1948.00	1986.40	19.10
PPw	UE-25a#1	1949.00	1985.40	18.63
PPw	UE-25a#1	1966.00	1968.40	19.47
PPw	UE-25a#1	1968.00	1966.40	18.00
PPw	UE-25a#1	1985.00	1949.40	14.50
PPw	UE-25a#1	1988.00	1946.40	13.08
PPw	USW GU-3	1637.20	3219.40	38.46
PPw	USW GU-3	1637.70	ND	35.55
PPw	USW GU-3	1652.60	3204.00	35.27
PPw	USW GU-3	1666.70	ND	31.52
PPw	USW GU-3	1698.70	3157.90	28.68
PPw	USW GU-3	1706.60	ND	26.46
PPw	USW GU-3	1711.50	3145.10	25.49
PPw	USW GU-3	1711.80	3144.80	24.71
PPw	USW GU-3	1730.90	3125.70	25.59
PPw	USW G-1	1926.60	2422.00	32.32
PPw	USW G-1	1930.00	2418.60	34.51
PPw	USW G-1	1947.00	2401.60	21.91
PPw	USW G-1	1948.00	2400.60	25.78
PPw	USW G-1	1973.70	2374.90	30.56
PPw	USW G-4	1822.80	ND	34.48
PPw	USW G-4	1870.70	ND	29.89
PPw	USW G-4	1915.80	ND	19.53
			Mean	25.57
			Standard Deviation =	6.90

Table B-2 (continued)

Unit	Hole	Depth (ft)	Elevation (ft)	Matrix Porosity (%)
PPn	UE-25a#1	2014.00	1920.40	16.70
PPn	UE-25a#1	2032.00	1902.40	22.44
PPn	UE-25a#1	2108.00	1826.40	22.18
PPn	UE-25a#1	2149.00	1785.40	22.52
PPn	UE-25a#1	2159.00	1775.40	9.70
PPn	UE-25a#1	2201.00	1733.40	15.38
PPn	UE-25a#1	2247.00	1687.40	22.98
PPn	UE-25a#1	2300.00	1634.40	18.26
PPn	UE-25a#1	2331.00	1603.40	16.12
PPn	USW GU-3	1749.00	3107.60	39.53
PPn	USW GU-3	1779.60	ND	39.58
PPn	USW GU-3	1780.30	3076.30	44.72
PPn	USW GU-3	1781.00	3075.60	44.31
PPn	USW GU-3	1793.00	3063.60	41.74
PPn	USW GU-3	1809.20	3047.40	38.40
PPn	USW GU-3	1813.50	ND	35.98
PPn	USW GU-3	1828.40	3028.20	38.59
PPn	USW GU-3	1851.30	3005.30	33.05
PPn	USW GU-3	1851.60	3005.00	35.12
PPn	USW GU-3	1866.90	ND	29.06
PPn	USW GU-3	1873.40	2983.20	33.33
PPn	USW GU-3	1894.70	2961.90	32.63
PPn	USW GU-3	1908.30	2948.30	35.29
PPn	USW GU-3	1912.70	ND	30.60
PPn	USW GU-3	1929.30	2927.30	35.93
PPn	USW GU-3	1950.00	2906.60	34.33
PPn	USW GU-3	1958.40	ND	34.32
PPn	USW GU-3	1970.90	2885.70	37.82
PPn	USW GU-3	1997.00	2859.60	31.09
PPn	USW GU-3	2008.40	ND	30.08
PPn	USW GU-3	2014.30	2842.30	32.91
PPn	USW GU-3	2027.80	2828.80	43.19
PPn	USW GU-3	2028.80	2827.80	39.08
PPn	USW GU-3	2050.50	2806.10	40.31
PPn	USW GU-3	2069.60	2787.00	35.14
PPn	USW G-1	2010.00	2338.60	31.40
PPn	USW G-1	2050.00	2298.60	28.15
PPn	USW G-1	2052.00	2296.60	32.11
PPn	USW G-1	2064.90	2283.70	27.00
PPn	USW G-1	2065.00	2283.60	29.24
PPn	USW G-1	2066.00	2282.60	29.29
PPn	USW G-1	2070.00	2278.60	28.63
PPn	USW G-1	2086.00	2262.60	31.67
PPn	USW G-1	2128.00	2220.60	31.54
PPn	USW G-1	2170.00	2178.60	27.64
PPn	USW G-1	2170.00	2178.60	26.32
PPn	USW G-1	2192.00	2156.60	30.89
PPn	USW G-1	2206.00	2142.60	32.51
PPn	USW G-1	2227.00	2121.60	38.52

Table B-2 (continued)

Unit	Hole	Depth (ft)	Elevation (ft)	Matrix Porosity (%)
PPn	USW G-1	2232.00	2116.60	38.52
PPn	USW G-1	2233.00	2115.60	35.00
PPn	USW G-1	2233.00	2115.60	38.00
PPn	USW G-1	2261.00	2087.60	36.10
PPn	USW G-1	2265.00	2083.60	36.48
PPn	USW G-1	2273.40	2075.20	35.39
PPn	USW G-1	2274.40	2074.20	31.60
PPn	USW G-1	2274.40	2074.20	35.00
PPn	USW G-1	2276.00	2072.60	34.17
PPn	USW G-1	2285.00	2063.60	36.67
PPn	USW G-1	2286.00	2062.60	35.56
PPn	USW G-1	2290.00	2058.60	33.00
PPn	USW G-1	2310.20	2038.40	37.08
PPn	USW G-1	2310.20	2038.40	38.87
PPn	USW G-1	2310.80	2037.80	39.11
PPn	USW G-1	2310.80	2037.80	35.56
PPn	USW G-1	2311.50	2037.10	36.44
PPn	USW G-1	2311.50	2037.10	35.74
PPn	USW G-1	2312.00	2036.60	35.86
PPn	USW G-1	2313.00	2035.60	38.43
PPn	USW G-4	2032.40	ND	34.82
PPn	USW G-4	2072.90	ND	20.59
PPn	USW G-4	2131.20	ND	24.17
PPn	USW G-4	2181.80	ND	29.17
PPn	USW G-4	2228.50	ND	28.45
			Mean	32.39
			Standard Deviation =	6.99

Table B-2 (continued)

Unit	Hole	Depth (ft)	Elevation (ft)	Matrix Porosity (%)
BFw	USW GU-3	2075.00	ND	30.12
BFw	USW GU-3	2091.10	2765.50	20.85
BFw	USW GU-3	2091.50	2765.10	27.91
BFw	USW GU-3	2110.00	ND	13.57
BFw	USW GU-3	2118.40	2738.20	17.12
BFw	USW GU-3	2129.80	2726.80	18.99
BFw	USW GU-3	2149.80	2706.80	21.01
BFw	USW GU-3	2167.50	ND	17.83
BFw	USW GU-3	2169.10	2687.50	24.81
BFw	USW GU-3	2175.50	2681.10	18.29
BFw	USW GU-3	2186.30	2670.30	25.29
BFw	USW GU-3	2204.90	ND	8.59
BFw	USW GU-3	2209.20	2647.40	18.36
BFw	USW GU-3	2231.00	2625.60	22.35
BFw	USW GU-3	2236.10	2620.50	9.77
BFw	USW GU-3	2249.20	2607.40	23.53
BFw	USW GU-3	2256.80	ND	8.56
BFw	USW GU-3	2265.70	2590.90	9.30
BFw	USW GU-3	2288.60	2568.00	10.08
BFw	USW GU-3	2290.40	2566.20	8.66
BFw	USW GU-3	2315.00	ND	8.53
BFw	USW GU-3	2317.40	2539.20	9.20
BFw	USW GU-3	2323.10	2533.50	8.91
BFw	USW GU-3	2348.00	2508.60	8.53
BFw	USW GU-3	2350.00	2506.60	8.49
BFw	USW GU-3	2356.70	ND	6.98
BFw	USW GU-3	2369.60	2487.00	7.34
BFw	USW GU-3	2404.30	2452.30	6.64
BFw	USW GU-3	2407.20	ND	7.03
BFw	USW GU-3	2408.80	2447.80	5.88
BFw	USW GU-3	2432.40	2424.20	5.88
BFw	USW GU-3	2447.30	2409.30	6.64
BFw	USW GU-3	2468.50	ND	5.77
BFw	USW GU-3	2471.80	2384.80	6.61
BFw	USW GU-3	2476.30	2380.30	8.08
BFw	USW GU-3	2488.80	2367.80	8.14
BFw	USW G-1	2321.00	2027.60	37.60
BFw	USW G-1	2321.00	2027.60	36.33
BFw	USW G-1	2321.00	2027.60	37.01
BFw	USW G-1	2321.00	2027.60	35.83
BFw	USW G-1	2321.00	2027.60	36.22
BFw	USW G-1	2321.00	2027.60	36.61
BFw	USW G-1	2332.00	2016.60	36.43
BFw	USW G-1	2333.00	2015.60	37.00
BFw	USW G-1	2333.00	2015.60	35.00

Table B-2 (continued)

Unit	Hole	Depth (ft)	Elevation (ft)	Matrix Porosity (%)
BFw	USW G-1	2338.00	2010.60	38.29
BFw	USW G-1	2338.00	2010.60	39.63
BFw	USW G-1	2338.00	2010.60	36.64
BFw	USW G-1	2338.00	2010.60	37.59
BFw	USW G-1	2338.00	2010.60	39.33
BFw	USW G-1	2338.00	2010.60	40.15
BFw	USW G-1	2338.00	2010.60	38.35
BFw	USW G-1	2338.00	2010.60	39.62
BFw	USW G-1	2355.00	1993.60	30.30
BFw	USW G-1	2355.90	1992.70	28.08
BFw	USW G-1	2367.90	1980.70	24.71
BFw	USW G-1	2371.00	1977.60	27.10
BFw	USW G-1	2380.00	1968.60	24.31
BFw	USW G-1	2380.90	1967.70	27.10
BFw	USW G-1	2380.90	1967.70	26.34
BFw	USW G-1	2380.90	1967.70	26.34
BFw	USW G-1	2382.90	1965.70	26.15
BFw	USW G-1	2385.30	1963.30	27.20
BFw	USW G-1	2385.30	1963.30	28.41
BFw	USW G-1	2385.30	1963.30	26.79
BFw	USW G-1	2385.30	1963.30	27.44
BFw	USW G-1	2385.30	1963.30	28.79
BFw	USW G-1	2388.00	1960.60	26.34
BFw	USW G-1	2388.00	1960.60	26.72
BFw	USW G-1	2388.00	1960.60	25.95
BFw	USW G-1	2392.00	1956.60	25.57
BFw	USW G-1	2405.00	1943.60	26.44
BFw	USW G-1	2405.00	1943.60	26.44
BFw	USW G-1	2405.00	1942.80	25.48
BFw	USW G-1	2414.00	1934.60	28.74
BFw	USW G-1	2414.00	1934.60	26.85
BFw	USW G-1	2428.00	1920.60	30.15
BFw	USW G-1	2428.00	1920.60	29.01
BFw	USW G-1	2428.00	1920.60	29.43
BFw	USW G-1	2428.00	1920.60	27.86
BFw	USW G-1	2428.00	1920.60	31.06
BFw	USW G-1	2428.00	1920.60	28.41
BFw	USW G-1	2428.00	1920.60	28.63
BFw	USW G-1	2428.00	1920.60	28.35
BFw	USW G-1	2428.00	1920.60	30.15
BFw	USW G-1	2428.00	1920.60	34.60
BFw	USW G-1	2428.00	1920.60	28.14
BFw	USW G-1	2429.00	1919.60	27.48
BFw	USW G-1	2429.00	1919.60	27.31
BFw	USW G-1	2445.00	1903.60	25.86
BFw	USW G-1	2468.00	1880.60	25.38
BFw	USW G-1	2472.30	1876.30	34.09
BFw	USW G-1	2472.30	1876.30	30.38
BFw	USW G-1	2472.50	1876.10	28.14
BFw	USW G-1	2472.50	1876.10	27.17

Table B-2 (continued)

Unit	Hole	Depth (ft)	Elevation (ft)	Matrix Porosity (%)
BFw	USW G-1	2473.50	1875.10	28.35
BFw	USW G-1	2473.50	1875.10	28.52
BFw	USW G-1	2474.00	1874.60	30.92
BFw	USW G-1	2474.00	1874.60	30.15
BFw	USW G-1	2480.00	1868.60	25.67
BFw	USW G-1	2485.60	1863.00	23.35
BFw	USW G-1	2493.00	1855.60	27.10
BFw	USW G-1	2493.00	1855.60	25.67
BFw	USW G-1	2501.00	1847.60	23.75
BFw	USW G-1	2509.00	1839.60	22.90
BFw	USW G-1	2510.00	1838.60	23.23
BFw	USW G-1	2517.00	1831.60	19.85
BFw	USW G-1	2518.00	1830.60	20.38
BFw	USW G-1	2530.00	1818.60	19.92
BFw	USW G-1	2536.20	1812.40	23.68
BFw	USW G-1	2536.20	1812.40	19.77
BFw	USW G-1	2538.00	1810.60	23.64
BFw	USW G-4	2298.00	ND	24.90
BFw	USW G-4	2336.80	ND	24.51
BFw	USW G-4	2381.60	ND	20.77
BFw	USW G-4	2436.10	ND	25.57
BFw	USW G-4	2478.00	ND	25.19
BFw	USW G-4	2523.70	ND	21.79
BFw	USW G-4	2577.70	ND	17.94
BFw	USW G-4	2637.50	ND	11.15
			Mean	23.91
			Standard Deviation =	9.39

Table B-2 (continued)

Unit	Hole	Depth (ft)	Elevation (ft)	Matrix Porosity (%)
BFn	USW GU-3	2513.20	2343.40	11.24
BFn	USW GU-3	2515.80	2340.80	9.02
BFn	USW GU-3	2521.50	ND	9.84
BFn	USW GU-3	2529.30	2327.30	12.99
BFn	USW GU-3	2551.40	2305.20	35.89
BFn	USW GU-3	2562.40	ND	26.81
BFn	USW GU-3	2568.00	2288.60	23.14
BFn	USW GU-3	2568.70	2287.90	20.66
BFn	USW GU-3	2592.00	2264.60	31.69
BFn	USW GU-3	2617.50	ND	21.63
BFn	USW G-1	2549.00	1799.60	31.85
BFn	USW G-1	2550.00	1798.60	25.93
BFn	USW G-1	2551.50	1797.10	23.98
BFn	USW G-1	2561.00	1787.60	23.46
BFn	USW G-1	2563.00	1785.60	21.46
BFn	USW G-1	2568.10	1780.50	31.71
BFn	USW G-1	2568.10	1780.50	28.39
BFn	USW G-1	2568.70	1779.90	28.57
BFn	USW G-1	2568.70	1779.90	33.60
BFn	USW G-1	2569.10	1779.50	29.83
BFn	USW G-1	2569.10	1779.50	33.33
BFn	USW G-1	2585.00	1763.60	24.27
BFn	USW G-1	2587.00	1761.60	26.64
BFn	USW G-1	2588.00	1760.60	26.64
BFn	USW G-1	2607.00	1741.60	25.41
BFn	USW G-1	2608.00	1740.60	23.48
BFn	USW G-1	2641.00	1707.60	27.71
BFn	USW G-1	2653.00	1695.60	29.92
BFn	USW G-1	2658.40	1690.20	30.74
BFn	USW G-1	2658.60	1690.00	22.51
BFn	USW G-1	2658.80	1689.80	26.72
BFn	USW G-1	2659.00	1689.60	21.52
BFn	USW G-1	2659.40	1689.20	28.87
BFn	USW G-1	2691.00	1657.60	23.05
BFn	USW G-1	2701.20	1647.40	29.75
BFn	USW G-1	2701.20	1647.40	30.71
BFn	USW G-1	2725.00	1623.60	28.69
BFn	USW G-4	2694.60	ND	28.05
BFn	USW G-4	2719.50	ND	25.32
BFn	USW G-4	2826.20	ND	27.87
			Mean	20.38
			Standard Deviation =	3.93

TABLE B-3

Residual Saturation for Each Hydrogeologic Unit

Unit	Sample Code	Depth (ft)	S_r
TSw	G-4	247	0.0600
TSw	G-4	864	0.0662
TSw	G-4	864	0.0578
TSw	G-4	1158	0.0801
TSw	G-4	1215	0.1199
TSw	G-4	1256	0.0704
TSw	G-4	1278	0.1198
TSw	G-4	1299	0.0517
TSw	G-4	1324	0.0026
TSw	GU-3	1132	0.0075
TSw	GU-3	1197	0.3757
TSw	GU-3	1240	0.0804
		Mean:	0.0910
CHnv	G-4	1359	0.1638
CHnv	GU-3	1311	0.0497
CHnv	GU-3	1331	0.0479
CHnv	GU-3	1440	0.0405
CHnv	GU-3	1499	0.0200
CHnv	GU-3	1555	0.1892
		Mean:	0.0852

TABLE B-3 (continued)

Unit	Sample Code	Depth (ft)	S_r
CHnz	G-4	1405	0.0100
CHnz	G-4	1548	0.1095
CHnz	G-4	1551	0.2017
CHnz	G-4	1686	0.0600
CHnz	G-4	1737	0.1000
CHnz	G-4	1769	0.2154
CHnz	G-4	1778	0.1330
CHnz	G-4	1778	0.1939
CHnz	G-4	1787	0.0370
		Mean:	0.1211
PPw	G-4	1899	0.0658
PPw	GU-3	1628	0.0180
PPw	GU-3	1680	0.0665
PPw	GU-3	1730	0.1239
		Mean:	0.0686
BFw	G-4	2006	0.1346
BFw	G-4	2101	0.3217
		Mean:	0.2282
BFn	G-4	2401	0.0608
BFn	G-4	2407	0.0559
		Mean:	0.0584

TABLE B-4

Mean and Standard Deviation of Effective Porosity

Unit	Effective Porosity	
	Mean	Standard Deviation
TSw	0.1062	0.0458
CHnv	0.3239	0.0880
CHnz	0.2693	0.0468
PPw	0.2382	0.0650
PPn	0.2500	0.0622
BFw	0.2251	0.0884
BFn*	0.2500	0.0622

*Assumed to be hydrologically identical to PPn.

B-2 Saturated Matrix Hydraulic Conductivity Data

Saturated matrix hydraulic conductivity (K_s) data were obtained from TUFFDB (1985), and Peters et al. (1984). The drillholes for which data exist are UE-25a#1, USW G-4, and USW GU-3. Plots of saturated matrix hydraulic conductivity as a function of depth for each drillhole are shown in Figure B-2. Again, using the stratigraphies for these drillholes, the conductivities were grouped by hydrologic unit in Table B-5. The natural logarithms for the conductivity values were calculated, and these are also presented in Table B-5 along with the corresponding means and standard deviations for each unit. To obtain some measure of the distribution of the conductivity values, one standard deviation was added or subtracted from the mean of the logarithms, and the inverse logarithm was then computed as follows:

$$\ln^{-1}(\text{mean}[\ln K_s] \pm \sigma[\ln K_s]) \quad .$$

Conductivity values are expressed in units of m/s, but were subsequently converted to mm/yr in Table 1 for the travel-time calculations.

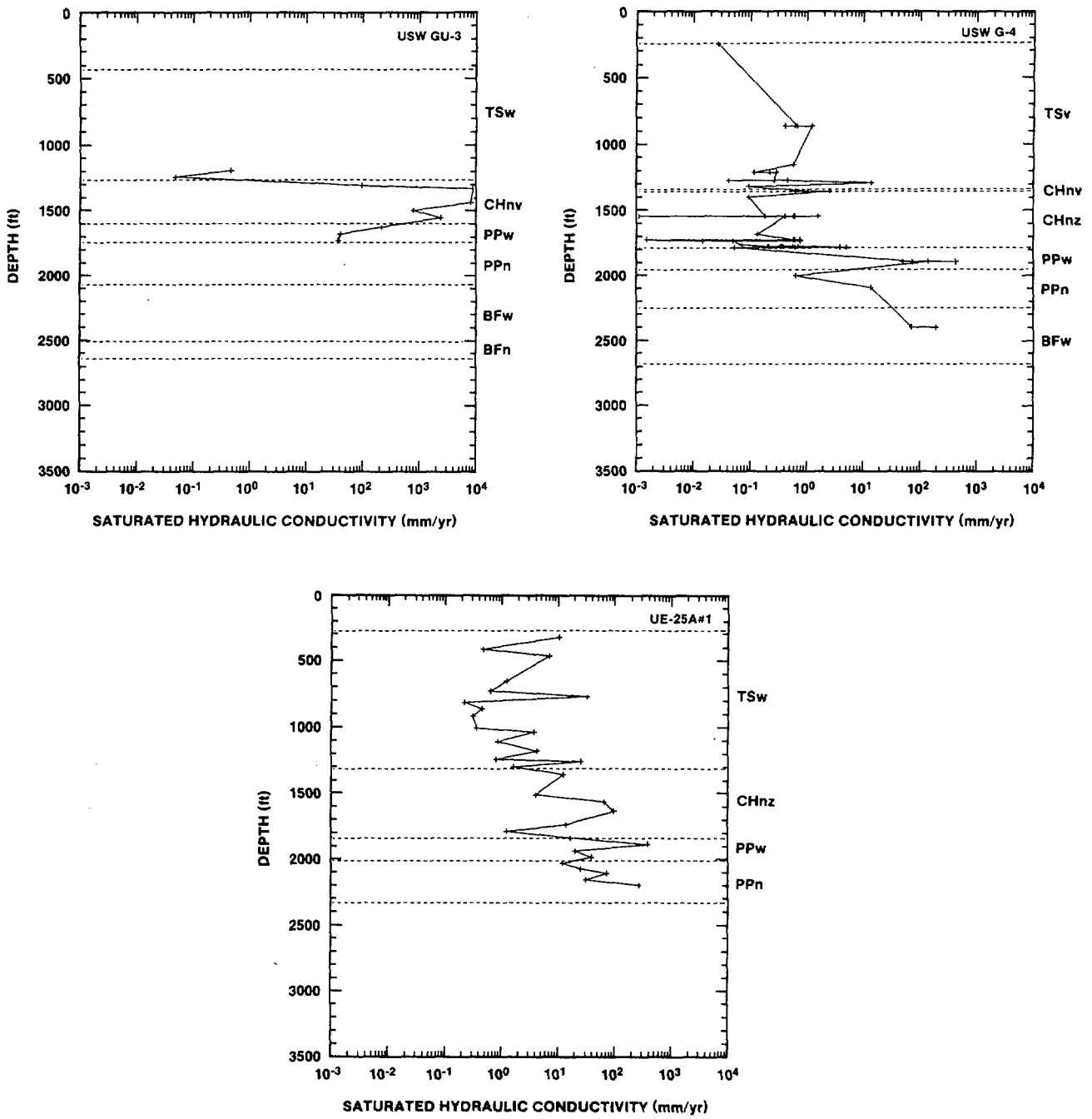

Figure B-2. Plots of saturated matrix hydraulic conductivity data as a function of depth for drillhole UE-25a#1, USW G-4, and USW GU-3.

TABLE B-5

Saturated Matrix Hydraulic Conductivity Data
from Tuff Data Base System 2000

Unit	Hole	Depth (ft)	K_s (m/s)	ln K_s (m/s)
TSw	USW G-4	247	.860D-12	-.278D+02
TSw	USW G-4	864	.217D-10	-.246D+02
TSw	USW G-4	864	.131D-10	-.251D+02
TSw	USW G-4	864	.197D-10	-.247D+02
TSw	USW G-4	864	.217D-10	-.246D+02
TSw	USW G-4	864	.390D-10	-.240D+02
TSw	USW G-4	1158	.186D-10	-.247D+02
TSw	USW G-4	1215	.377D-11	-.263D+02
TSw	USW G-4	1215	.711D-11	-.257D+02
TSw	USW G-4	1215	.919D-11	-.254D+02
TSw	USW G-4	1278	.858D-11	-.255D+02
TSw	USW G-4	1278	.134D-11	-.273D+02
TSw	USW G-4	1278	.148D-10	-.249D+02
TSw	USW G-4	1299	.447D-09	-.215D+02
TSw	USW G-4	1324	.302D-11	-.265D+02
TSw	USW GU-3	1197	.146D-10	-.249D+02
TSw	USW GU-3	1246	.152D-11	-.272D+02
TSw	UE-25a#1	328	.335D-09	-.218D+02
TSw	UE-25a#1	421	.150D-10	-.249D+02
TSw	UE-25a#1	471	.220D-09	-.222D+02
TSw	UE-25a#1	660	.391D-10	-.240D+02
TSw	UE-25a#1	733	.200D-10	-.246D+02
TSw	UE-25a#1	772	.103D-08	-.207D+02
TSw	UE-25a#1	816	.687D-11	-.257D+02
TSw	UE-25a#1	866	.143D-10	-.250D+02
TSw	UE-25a#1	921	.989D-11	-.253D+02
TSw	UE-25a#1	1010	.113D-10	-.252D+02
TSw	UE-25a#1	1040	.119D-09	-.229D+02
TSw	UE-25a#1	1112	.271D-10	-.243D+02
TSw	UE-25a#1	1183	.135D-09	-.227D+02
TSw	UE-25a#1	1249	.249D-10	-.244D+02
TSw	UE-25a#1	1266	.803D-09	-.209D+02
TSw	UE-25a#1	1304	.510D-10	-.237D+02

Mean; ln (K_s) = -.245D+02 (m/s)
Standard Deviation ln (K_s) = .173D+01 (m/s)

TABLE B-5 (continued)

Unit	Hole	Depth (ft)	K_s (m/s)	ln K_s (m/s)
CHvn	USW G-4	1359	.325D-10	-.241D+02
CHvn	USW G-4	1359	.199D-10	-.246D+02
CHvn	USW G-4	1359	.803D-10	-.232D+02
CHvn	USW GU-3	1311	.315D-08	-.196D+02
CHvn	USW GU-3	1331	.292D-06	-.150D+02
CHvn	USW GU-3	1440	.268D-06	-.151D+02
CHvn	USW GU-3	1499	.257D-07	-.175D+02
CHvn	USW GU-3	1555	.790D-07	-.164D+02

Mean ln (K_s) = -.195D+02 (m/s)
Standard Deviation ln (K_s) = .404D+01 (m/s)

CHnz	USW G-4	1405	.299D-11	-.265D+02
CHnz	USW G-4	1548	.590D-11	-.259D+02
CHnz	USW G-4	1548	.197D-10	-.247D+02
CHnz	USW G-4	1548	.237D-13	-.314D+02
CHnz	USW G-4	1551	.506D-10	-.237D+02
CHnz	USW G-4	1551	.188D-10	-.247D+02
CHnz	USW G-4	1551	.133D-10	-.250D+02
CHnz	USW G-4	1686	.424D-11	-.262D+02
CHnz	USW G-4	1728	.186D-10	-.247D+02
CHnz	USW G-4	1728	.245D-10	-.244D+02
CHnz	USW G-4	1728	.197D-10	-.247D+02
CHnz	USW G-4	1728	.469D-13	-.307D+02
CHnz	USW G-4	1737	.459D-12	-.284D+02
CHnz	USW G-4	1737	.248D-10	-.244D+02
CHnz	USW G-4	1737	.159D-11	-.272D+02
CHnz	USW G-4	1769	.230D-11	-.268D+02
CHnz	USW G-4	1778	.647D-11	-.258D+02
CHnz	USW G-4	1778	.689D-11	-.257D+02
CHnz	USW G-4	1778	.183D-10	-.247D+02
CHnz	USW G-4	1778	.225D-10	-.245D+02
CHnz	USW G-4	1787	.161D-09	-.225D+02
CHnz	USW G-4	1787	.197D-10	-.247D+02
CHnz	USW G-4	1787	.124D-09	-.228D+02
CHnz	USW G-4	1787	.168D-11	-.271D+02
CHnz	UE-25a#1	1361	.397D-09	-.216D+02
CHnz	UE-25a#1	1516	.128D-09	-.228D+02
CHnz	UE-25a#1	1568	.207D-08	-.200D+02
CHnz	UE-25a#1	1638	.314D-08	-.196D+02
CHnz	UE-25a#1	1741	.448D-09	-.215D+02
CHnz	UE-25a#1	1791	.388D-10	-.240D+02
CHnz	UE-25a#1	1842	.526D-09	-.214D+02

Mean ln (K_s) = -.248D+02 (m/s)
Standard Deviation ln (K_s) = .266D+01 (m/s)

TABLE B-5 (concluded)

Unit	Hole	Depth (ft)	K_s (m/s)	ln K_s (m/s)
PPw	USW G-4	1899	.234D-08	-.199D+02
PPw	USW G-4	1899	.138D-07	-.181D+02
PPw	USW G-4	1899	.158D-08	-.203D+02
PPw	USW G-4	1899	.446D-08	-.192D+02
PPw	USW GU-3	1628	.692D-08	-.188D+02
PPw	USW GU-3	1680	.128D-08	-.205D+02
PPw	USW GU-3	1730	.118D-08	-.206D+02
PPw	UE-25a#1	1888	.124D-07	-.182D+02
PPw	UE-25a#1	1942	.644D-09	-.212D+02
PPw	UE-25a#1	1988	.127D-08	-.205D+02
		Mean ln (K_s) = -.197D+02 (m/s)		
		Standard Deviation ln (K_s) = .109D+01 (m/s)		
PPn	USW G-4	2006	.203D-10	-.246D+02
PPn	USW G-4	2101	.436D-09	-.216D+02
PPn	UE-25a#1	2032	.383D-09	-.217D+02
PPn	UE-25a#1	2078	.805D-09	-.209D+02
PPn	UE-25a#1	2108	.236D-08	-.199D+02
PPn	UE-25a#1	2159	.101D-08	-.207D+02
PPn	UE-25a#1	2201	.891D-08	-.185D+02
		Mean ln (K_s) = -.211D+02 (m/s)		
		Standard Deviation ln (K_s) = .188D+01 (m/s)		
PFw	USW G-4	2401	.231D-08	-.199D+02
PFw	USW G-4	2407	.626D-08	-.189D+02
		Mean ln (K_s) = -.194D+02 (m/s)		
		Standard Deviation ln (K_s) = .707D+00 (m/s)		

B-3 Brooks-Corey Exponent Data

One way to estimate the relative conductivity (K_r) is to use the power formulation for effective saturation proposed by Brooks and Corey (1966). The formulation for the wetting phase relative conductivity is

$$K_r = \frac{K}{K_s} = (S_e)^{\varepsilon} = \left(\frac{S - S_r}{1 - S_r}\right)^{\varepsilon} \quad . \tag{B-3}$$

The quantity $(S - S_r)/(1 - S_r)$ is called effective saturation, S_e, and S_r is the residual saturation. Values of the exponent, ε, depend upon the pore structure of the medium under consideration and can be determined from saturation versus capillary pressure. The relative conductivity versus pressure head for each unit can be estimated from Equation B-3.

Brooks and Corey showed that ε, the slope of the curve of log K_r, is related to $-\lambda$, the slope of the curve of log S_e as a function of the logarithm of capillary pressure, by

$$\varepsilon = 3 + (2/\lambda) \quad . \tag{B-4}$$

By experimentally determining saturation versus pressure head, λ can be estimated. Brooks and Corey suggested plotting the logarithm of the effective saturation, S_e, versus the logarithm of the capillary

pressure ψ. They observed that the relationship of Equation B-4 is found to be generally valid for the consolidated rock cores analyzed in their studies.

In this analysis the relation between S_e and ψ was taken from Peters et al. (1984), by finding a straight line that fits the data fit as closely as possible when plotted on log-log scale. The exponent ϵ is then calculated by Equation B-4. The ϵ for each unit is obtained by averaging the ϵ values in Table B-6 estimated from the available retention curves within each unit.

TABLE B-6

Brooks-Corey Exponent for Each Hydrogeologic Unit

Unit	Sample Code	Depth (ft)	λ	ε
TSw	G4-5	864	0.53	6.79
TSw	G4-24	864	0.77	5.60
TSw	G4-6	1158	0.78	5.56
TSw	G4-7	1256	0.87	5.30
TSw	G4-8	1299	0.60	6.33
TSw	G4-9	1324	0.67	5.97
TSw	GU3-9	1132	0.47	7.24
TSw	GU3-10	1197	2.94	3.68
TSw	GU3-11	1246	2.17	3.93
			Average ε =	5.9
CHnv	GU3-12	1811	2.27	3.88
CHnv	GU3-13	1331	3.23	3.62
CHnv	GU3-14	1440	2.86	3.70
CHnv	GU3-15	1499	0.59	6.38
			Average ε =	4.2
CHnz	G4-10	1405	0.21	12.59
CHnz	G4-11	1548	0.60	6.31
CHnz	G4-12	1686	0.45	4.74
CHnz	G4-13	1728	0.70	5.86
CHnz	G4-14	1737	0.57	6.85
CHnz	G4-15	1769	1.50	4.33
CHnz	G4-16	1778	0.58	6.42
CHnz	G4-17	1787	0.67	6.00
CHnz	GU3-16	1555	9.09	3.22
			Average ε =	7.0
PPw	G4-18	1899	1.61	4.25
PPw	GU3-17	1628	2.44	3.82
PPw	GU3-18	1680	2.44	3.82
			Average ε =	4.0

TABLE B-6 (concluded)

Unit	Sample Code	Depth (ft)	λ	ε
PPn	G4-19	2006	1.02	4.96
PPn	G4-20	2101	0.86	5.33
PPn	GU3-19	1730	1.85	4.08
			Average ε =	5.2
BFw	G4-21	2401	1.21	4.64
BFw	G4-22	2407	0.39	8.11
			Average ε =	4.6

APPENDIX C. LISTS OF COMPUTER PROGRAMS

C-1 FORTRAN Program for Calculating Groundwater Travel Times.

```
C**********************************************************************
C
C       Travel Time Calculations
C
C       Calculate travel times for piecewise unit depths.  Break up unit
C       into constant distance intervals and select constants from
C       supplied distribution curves.  Save fracture flow and velocity
C       for each cell, travel times and # of fracture flows for each
C       unit per column, and travel time and # of fracture flows for each
C       column.
C
C       Calculations are performed in units of feet and years.
C
C**********************************************************************
C
C        Variables
C        ---------
C        colrtttc - verticle column travel time for Technetium
C        colrttu  -        "        "        "      Uranium
C        d        - distance used to calculate travel time for this cell
C        deltad   - maximum distance with which to calculate travel time
C        flux     - flux constant
C        fp       - porosity constant for fracture flow
C        fraction - saturated hydraulic conductivitiy divided by flux
C        fracture - Logical flag: T -> fracture flow conditions
C                                 F -> matrix   flow conditions
C        ftpermm  - constant for converting milimeters to feet
C        i        - temporary loop counters
C        irs      - integer random seed
C        igp      - Grid point loop counter
C        iskip    - # of units to skip before desired unit
C        itt      - ident of desired travel time: 1 -> water
C                                                 2 -> Uranium
C                                                 3 -> Technetium
C        iu       - unit loop counter
C        j,k,l,m  - temporary counters and variables
C        mefile   - character string: multiple unit elevation file name
C        mp       - sample of distributed matrix porosity
C        noc      - # of columns for this GTM
C        nocells  - # of equal-distant elements within a unit
C        nocolff  - # of fracture flows: this verticle column
C        nor      - # of rows for this GTM
C        nou      - # of units for this verticle column
C        nounitff - # of fracture flows: this unit, this verticle column
C        ratio    - constant ratio which determines fracture flow
C        rtttc    - cell travel time for Technetium
C        rttu     -      "        "    Uranium
C        shc      - sample: distributed saturated hydraulic conductivity
C        sumfile  - character string: travel time summary file name
C        sx       - x-coord of lower left point for this GTM
C        sy       - y-coord of lower left point for this GTM
C        thick    - remaining thickness of this unit
C        tt       - calculated water travel time for this cell
C        ttcol    - sum of travel times for this verticle column
C        ttcolm   - "      "       "       "       "       "  (matrix)
C        ttfile   - Character string of name of travel time file
C        ttmatrix - calculated travel time for matrix flow
C        ttunit   - sum of travel times: this unit, this column
C        ttunitm  - "      "       "       "       "       (matrix)
C        unitrtttc- "      "       "       "       "       (Technitium)
C        unitrttu - "      "       "       "       "       (Uranium)
C        velfrac  - calculated velocity of fracture flow for this cell
C        velmatrix- "      "       "     matrix flow   "     "
```

```
C       x         - temporary variable
C
C       Arrays
C       ------
C       epsilon   - unit dependent coefficients for calculating matrix
C                   velocities
C       kdtc      - unit dependent coefficients for calculating travel
C                   times of Technetium
C       kdu       - unit dependent coefficients for calculating travel
C                   times of Uranium
C       sbd       - unit dependent coefficients for calculating travel
C                   times of the radionuclides
C       unit      - thickness of each unit in this verticle column
C
C       Files
C       -----
C       Unit 1    - Input:  Multiple unit elevation file
C       Unit 2    - Output: Travel time results file
C       Unit 3    - Output: Travel time summary file
C
C       Subroutines
C       -----------
C       getdist   - Get distribution of saturated hydraulic condutivity
C                   and matrix porosity
C
C       Functions
C       ---------
C       amod      - Modulo function
C       idate     - Get system date for initializing random seed
C       random    - Random number generator
C       secnds    - "       "    seconds       "         "         "
C
C*************************************************************************
C
C       Modifications:
C        9/10/85 - Correct negative unit check                          V2.1
C        9/12/85 - New matrix velocity calculations                     V2.2
C                - Radionuclide retardation travel time calculations    V2.3
C        9/13/85 - Do not allow distribution beyond 3 sigma             V2.4
C                - Change distribution coefficients                     V2.5
C                - User input of control parameters and constants       V2.6
C        9/17/85 - Generate summary output file                         V3.1
C        9/30/85 - Allow for Fracture Flow ratio < 1.0                  V4.1
C                - Make sure porosity > 0.0                             V4.2
C       10/ 1/85 - Use largest velocity in Fracture Flow calculations   V4.3
C
C*************************************************************************
C
      CHARACTER*80 mefile,ttfile
      CHARACTER*80 sumfile                                              V3.1
C
      REAL unit(10),mp
      REAL epsilon(10)                                                  V2.2
      REAL sbd(10),kdu(10),kdtc(10)                                     V2.3
C
      LOGICAL fracture
C
      DATA   ftpermm
     +    /.00328084/
C
C                  TS   CHV  CHZ  PPW  CFU  BFW  CFM
      DATA epsilon/5.90,4.20,7.00,4.00,5.20,4.60,5.20,3*1./             V2.2
      DATA sbd    /2.36,1.85,1.95,2.20,2.00,2.23,2.00,3*0./             V2.3
```

```
      DATA kdu    /1.80,1.30,5.30,1.30,1.30,1.30,1.30,3*0./          V2.3
      DATA kdtc   /0.30,0.20,0.20,0.20,0.20,4.20,0.20,3*0./          V2.3
C
C..... Identify program to user
C
      type *,' '
      type *,'   Travel Time Calculations'
      type *,'Version 4 ... September 30,1985'
      type *,' '
C
C..... Initialize
C
      nounitff=0
      nocolff=0
      ttunit=0
      ttunitm=0
      ttcol=0
      ttcolm=0
      unitrttu =0                                                    V2.3
      unitrtttc=0                                                    V2.3
      colrttu =0                                                     V2.3
      colrtttc=0                                                     V2.3
C
      do 2 i=1,10                                                    V2.2
    2 epsilon(i)=-1./epsilon(i)                                      V2.2
C
C..... Set up random generator
C
      call idate (i,j,k)
      x=secnds (0.)
      m=amod (x,500.)
      irs=i*j+m+x/3.
      k=x/3.
      do 10 l=1,m
   10 x=ran(irs)
      type *,'Random seed:',irs
C
C..... Open multiple elevations and travel time files
C
      type *,'Enter Multiple Elevations file:'
      accept 9502,mefile
      type *,mefile
      open (unit=1,name=mefile,type='OLD',READONLY)
      read (1,*) nou,nor,noc,sx,sy
C
      type *,'Enter Travel Time output file:'
      accept 9502,ttfile
      type *,ttfile
      open (unit=2,name=ttfile,type='NEW',carriagecontrol='LIST')
      write (2,*) nou,nor,noc,sx,sy
C
      type *,'Enter Travel Time Summary output file:'                V3.1
      accept 9502,sumfile                                            V3.1
      type *,sumfile                                                 V3.1
      open (unit=3,name=sumfile,type='NEW',carriagecontrol='LIST')   V3.1
      write (3,*) nou,nor,noc,sx,sy                                  V3.1
C
C..... Get process control parameters
C
      type *,'Enter flux :(ft/year)'                                 V2.6
      accept *,flux                                                  V2.6
      type *,flux                                                    V2.6
C
```

```
      type *,'Enter depth increment: (ft)'                              V2.6
      accept *,deltad                                                   V2.6
      type *,deltad                                                     V2.6
C
      type *,'Enter porosity for fracture flow: '                       V2.6
      accept *,fp                                                       V2.6
      type *,fp                                                         V2.6
C
      type *,'Enter ratio of hydraulic conductivity to flux '           V2.6
      type *,'  which determines existence of fracture flow:'           V2.6
      accept *,ratio                                                    V2.6
      type *,ratio                                                      V2.6
C
C..... Read next column of elevations
C
 1000 read (1,*,end=8000) (unit(k),k=1,nou)
      do 1010 i=1,nou
         if (unit(i).lt.0) unit(i)=0                                    V2.1
 1010 continue
C
C..... Loop on units in column
C
      iu=1
      do while (iu.le.nou)
C
C..... Loop on cells in unit
C
         thick=unit(iu)
         nocells=thick/deltad
         if (amod(thick,deltad).gt.0.) nocells=nocells+1
         write (2,*) nocells
         do while (thick.gt.0)
            d=deltad
            if (d.gt.thick) d=thick
            thick=thick-d
C
C..... Get distribution numbers
C
            mp=0.                                                       V4.2
            do while (mp.le.0.)                                         V4.2
               call getdist (iu,mp,shc,irs)
            end do                                                      V4.2
            shc=shc*ftpermm
C
C..... Identify fracture flow
C
            fraction=flux/shc                                           V4.1
            if (fraction.ge.ratio) then                                 V4.1
               fracture=.true.
               nounitff=nounitff+1
               nocolff=nocolff+1
            else
               fracture=.false.
            end if
            if (fracture) then
C
C..... Compute fracture velocities and Travel Times
C
               if (fraction.le.1.) shc=ratio*shc                        V4.1
               velmatrix=shc/mp
               velfrac=(flux-shc)/fp
               if (velfrac.gt.velmatrix) then                           V4.3
                  tt=d/velfrac
```

```
                  else                                                    V4.3
                     tt=d/velmatrix                                       V4.3
                  end if                                                  V4.3
                  rttu =tt*400.                                           V2.3
                  rtttc=rttu                                              V2.3
               else
C
C..... Compute matrix velocities and Travel Times
C
                  velmatrix=(flux/mp)*(flux/shc)**epsilon(iu)             V2.2
                  tt=d/velmatrix
                  velfrac=0
                  rttu =tt*(1.+kdu (iu)*sbd(iu)/mp)                       V2.3
                  rtttc=tt*(1.+kdtc(iu)*sbd(iu)/mp)                       V2.3
               end if
               ttmatrix=d/velmatrix
C
C..... Store cell data
C
               write (2,*) tt,fracture,velmatrix,velfrac,shc,mp
               ttunit=ttunit+tt
               ttunitm=ttunitm+ttmatrix
               unitrttu =unitrttu +rttu                                   V2.3
               unitrtttc=unitrtttc+rtttc                                  V2.3
            end do
C
C..... Store unit data
C
            write (2,*) ttunit,nounitff,ttunitm,unitrttu,unitrtttc        V2.3
            write (3,9301)                                                V3.1
     +         nocells,ttunit,nounitff,ttunitm,unitrttu,unitrtttc         V3.1
            ttcol=ttcol+ttunit
            ttcolm=ttcolm+ttunitm
            colrttu =colrttu +unitrttu                                    V2.3
            colrtttc=colrtttc+unitrtttc                                   V2.3
            ttunit=0
            ttunitm=0
            nounitff=0
            unitrttu =0                                                   V2.3
            unitrtttc=0                                                   V2.3
            iu=iu+1
         end do
C
C..... Store column data
C
         write (2,*) ttcol,nocolff,ttcolm,colrttu,colrtttc                V2.3
         write (3,9302) ttcol,nocolff,ttcolm,colrttu,colrtttc             V3.1
         ttcol=0
         ttcolm=0
         nocolff=0
         colrttu =0                                                       V2.3
         colrtttc=0                                                       V2.3
C
         go to 1000
C
C..... End of input file
C
 8000 continue
C
C..... Terminate
C
 8800 stop 'Travel Time Calculations Complete'
C
```

```
C..... Formats
C
 9301 format (i5,f15.3,i5,3f15.3)                                        V3.1
 9302 format (5x,f15.3,i5,3f15.3)                                        V3.1
C
 9501 format (a1)
 9502 format (a80)
C
      end
      subroutine getdist (i,rnor,rlnor,irs)
C*************************************************************************
C
C        Get samples for a normal distribution (RNOR) and a log-normal
C        distribution (RLNOR) for unit 'i'.  The mean and standard
C        deviations for each unit are given as data statements.
C
C*************************************************************************
C
C        Variables
C        ---------
C        i         - ident of unit   1->Topopah Springs welded below
C                                       the disturbed zone
C                                    2->Calico Hills nonwelded vitrified
C                                    3->Calico Hills welded zelotized
C                                    4->Prow Pass welded
C                                    5->Prow Pass nonwelded
C                                       (Crater Flats, Upper Unit)
C                                    6->Bullfrog welded
C                                    7->Bullfrog nonwelded
C                                       (Crater Flats, Middle Unit)
C        irs       - integer random seed
C        rlnor     - returned value of log-normal distribution for
C                    saturated hydraulic conductivity
C        rnor      - returned value fo normal ditribution for porosity
C        skmu      - unit dependent means of saturated hydraulic
C                    conductivity
C        sksd      - unit dependent standard deviations of saturated
C                    hydraulic conductivity
C        thmu      - unit dependent means of matrix porosity
C        thsd      - unit dependent standard deviations of matrix porosity
C
C        Subroutines
C        -----------
C        lnormal   - returns sample of log-normal distribution
C        normal    - "      "        " normal          "
C
C*************************************************************************
C
      DIMENSION THMIN(7),SKMIN(7),THMU(7),THSD(7),SKMU(7),SKSD(7)        V2.5
C
C                      TS     CHV    CHZ    PPW    CFU    BFW    CFM
      DATA THMU    /.1062,.3239,.2693,.2382,.2500,.2251,.2500/           V2.5
      DATA THSD    /.0458,.0880,.0468,.0650,.0622,.0884,.0622/           V2.5
      DATA SKMU    /-.326, 4.67,-.626, 4.47, 3.07, 4.77, 3.07/           V2.5
      DATA SKSD    / 1.73, 4.04, 2.66, 1.09, 1.88, .707, 1.88/           V2.5
C
      CALL NORMAL(THMU(I),THSD(I),RNOR,irs)
      CALL LNORMAL(SKMU(I),SKSD(I),RLNOR,irs)
C
      return
      END
      SUBROUTINE NORMAL (U,S,R,irs)
C*************************************************************************
```

```
C
C        Return sample from normal distribution
C       U=MEAN,S=STD,R=NORMAL RANDOM DEVIATE
C
C*************************************************************************
C
      DIMENSION X(12)
C
    1 SUMX=0.
C
      DO 10 I=1,12
      X(I)=RAN(irs)
   10 SUMX=SUMX+X(I)
      R=S*SUMX+(U-6.*S)
      if (abs(r-u).gt.3.*s) go to 1                                    V2.4
C
      RETURN
      END
      SUBROUTINE LNORMAL (U,S,rr,irs)                                  V2.4
C*************************************************************************
C
C        Return sample from log-normal distribution
C       U=MEAN,S=STD,R=NORMAL RANDOM DEVIATE
C
C*************************************************************************
C
      DIMENSION X(12)
C
    1 SUMX=0.
C
      DO 10 I=1,12
      X(I)=RAN(irs)
   10 SUMX=SUMX+X(I)
      R=S*SUMX+(U-6.*S)                                                V2.4
      if (abs(r-u).gt.3.*s) go to 1                                    V2.4
      rr=exp(r)                                                        V2.4
C
      RETURN
      END
```

C-2. FORTRAN Program for Calculating Expected Cumulative Discharge of Radionuclides.

```
      PROGRAM RELEASE
C
C RELEASE CALCULATES THE MEAN RELEASE FOR RADIONUCLIDES IN GIVEN
C FLUXES AT GIVEN TRANSPORT TIMES.  RELEASE SOLVES THE FOLLOWING EQUATION
C FOR A GIVEN RADIONUCLIDE AT A GIVEN PERCOLATION FLUX AND A GIVEN
C TRANSPORT TIME:
C
C     XBAR = .5 * AA
C            * (EXP(RDC * (TAUBAR + .5 * RDC * VAR))
C                * (1. + ERF((TAUBAR + RDC * VAR) / (SQRT2 * STDDEV)))
C              - EXP(-R * (TAUBAR - .5 * R * VAR))
C                * (1. + ERF((TAUBAR - R * VAR) / (SQRT2 * STDDEV))))
C
C     WHERE THE VARIABLES IN THE ABOVE EQUATION AND IN THE CODE ARE
C     DEFINED AS FOLLOWS:
C
C           A         -- EFFECTIVE WATER INTERCEPT AREA OF A WASTE
C                        PACKAGE (M**2)
C           AA        -- RADIONUCLIDE ACTIVITY (CURIES)...
C                        ALPHA * N * R * RIM / (RDC + R) * EXP(-RDC * T)
C           ALPHA     -- RADIONUCLIDE SPECIFIC ACTIVITY (CURIES/KG)
C           I         -- RADIONUCLIDE INDEX
C           J         -- PERCOLATION FLUX INDEX
C           K         -- TRANSPORT TIME INDEX
C           N         -- NUMBER OF CANISTERS
C           Q         -- PERCOLATION FLUX (M**3/M**2*YR)
C           R         -- RADIONUCLIDE FRACTIONAL RELEASE RATE (1/YR)...
C                        Q * A * S / WM
C           RDC       -- RADIONUCLIDE DECAY CONSTANT (1/YR)
C           RIM       -- RADIONUCLIDE INVENTORY MASS (KG)
C           RNN       -- RADIONUCLIDE NAMES
C           S         -- MIN(SR,SM), WHERE SR IS THE SOLUBILITY OF A
C                        RADIONUCLIDE AND SM IS THE SOLUBILITY OF THE
C                        WASTE PACKAGE MATRIX (KG/M**3)
C           SQRT2     -- SQUARE ROOT OF 2
C           STDDEV    -- STANDARD DEVIATON OF THE TRANSPORT TIME
C           T         -- PROBLEM TIME (YR)
C           TAUBAR    -- (YR)... T - (TSUBC + TBAR)
C           TBAR      -- MEAN VALUE OF THE TRANSPORT TIME (YR)
C           TSUBC     -- WASTE PACKAGE CONTAINMENT TIME (YR)
C           VAR       -- VARIANCE OF THE TRANSPORT TIME
C           WM        -- MASS OF THE WASTE PACKAGE MATRIX (KG)
C           XBAR      -- THE MEAN VALUE OF THE RADIONUCLIDE RELEASE
C                        (CURIES)
C
      IMPLICIT NONE
      EXTERNAL ERF
      REAL ERF
      CHARACTER*8 RNN(3)
      REAL*8 ALPHA(3),RDC(3),RIM(3),S(3)
      REAL*8 Q(2),T(2),TBAR(2),STDDEV(2)
      REAL*8 A,WM,N,TSUBC
      REAL*8 AA,R,SQRT2,TAUBAR,VAR,XBAR
      INTEGER I,J,K
      DATA RNN /'C-14', 'TC-99', 'I-129'/
      DATA ALPHA /4.45E+3, 1.70E+1, 1.74E-1/
      DATA RDC /1.21E-4, 3.22E-6, 4.36E-8/
      DATA RIM /6.0E-4, 2.55, 6.32E-1/
      DATA S /5.0E-2, 5.0E-2, 5.0E-2/
      DATA Q /5.E-4, 1.E-3/
```

```
      DATA T /1.E+4, 1.E+5/
      DATA TBAR /4.42E+4, 2.15E+4/
      DATA STDDEV /1.25E+4, 7.94E+3/
      DATA A,WM,N,TSUBC /0.332, 3.33E+3, 2.1E+4, 3.E+3/
      SQRT2=SQRT(2.)
      DO 20 K=1,2
      DO 15 J=1,2
      TAUBAR=T(K)-(TSUBC+TBAR(J))
      VAR=STDDEV(J)*STDDEV(J)
      DO 10 I=1,3
      R=Q(J)*A*S(I)/WM
      AA=ALPHA(I)*N*R*RIM(I)/(RDC(I)+R)*EXP(-RDC(I)*T(K))
      XBAR=.5*AA*(EXP(RDC(I)*(TAUBAR+.5*RDC(I)*VAR))
     *     *(1.+ERF((TAUBAR+RDC(I)*VAR)/(SQRT2*STDDEV(J))))
     *     -EXP(-R*(TAUBAR-.5*R*VAR))
     *     *(1.+ERF((TAUBAR-R*VAR)/(SQRT2*STDDEV(J)))))
      WRITE(4,5) T(K),Q(J),RNN(I),XBAR
 5    FORMAT(' TIME:  ',F8.0,'  FLUX:  ',F5.4,
     *     '  NUCLIDE:  ',A8,'MEAN RELEASE:  ',G12.5)
 10   CONTINUE
 15   CONTINUE
 20   CONTINUE
      STOP
      END
C
      REAL*8 FUNCTION ERF(X)
C
C ERF IS AN APPROXIMATION OF THE ERROR FUNCTION; TAKEN (ORIGINALLY) FROM:
C     C. HASTINGS, JR., APPROXIMATIONS FOR DIGITAL COMPUTERS.
C     PRINCETON UNIVERSITY PRESS, PRINCETON, N. J., 1955.
C
      IMPLICIT NONE
      REAL*8 X,ISGN
      REAL*8 T,T2,T3,T4,T5
      REAL*8 P,A1,A2,A3,A4,A5
      DATA P,A1,A2,A3,A4,A5
     *     /.3275911, .254829592, -.284496736, 1.421413741,
     *      -1.453152027, 1.061405429/
      ISGN=1.
      IF(X.LT.0) ISGN=-1.
      X=ABS(X)
      T=1./(1.+P*X)
      T2=T*T
      T3=T2*T
      T4=T3*T
      T5=T4*T
      ERF=ISGN*(1.-(A1*T+A2*T2+A3*T3+A4*T4+A5*T5)*EXP(-X*X))
      RETURN
      END
```

APPENDIX D

INFORMATION RELEVANT TO THE REFERENCE INFORMATION BASE

D-1 Source of Data Used in the Report

1. The map of Yucca Mountain Site shown in Figure 2 was generated by Interactive Graphics Information System (IGIS, Product Number CAL-0119, SNL, 1986).

2. General hydrologic cross section of Yucca Mountain, shown in Figure 2, was modified from IGIS product number CAL-0115. The modification is necessary to show the wavy arrows for percolation flux and the unsaturated zone between the disturbed zone and the water table. The legend for hydrologic units was changed to be consistent with NNWSI EA (1986).

3. Grid map of the calculational elements for the repository studying area shown in Figure 3 was generated by the Interactive Graphics Information System (IGIS, Product Number CAL-0114, SNL, 1986).

4. Isopach contour maps shown in Figure 4 were generated by Interactive Graphics Information System (IGIS Product Numbers CAL-0047 through CAL-0053, and CAL-0060).

5. Parameters listed in Table 1 were summarized from data in Appendix B.

6. Histograms of total bulk porosity for each unit shown in Figure 5 and histograms of the logarithm of saturated matrix hydraulic conductivity were derived from data in Appendix B.

7. Values for the modeling parameters listed in Table 2 were chosen for the parametric analyses. The flux of 0.5 mm/yr and vertical correlation length of 10 ft used for baseline case were based on the understanding at the time, of the upper limit of percolation flux.

8. Values for the parameters used in the calculation of cumulative releases are the same as those specified in the EA (DOE, 1986). Computations for this report were based on the emplacement, approximately, of 21,000 canisters (or 70,000 MTHM).

9. The hydrological unit and drill hole data listed in Table B-1 were based on Reference Information Base, version 01.001, SNL, 1985.

10. Matrix porosity (Table B-2), residual saturation (Table B-3), and saturated matrix hydraulic conductivity (Table B-5) were obtained from Tuff Data Base System 2000, version 11001, Product Nos. 1 and 2, SNL, 1985.

D-2 Data Recommended for Inclusion Into the Reference Information Base

1. Data for the hydrological parameters used in the calculations of the baseline case groundwater travel time are the first of their kind compiled from RIB and TUFFDB. The data for baseline case shown in Tables 1 and 2 are candidates for inclusion in the RIB.

2. Based on the present calculational model, the estimates of groundwater travel time (as shown in Figures 8D and 12) for the baseline case, are candidates for inclusion in the RIB.

3. Cumulative releases to the water table listed in Table 4 are also candidates for inclusion in the RIB.

D-3 Data Recommended for Inclusion Into the Tuff Data Base

None.

DISTRIBUTION LIST

B. C. Rusche (RW-1)
Director
Office of Civilian Radioactive
Waste Management
U.S. Department of Energy
Forrestal Building
Washington, DC 20585

T. P. Longo (RW-25)
Program Management Division
Office of Geologic Repositories
U.S. Department of Energy
Forrestal Building
Washington, DC 20585

Ralph Stein (RW-24)
Office of Geologic Repositories
U.S. Department of Energy
Forrestal Building
Washington, DC 20585

Cy Klingsberg (RW-24)
Geosciences and Technology Division
Office of Geologic Repositories
U. S. Department of Energy
Forrestal Building
Washington, DC 20585

J. J. Fiore, (RW-22)
Office of Geologic Repositories
U.S. Department of Energy
Forrestal Building
Washington, DC 20585

B. G. Gale (RW-25)
Office of Geologic Repositories
U.S. Department of Energy
Forrestal Building
Washington, DC 20585

M. W. Frei (RW-24)
Office of Geologic Repositories
U.S. Department of Energy
Forrestal Building
Washington, DC 20585

R. J. Blaney (RW-22)
Program Management Division
Office of Geologic Repositories
U.S. Department of Energy
Forrestal Building
Washington, DC 20585

E. S. Burton (RW-25)
Siting Division
Office of Geologic Repositories
U.S. Department of Energy
Forrestal Building
Washington, D.C. 20585

R. W. Gale (RW-40)
Office of Geologic Repositories
U.S. Department of Energy
Forrestal Building
Washington, DC 20585

C. R. Cooley (RW-24)
Geosciences & Technology Division
Office of Geologic Repositories
U.S. Department of Energy
Forrestal Building
Washington, DC 20585

J. E. Shaheen (RW-44)
Outreach Programs
Office of Policy, Integration and
Outreach
U.S. Department of Energy
Forrestal Building
Washington, DC 20585

V. J. Cassella (RW-22)
Office of Geologic Repositories
U.S. Department of Energy
Forrestal Building
Washington, DC 20585

J. O. Neff, Manager
Salt Repository Project Office
U.S. Department of Energy
505 King Avenue
Columbus, OH 43201

D. C. Newton (RW-23)
Engineering & Licensing Division
Office of Geologic Repositories
U.S. Department of Energy
Forrestal Building
Washington, DC 20585

O. L. Olson, Manager
Basalt Waste Isolation Project Office
U.S. Department of Energy
Richland Operations Office
Post Office Box 550
Richland, WA 99352

D. L. Vieth, Director (4)
Waste Management Project Office
U.S. Department of Energy
Post Office Box 14100
Las Vegas, NV 89114

D. F. Miller, Director
Office of Public Affairs
U.S. Department of Energy
Post Office Box 14100
Las Vegas, NV 89114

P. M. Bodin (12)
Office of Public Affairs
U.S. Department of Energy
Post Office Box 14100
Las Vegas, NV 89114

B. W. Church, Director
Health Physics Division
U.S. Department of Energy
Post Office Box 14100
Las Vegas, NV 89114

Chief, Repository Projects Branch
Division of Waste Management
U.S. Nuclear Regulatory Commission
Washington, D.C. 20555

Document Control Center
Division of Waste Management
U.S. Nuclear Regulatory Commission
Washington, D.C. 20555

S. A. Mann, Manager
Crystalline Rock Project Office
U.S. Department of Energy
9800 South Cass Avenue
Argonne, IL 60439

K. Street, Jr.
Lawrence Livermore National
Laboratory
Post Office Box 808
Mail Stop L-209
Livermore, CA 94550

L. D. Ramspott (3)
Technical Project Officer for NNWSI
Lawrence Livermore National
Laboratory
P.O. Box 808
Mail Stop L-204
Livermore, CA 94550

W. J. Purcell (RW-20)
Associate Director
Office of Geologic Repositories
U.S. Department of Energy
Forrestal Building
Washington, DC 20585

D. T. Oakley (4)
Technical Project Officer for NNWSI
Los Alamos National Laboratory
P.O. Box 1663
Mail Stop F-619
Los Alamos, NM 87545

W. W. Dudley, Jr. (3)
Technical Project Officer for NNWSI
U.S. Geological Survey
Post Office Box 25046
418 Federal Center
Denver, CO 80225

NTS Section Leader
Repository Project Branch
Division of Waste Management
U.S. Nuclear Regulatory Commission
Washington, D.C. 20555

V. M. Glanzman
U.S. Geological Survey
Post Office Box 25046
913 Federal Center
Denver, CO 80225

P. T. Prestholt
NRC Site Representative
1050 East Flamingo Road
Suite 319
Las Vegas, NV 89109

J. S. Wright
Technical Project Officer for NNWSI
Westinghouse Electric Corporation
Waste Technology Services Division
Nevada Operations
Post Office Box 708
Mail Stop 703
Mercury, NV 89023

M. E. Spaeth
Technical Project Officer for NNWSI
Science Applications
International Corporation
Suite 407
101 Convention Center Drive
Las Vegas, NV 89109

ONWI Library
Battelle Columbus Laboratory
Office of Nuclear Waste Isolation
505 King Avenue
Columbus, OH 43201

SAIC-T&MSS Library (2)
Science Applications
International Corporation
Suite 407
101 Convention Center Drive
Las Vegas, NV 89109

W. M. Hewitt, Program Manager
Roy F. Weston, Inc.
2301 Research Blvd., 3rd Floor
Rockville, MD 20850

W. S. Twenhofel, Consultant
Science Applications
International Corp.
820 Estes Street
Lakewood, CO 89215

H. D. Cunningham
General Manager
Reynolds Electrical &
Engineering Co., Inc.
Post Office Box 14400
Mail Stop 555
Las Vegas, NV 89114

A. E. Gurrola
General Manager
Energy Support Division
Holmes & Narver, Inc.
Post Office Box 14340
Las Vegas, NV 89114

T. Hay, Executive Assistant
Office of the Governor
State of Nevada
Capitol Complex
Carson City, NV 89710

J. A. Cross, Manager
Las Vegas Branch
Fenix & Scisson, Inc.
Post Office Box 15408
Las Vegas, NV 89114

R. R. Loux, Jr., Director (3)
Nevada Agency for Nuclear Projects
Nuclear Waste Project Office
State of Nevada
Capitol Complex
Carson City, NV 89710

Neal Duncan (RW-44)
Office of Policy, Integration, and
Outreach
U.S. Department of Energy
Forrestal Building
Washington, DC 20585

C. H. Johnson, Technical
Program Manager
Nevada Agency for Nuclear Projects
Nuclear Waste Project Office
State of Nevada
Capitol Complex
Carson City, NV 89710

John Fordham
Desert Research Institute
Water Resources Center
Post Office Box 60220
Reno, NV 89506

Department of Comprehensive Planning
Clark County
225 Bridger Avenue, 7th Floor
Las Vegas, NV 89155

Lincoln County Commission
Lincoln County
Post Office Box 90
Pioche, NV 89043

Community Planning and Development
City of North Las Vegas
Post Office Box 4086
North Las Vegas, NV 89030

City Manager
City of Henderson
Henderson, NV 89015

N. A. Norman
Project Manager
Bechtel National Inc.
P. O. Box 3965
San Francisco, CA 94119

Flo Butler
Los Alamos Technical Associates
1650 Trinity Drive
Los Alamos, New Mexico 87544

Timothy G. Barbour
Science Applications International Corporation
1626 Cole Boulevard, Suite 270
Golden, CO 80401

E. P. Binnall
Field Systems Group Leader
Building 50B/4235
Lawrence Berkeley Laboratory
Berkeley, CA 94720

Dr. Martin Mifflin
Desert Research Institute
Water Resources Center
Suite 1
2505 Chandler Avenue
Las Vegas, NV 89120

Planning Department
Nye County
Post Office Box 153
Tonopah, NV 89049

Economic Development Department
City of Las Vegas
400 East Stewart Avenue
Las Vegas, NV 89101

Director of Community Planning
City of Boulder City
Post Office Box 367
Boulder City, NV 89005

Commission of the European Communities
200 Rue de la Loi
B-1049 Brussels
BELGIUM

Technical Information Center
Roy F. Weston, Inc.
2301 Research Boulevard, Third Floor
Rockville, MD 20850

R. Harig
Parsons Brinkerhoff Quade & Douglas, Inc.
1625 Van Ness Ave.
San Francisco, CA 94109-3678

Dr. Madan M. Singh, President
Engineers International, Inc.
98 East Naperville Road
Westmont, IL 60559-1595

Roger Hart
Itasca Consulting Group, Inc.
P.O. Box 14806
Minneapolis, Minnesota 55414

T. H. Isaacs (RW-22)
Office of Geologic Repositories
U.S. Department of Energy
Forrestal Building
Washington, DC 20585

J. P. Knight (RW-23)
Office of Geologic Repositories
U.S. Department of Energy
Forrestal Building
Washington, DC 20585

D. H. Alexander (RW-24)
Office of Geologic Repositories
U.S. Department of Energy
Forrestal Building
Washington, DC 20585

Allen Jelacic (RW-24)
Office of Geologic Repositories
U.S. Department of Energy
Forrestal Building
Washington, DC 20585

E. S. Burton (RW-25)
Office of Geologic Repositories
U.S. Department of Energy
Forrestal Building
Washington, DC 20585

Gerald Parker (RW-25)
Office of Geologic Repositories
U.S. Department of Energy
Forrestal Building
Washington, DC 20585

B. J. King, Librarian (2)
Basalt Waste Isolation Project
Library
Rockwell Hanford Operations
Post Office Box 800
Richland, WA 99352

J. R. Rollo
Deputy Assistant Director
for Engineering Geology
U.S. Geological Survey
106 National Center
12201 Sunrise Valley Drive
Reston, VA 22092

David K. Parrish
RE/SPEC Inc.
3815 Eubank, N.E.
Albuquerque, NM 87191

R. Lindsay Mundell
United States Bureau of Mines
P.O. Box 25086
Building 20
Denver Federal Center
Denver, Colorado 80225

Martin Marietta Energy Systems, Inc.
Attn: Cathy D. Long
4500 N 1103
P. O. Box X
Oak Ridge, TN 37831

6300 R. W. Lynch
6310 T. O. Hunter
6310 72/12141/13/TBD
6310 73/12144/13/TBD
6311 L. W. Scully
6311 C. Mora
6312 F. W. Bingham
6312 M. S. Tierney (10)
6312 G. E. Barr
6313 T. E. Blejwas
6314 J. R. Tillerson
6315 S. Sinnock (10)
6315 Y. T. Lin (10)
6315 P. G. Kaplan
6315 M. J. Eatough
6332 WMT Library (20)
6430 N. R. Ortiz
3141 S. A. Landenberger (5)
3151 W. L. Garner (3)
8024 P. W. Dean
3154-3 C. H. Dalin (28)
for DOE/OSTI

Org.	Bldg.	Name	Rec'd by	Org.	Bldg.	Name	Rec'd by

Sandia National Laboratories